

**University of São Paulo
“Luiz de Queiroz” College of Agriculture**

**Estimating the longitudinal concordance correlation through fixed
effects and variance components of polynomial mixed-effects
regression model**

Thiago de Paula Oliveira

Thesis presented to obtain the degree of Doctor in Sci-
ence Area: Statistics and Agricultural Experimentation

**Piracicaba
2018**

Thiago de Paula Oliveira
Agronomy Engineer

**Estimating the longitudinal concordance correlation through fixed
effects and variance components of polynomial mixed-effects
regression model**

versão revisada de acordo com a resolução CoPGr 6018 de 2011

Advisor:

Prof. Dr. **SILVIO SANDOVAL ZOCCHI**

Thesis presented to obtain the degree of Doctor in Sci-
ence Area: Statistics and Agricultural Experimentation

Piracicaba
2018

**Dados Internacionais de Catalogação na Publicação
DIVISÃO DE BIBLIOTECA - DIBD/ESALQ/USP**

Oliveira, Thiago de Paula

Estimating the longitudinal concordance correlation through fixed effects and variance components of polynomial mixed-effects regression model / Thiago de Paula Oliveira. -- versão revisada de acordo com a resolução CoPGr 6018 de 2011. -- Piracicaba, 2018 .

117 p.

Tese (Doutorado) -- USP / Escola Superior de Agricultura "Luiz de Queiroz".

1. Dados longitudinais 2. Modelo de regressão linear misto 3. Concordância longitudinal 4. *Carica papaya* L. 5. Análise de cor 6. Software R .
I. Título.

DEDICATORY

To my parents José Aparecido and Rosângela,
And my fiancé Letícia.
I love you.

ACKNOWLEDGMENTS

I thank to the University of São Paulo, especially “Luiz de Queiroz” College of Agriculture (ESALQ) for my professional qualification and National University of Ireland, that supported this research project. Financial support from the CNPq (“Conselho Nacional de Desenvolvimento Científico e Tecnológico”); and the CAPES (“Coordenação de Aperfeiçoamento de Pessoal de Nível Superior”) is gratefully acknowledged. Additional support was provided by FAPESP (“Fundação de Amparo à Pesquisa do Estado de São Paulo”) and by Departamento de Ciências Exatas of ESALQ.

Special acknowledgment goes to my advisor Prof. Silvio Sandoval Zocchi, who has always believed in my potential, and to my supervisor abroad John Hinde for the support of my Ph.D thesis and for their academic and friendly advices. I am also very thankful to my friends from Departamento de Ciências Exatas (ESALQ/USP) and from Statistical Genetics Laboratory (ESALQ/USP).

I would like to extend my acknowledgments to my family (Cido, Rose, and Tati) and my family in law (José Maurício, Liberaci, Renato, Bruna, Lais, and Gabriel), for their unconditional support during all stages of my life and for always believing in my potential. I could not forget to mention my other two families Vic, Ronaldo, Renan, Marina and Enzo, and Estela, Ronaldo, Rafael, Marcus, Ana, and Bruno that will always be kept in my heart.

I also need to thank my friends and siblings: Silvio Zocchi for his support, friendship, and confidence; Idemauro Lara, who became a great friend and part of my family; Rafael Moral, with whom I have always shared every stage of my life; and Aline, Adriano, Isabela and Fábio, who are loyal friends.

Finally, I would like to thank my fiancé Letícia Aparecida de Castro Lara for all comprehension, attention and love that she had with me through all these years.

“Live as if you were to die tomorrow. Learn as if you were to live forever.”

Mahatma Gandhi

Até a calmaria chegar

Eu estou sozinho
Não posso nem mesmo imaginar
As incertezas do caminho
De um barco perdido em alto mar

Onde está a estrela que há tanto tempo procuro?
Às vezes fico assim pensando...
Em episódios arrítmicos
E, assim, enlouquecendo a procura de um lar!

Estou completamente perdido nessa imensidão
Como posso, então, fixar meu olhar
Em estrelas que me confundem o tempo todo?
São apenas portas aberta aos tolos sob a luz do luar!

Lá se vai meu pequeno barco novamente
Levado por outra onda doutro amor luzente
Até a calmaria chegar!

Thiago de Paula Oliveira

SUMMARY

Resumo	9
Abstract	10
List of Figures	11
List of Tables	13
Lista de Abreviaturas e Siglas	14
Lista de Símbolos	15
1 Introduction	17
References	18
2 Literature review	21
2.1 Importance of papaya, methods for measurement fruit's color and agreement indexes	21
2.2 Longitudinal data and mixed effects models	26
2.2.1 Estimation methods	28
2.2.2 Selecting the covariance structure	32
2.3 Prediction of random effects	37
2.4 Conditional test for fixed effect parameters	38
2.5 The top-down strategy	39
References	39
3 Longitudinal concordance correlation function based on variance components: an application in fruit color analysis	45
3.1 Introduction	46
3.2 Experimental data and descriptive analysis	48
3.3 Definition of the longitudinal concordance correlation (LCC)	51
3.3.1 The multiple mixed effects regression model for longitudinal data	51
3.3.2 Model extensions	52
3.3.3 The longitudinal concordance correlation	53
3.4 Estimation of the LCC using variance components	55
3.5 Non-parametric bootstrap confidence intervals	56
3.6 Simulation study	57
3.7 Papaya's peel hue data analysis	60
3.8 Discussion	65
3.9 Conclusions	66
References	67
4 Estimation of the longitudinal concordance correlation function in R: The lcc package	71
4.1 Introduction	72
4.2 The longitudinal concordance correlation (LCC)	73
4.2.1 Estimation	74
4.3 Overview of the package lcc and R syntax	76

4.3.1	Output of the <code>lcc</code> function	81
4.4	Specifying models in the <code>lcc</code>	82
4.5	The papaya's peel hue dataset	83
4.6	Comparison with <code>cccrm</code> package	86
4.7	Discussion	88
4.8	Future works	88
4.9	Conclusions	89
	References	89
5	Conclusions	91
	Appendix	93
	Annex	99

RESUMO

Estimando a correlação de concordância longitudinal por meio de efeitos fixos e componentes de variâncias do modelo de regressão polinomial de efeitos mistos

Resumo: No setor de pós-colheita é muito comum a utilização de colorímetros para avaliar a cor média da casca de frutos ao longo do tempo. No entanto, muitas vezes as técnicas de amostragem utilizando esse equipamento podem levar a medidas tendenciosas da média amostral. Alternativamente, a utilização de imagens digitais pode levar a um menor viés, uma vez que toda a região da casca do fruto é amostrada de forma sistemática. No entanto, ainda é necessária a comparação de ambas abordagens, pois o colorímetro tem vantagens em relação a facilidade de utilização e menor tempo para realizar a amostragem em cada fruto quando comparado a um scanner de mesa. Assim, no caso de variáveis respostas medidas em uma escala contínua, a reprodutibilidade das medidas tomadas por ambos equipamentos pode ser avaliada por meio do coeficiente de correlação de concordância. Dessa forma, para avaliar o perfil da concordância entre métodos, nós propomos uma correlação de concordância longitudinal (LCC), baseada em um modelo de regressão polinomial com efeitos mistos. Os resultados sugeriram que as técnicas por meio de imagens digitais devem ser utilizadas para a quantificação da tonalidade média de frutos. Adicionalmente, a partir do perfil de concordância estimado notamos que existe um período em que ambos os equipamentos podem ser utilizados. A performance do coeficiente de concordância longitudinal foi avaliada por meio de um estudo de simulação, o qual sugeriu que nossa metodologia é robusta a dados desbalanceados (“dropout”) e que a probabilidade de convergência é aceitável para uma amostra de 20 frutos e ideal para amostras a partir de 100 frutos. Uma vez que ainda não existem pacotes disponibilizados no ambiente computacional R para a estimação da correlação de concordância longitudinal, nós estamos desenvolvendo um pacote intitulado **lcc**, o qual será submetido ao “Comprehensive R Archive Network” (CRAN). Nesse pacote nós implementamos procedimentos para estimação da correlação de concordância longitudinal, da correlação de Person longitudinal e de uma medida de acurácia longitudinal. Além disso, nosso pacote foi desenvolvido para dados balanceados e desbalanceados, permitindo modelar a heteroscedasticidade entre erros dentro do grupo usando ou não o tempo como covariável, e, também, permitindo a inclusão de covariáveis no preditor linear para controlar variações sistemáticas na variável resposta.

Palavras-chave: Dados longitudinais, Modelo de regressão linear misto, Concordância longitudinal, *Carica papaya* L., Análise de cor, Software R

ABSTRACT

Estimating the longitudinal concordance correlation through fixed effects and variance components of polynomial mixed-effects regression model

In the post-harvest area, a common approach to quantify the average color of fruits peel over time is the sampling of small number of points generally on its equatorial region using a colorimeter. However, when we use a colorimeter to classify an uneven-colored fruit misclassification may occur because points in the peel region may not be representative of average color of fruit. The main problem when we use this method is to determine the number of points to be sampled as well as the location of these points on the fruit's surface. An alternative method to evaluate measure of color is digital image analysis because it covers whole of the object surface, by using a sample of pixels taken from the image. As the colorimeter approach is faster and easier than image analysis, it may not be suitable for assessing the overall mean color of the papaya's peel and its performance will depend on the number of measured points and choice of sampled region. In this sense, the comparison between these approach is still necessary because we need to know if a sample on the equatorial region can reproduce a sample over the whole region, and if the colorimeter can compete with a scanner or digital camera in measuring the mean hue of papaya peel over time. Thus, we proposed a longitudinal concordance correlation (LCC) based on polynomial mixed-effects regression model to evaluate the extent of agreement among methods. The results show that ideally image analysis of whole fruit's region should be used to compute the mean hue and that the topography and curved surface of papaya fruit did not affect the mean hue obtained by the scanner. Since there are still no packages available to estimate the LCC in the free software environment R, we are developing a package called **lcc**, which provides functions for estimating the longitudinal concordance correlation (LCC) among methods based on variance components and fixed effects of polynomial mixed-effects model. Additionally, we implemented arguments in this function to estimating the longitudinal Pearson correlation (LPC), as precision measure, and longitudinal bias corrector factor (LA), as accuracy measure. Moreover, these components can be estimated using different structures for variance-covariance matrices of random effects and variance functions to model heteroscedasticity among within-group errors using or not the time as variance covariate.

Keywords: Longitudinal data, Mixed-effects regression, Longitudinal agreement, *Carica papaya* L., Color analysis, Software R

LIST OF FIGURES

2.1 CIELab (or CIELCh) color system with two-color representation: A as yellow hue, where $a = 8$ and $b = 54$ (or $C = 55$ and $H = 82^\circ$) and B as red hue, where $a^* = 50$ and $b^* = 22$ (or $C^* = 55$ and $h^* = 24^\circ$)	23
3.1 Equatorial region of both sides of one fruit (above) and separation of the equatorial region (in blank) of the black background using the <code>autoThreshold</code> function (a), both sides of one fruit stacked in one image (b) and separation of fruit's peel of the black background through the <code>autoThreshold</code> function as well (c)	49
3.2 Vector of mean hue obtained from observed points on equatorial region by the colorimeter and scanner, and whole region by the scanner	50
3.3 Individual profiles of 20 fruits assessed on the equatorial region by the scanner and colorimeter, and whole region by the scanner over time	50
3.4 Estimated simultaneous coverage rate based on 95% confidence intervals for $S_{jl,j'l'}(t_k)$ and $LCC(t_k)$, both considering $N \in \{20, 50, 100\}$ fruits in the balanced (A) and unbalanced (B) designs	59
3.5 Systematic differences between CE and ScE; CE and ScW; and ScE and ScW over the time, where CE and ScE indicate, respectively, observations measured by the colorimeter and scanner on the equatorial region while ScW indicates observations measured by the scanner on the whole region	61
3.6 Estimate and 95% confidence interval (CI) for the longitudinal concordance correlation (a); longitudinal Pearson correlation (b); and longitudinal accuracy (c) between observations measured on the equatorial region by the scanner and colorimeter with addition of points that represent the concordance correlation coefficient considering independent measurements taken over time	63
3.7 Estimate and 95% confidence interval (CI) for the longitudinal concordance correlation (a); longitudinal Pearson correlation (b); and longitudinal accuracy (c) between observations measured on the equatorial region by the colorimeter and whole region by the scanner with addition of respective observed values considering independent measurements taken over time (points)	64
3.8 Estimate and 95% confidence interval (CI) for the longitudinal concordance correlation (a); longitudinal Pearson correlation (b); and longitudinal accuracy (c) between observations measured on the equatorial and whole regions by the scanner with addition of respective observed values considering independent measurements taken over time (points)	64
4.1 (a) Individual profiles of 20 fruits assessed on the equatorial region by colorimeter and scanner, (b) scatter plot of hue data considering all repeated measurements, and (c) individual 95% confidence intervals for second degree polynomial coefficients	84

4.2 Estimate and 95% bootstrap confidence interval for the (a) longitudinal concordance correlation (LCC); (b) longitudinal Pearson correlation; and (c) longitudinal accuracy between observations measured on the equatorial region by the scanner and colorimeter with addition of points that represent the sample CCC, sample Pearson correlation coefficient, and sample accuracy, respectively	85
4.3 (a) Normal plot of within-group standardized residuals, (b) scatter plots of standardized residuals versus fitted values for the homoscedastic fitted, and (c) plot of standardized residuals versus time for <code>m1</code> fitted object	85
4.4 Estimate and 95% bootstrap confidence interval for the (a) longitudinal concordance correlation (LCC); (b) longitudinal Pearson correlation; and (c) longitudinal accuracy between observations measured on the equatorial region by the scanner and colorimeter with addition of points that represent the sample CCC, sample Pearson correlation coefficient, and sample accuracy, respectively	87
A.1 (a) Observed values versus the predicted values of the model; (b) the normality of residuals; and (c) the conditional residuals versus the predicted values. Here ‘Col’ represent observations measured by colorimeter on equatorial region, ‘SER’ represent observations measured by scanner on equatorial region, and ‘STR’ represent observations measured by scanner on whole region	97

LIST OF TABLES

3.1 Overall mean of simulated scaled mean error (SME), in absolute values, and root mean square error (RMSE) for four examples of longitudinal concordance correlation based on 2.000 Monte Carlo samples for 20, 50 and 100 fruits in the balanced and unbalanced design cases	58
3.2 Coefficients, parameter estimates by REML and their 95% confidence interval obtained by the non-parametric bootstrap method	61
4.1 Input arguments for LCC package	77
4.2 Observations (<i>Obs</i>) from 1 to 4 and 278 to 281 of the hue color dataset. The response variable is <i>H_mean</i> , <i>Method</i> represents the method/observer variable, <i>Time</i> represents the time variable, and <i>Fruit</i> shows the subject identification variable	81
Annex A small part of hue data of papaya fruits measured by two methods (Colorimeter or Scanner) on two peel regions (Equatorial or Whole) over time	99

LISTA DE ABREVIATURAS E SIGLAS

ANOVA	analysis of variance
CCC	Concordance correlation coefficient
CCCrn	Concordance correlation coefficient for repeated measures
GIMP	GNU image manipulation program
LCC	Longitudinal concordance correlation
LPC	Longitudinal Pearson Correlation
LA	Longitudinal accuracy
MAR	Missing at random
MCAR	Missing completely at random
MNAR	Missing not at random
REML	Restricted maximum likelihood
RMSE	Root mean square error
SME	Scaled mean error
VC	variance components

LISTA DE SÍMBOLOS

L^*	Luminosity
C^*	Chroma
h^*	Hue
\bar{h}^*	Circular mean hue
Y_{ijklk}	Random variable observed on i th fruit by the j th method on l th region of the fruit's peel at time t_k
y_{ijklk}	a realization of random variable Y_{ijklk}
t_{ik}	Time variable associated with i th fruit and k th repeated measurement
τ_{ik}	Time in the log scale, $\tau_{ik} = \log(t_{ik} + 1)$
d_{ick}	Dummy variable for fruit i associated with category c at time k
$\mathbf{X}_i(t_{ik})$	Design matrix associated with fixed effects
$\mathbf{Z}_i(t_{ik})$	Design matrix associated with random effects
β	Vector of fixed effects
\mathbf{b}_i	Vector of random effects for i th fruit
α_i	Within method-region by-subject vector of random effects
\mathbf{u}_i	Vector of random effects for i th fruit, where $\mathbf{u}_i = [\mathbf{b}_i^T, \alpha_i^T]^T$
ϵ	Vector of error terms
\mathbf{G}	Variance covariance matrix of random effects
\mathbf{D}	Variance covariance matrix of random effects
$g(\cdot)$	Variance function
δ	Vector of variance parameters
\mathbf{R}	Variance covariance matrix of errors
Φ	Matrix of zeros
\mathbf{V}_i	Marginal variance covariance matrix, $\mathbf{V}_i = \mathbf{Z}_i(t_{ik}) \mathbf{D} \mathbf{Z}_i^T(t_{ik}) + \mathbf{R}_i$
ρ_c	Concordance correlation coefficient
ρ_p	Pearson correlation coefficient
C_b	Bias correction factor
$\rho_{c,rm}$	Concordance correlation coefficient for repeated measures
$\rho_{jl,j'l'}(t_k)$	Longitudinal concordance correlation
$\rho_{jl,j'l'}^P(t_k)$	Longitudinal Pearson correlation
$C_{jl,j'l'}(t_k)$	Longitudinal bias correction factor
$S_{jl,j'l'}$	Systematic difference

1 INTRODUCTION

Measuring the amount of agreement between two or more responses is a common research goal. When the data are categorical in nature, the Cohen's kappa (COHEN, 1960) and weighted kappa (COHEN, 1968) statistics are appropriated measures of agreement for ordinal and nominal categorical variables, respectively. On the other hand, when the data are measured in continuous scale, the concordance correlation coefficient (CCC) introduced by LIN (1989) should be used as agreement measure between two methods. This agreement index is calculated by measuring the variation of the linear relationship between each pair of observations from the 45° line through the origin. Therefore, the mainly advantage of this coefficient is not only measuring how far each observation deviates from the best-fit line (measure of precision), but also how far the best-fit line deviates from the 45° line through the origin (measure of accuracy). Moreover, some extensions of CCC to categorical data was developed to estimate agreement equivalently to Cohen's kappa and weighted kappa statistics (KRIPPENDORFF, 1970; KING and CHINCHILLI, 2001).

However, when subjects, methods, or covariates variation are considered in the estimation of CCC, CARRASCO and JOVER (2003) suggested the use of two-way linear mixed-effect model to estimate CCC through variance components (VC), which was extended to repeated measures by CARRASCO *et al.* (2009) and soon after to generalized linear mixed-effects models (GLMMs) for count data by CARRASCO (2010). Other research direction is to estimate CCC via generalized estimating equations (GEE) introduced by BARNHART and WILLIAMSON (2001), who proposed three sets of estimating equations to model CCC between two methods for continuous variables. This approach was also extended to multiple methods (BARNHART *et al.*, 2005). Additionally, TSAI (2015) demonstrated through simulation study that CCC under VC and GEE can be biased when the model is misspecified, consequently, it is very important to perform model selection in both approach. Besides, this author also show that VC approach is less affected by model misspecification than GEE one.

In longitudinal studies where multiple methods measure the same individual and the main goal is to evaluate whether the methods agree with each other, it is natural to want to know when interchangeably among them will be possible. This would allows the use of cheapest or most convenient method in place of others. Thus, in this thesis we proposed an extension of ideas presented by LIN (1989) and CARRASCO *et al.* (2009) based on the mixed-effects polynomial regression model rather than a mixed-effects ANOVA approach. Our approach allows to estimate the extent of agreement among pair of observations for multiple methods. Furthermore, we also proposed an R (R CORE TEAM, 2017) package called **lcc**, which provides functions for estimating the longitudinal concordance correlation (LCC) among methods based on variance components and fixed effects of polynomial mixed-effects model. We also add arguments in this function for estimating the longitudinal Pearson correlation (LPC), as precision measure, and longitudinal bias corrector factor (LA), as accuracy measure.

The remainder of the thesis is organized as follows. In Chapter 2, we present a brief review on papaya ripeness, color measurements, concordance correlation coefficient, longitudinal data, mixed effects models, estimation methods (likelihood-based estimation), and model selection. In Chapter 3 we define the longitudinal concordance correlation (LCC) based on fixed effects and variance components in a multiple mixed-effects regression model. We also present a bootstrap-based confidence intervals, a simulation study to demonstrate the performance of LCC, and illustrate our approach with an application to the papaya hue color, considering fruit classification and maturation studies in the post-harvest phase. We describe the implementation of R package called `lcc` and explain its technical arguments in the Chapter 4. Numerical and graphical summaries for the fitted and confidence intervals were implemented for ‘`lcc`’ object in order to facilitate the interpretation of results. The approach is illustrated using two real datasets. In Chapter 5, we make our general conclusion. Finally, in the Appendix section, we present some proofs, matrix algebra theory used in demonstrations discussed throughout of this thesis. Moreover, R code used in the development of Chapter 3 is available in the Appendix while R code used in Chapter 4 may be upon request to the author.

References

- BARNHART, H., J. SONG, and M. HABER, 2005 Assessing intra, inter, and total agreement with replicated measurements. *Stat. Med.* **24**: 1371–1384.
- BARNHART, H. X. and J. M. WILLIAMSON, 2001 Modeling concordance correlation via GEE to evaluate reproducibility. *Biometrics* **57**: 931–940.
- CARRASCO, J. L., 2010 A generalized concordance correlation coefficient based on the variance components generalized linear mixed models for overdispersed count data. *Biometrics* **66**: 897–904.
- CARRASCO, J. L. and L. JOVER, 2003 Estimating the Generalized Concordance Correlation Coefficient through Variance Components. *Biometrics* **59**: 849–858.
- CARRASCO, J. L., T. S. KING, and V. M. CHINCHILLI, 2009 The concordance correlation coefficient for repeated measures estimated by variance components. *Journal of biopharmaceutical statistics* **19**: 90–105.
- COHEN, J., 1960 A coefficient of agreement for nominal scales. *Educ. Psychol. Meas.* **20**: 37–46.
- COHEN, J., 1968 Weighted kappa: nominal scale agreement with provision for scaled disagreement or partial credit. *Psychol. Bull.* **70**: 213–220.
- KING, T. S. and V. M. CHINCHILLI, 2001 A generalized concordance correlation coefficient for continuous and categorical data. *Statistics in Medicine* **20**: 2131–2147.

- Krippendorff, K., 1970 Bivariate Agreement Coefficients for Reliability of Data. *Sociological Methodology* **2**: 139–150.
- Lin, L. I., 1989 A Concordance Correlation Coefficient to Evaluate Reproducibility. *Biometrics* **45**: 255–268.
- R CORE TEAM, 2017 The R environment.
- Tsai, M.-Y., 2015 Comparison of concordance correlation coefficient via variance components, generalized estimating equations and weighted approaches with model selection. *Computational Statistics and Data Analysis* **82**: 47–58.

2 LITERATURE REVIEW

In this chapter, we present a brief review about some important topics. In Section 2.1, we discuss the importance of papaya fruits, what methods can be used to evaluate the peel color of these fruits, and how we can assess the agreement among these methods. Longitudinal data analysis involving multiples outcomes or covariates is described in Section 2.2. In the Section 2.3, we presented how the prediction of random effects is made. The fixed effect selection procedure that can be made using the conditional *F*-test is presented in Section 2.4. Finally, the top-down strategy to model selection is presented in Section 2.5.

2.1 Importance of papaya, methods for measurement fruit's color and agreement indexes

The global demand of papaya (*Carica papaya* L.) has grown over the last years. The Brazilian production in 2012 was approximately 1.5 million tons of fruit in around 31,000 hectares of cropped area (EMBRAPA, 2012). Regions with higher productivity are the Northeast and Southeast, whose productions are approximately 0.92 and 0.55 million tons, respectively (SECRETARIA DA AGRICULTURA, PECUÁRIA, IRRIGAÇÃO, PESCA E AQUICULTURA, 2014).

On the other hand, producers face a challenge when ensuring pre- and post-harvest quality of the fruit when aiming to export. In September 2014, around 2,896 tons of papaya were sold for the exportation market, representing an increase of 24.94% when compared with 2013 (SECRETARIA DA AGRICULTURA, PECUÁRIA, IRRIGAÇÃO, PESCA E AQUICULTURA, 2014). However, one of the main problems related to exporting is the misclassification of fruits that may cause non-uniformity in a box and among boxes. Generally, fruits in advanced ripening stages may increase the ripening velocity of other fruits due to ethylene emission, causing a reduction in fruits lifetime and consequently affecting its exportation (FONSECA *et al.*, 2007).

Fruit quality depends on maturation stage, but does not depend on the cultivar. According to BRON and JACOMINO (2006), the maturation stages can be determined by the peel color that is considered a reliable variable to establish a maturation index. Moreover, maturation stage can also be used to determine harvest and consumption times of several fruits (FONSECA *et al.*, 2007).

Harvest point can influence directly on aroma, flavor, shelf life, and ripeness process. As consequence, fruits harvested before or after this point can also have its market price reduced. (BRON and JACOMINO, 2006). In general, the visual appearance has a larger influence on fruit purchasing decisions by consumers (CHITARRA and CHITARRA, 2005). They have a greater preference for fruits with bright-yellow or bright-orange peel coloring (FIORAVANÇO *et al.*, 1994). Thus, the acceptance or rejection of fruits by consumers is directly associated with its peel color, more specifically with hue color component.

Although coloration is important to classification and study of ripening process, techniques used to quantify the papaya peel color may be strongly biased (OLIVEIRA *et al.*, 2017). In general, researchers do not take into account the non-uniformity of peel color among fruits

evaluated at same time and within-fruits measured over time in the sampling. Thus, as the sampling may not properly represent the target population, the sampled mean color can be biased.

Currently, we have three techniques to color quantification that are visual, instrumental, and image analysis. Color quantification by visual method is based on comparison of peel color with standard color scales, as Munsell color charts for plant tissues proposed by MUNSELL COLOR COMPANY (1952). However, this method can be naturally biased because it is possible to get different interpretation for a same fruit measured by distinct classifiers, or for a same fruit measured at different times by the same classifier (AVILA *et al.*, 2015). Besides, bias in fruit classification can increase with fatigue of the classifier (AVILA *et al.*, 2015). Consequently, this process can lead to non-uniformity of fruits color in the same box and/or among boxes (OLIVEIRA *et al.*, 2002).

When we use a colorimeter to classify an uneven-colored fruit, misclassification may occur because sampled points in the peel region may not be representative of target population. To understand the possible failures when using the colorimeter methodology, we must initially understand how it works. A colorimeter is a relatively simple sensor device consisting of a cuvette (a small tube of circular cross section, sealed at one end, made of plastic and designed to sample a small area of objects), a light source and light intensity sensor (MINOLTA, 1991). In the post-harvest, it is used to evaluate the entire peel mean color of several fruits, such as mango, papaya, banana, lemon, orange and others. Thus, the main problem when we use this method is to determine the number of points to be sampled as well as the location of these points on the fruit surface. It is common, for example, the sampling of four points on the equatorial region in papaya fruit (CHÁVEZ-SÁNCHEZ *et al.*, 2013; MARTINS *et al.*, 2014), however, as this fruit do not have a uniform coloration, sampling only equatorial region could not be representative of its entire surface (OLIVEIRA *et al.*, 2017). Despite of this problem, colorimeter methodology can be very efficient when the goal is to measure the mean color of fruits whose peel has uniform coloration.

An alternative method to evaluate uneven color fruits is digital image analysis because it covers the whole of the object surface, by using a sample of pixels taken from the image. Besides, it also offers many versatile possibilities, such as to evaluate the fruit's shape (O'SULLIVAN *et al.*, 2003; DARRIGUES *et al.*, 2008; WU and SUN, 2013). Furthermore, digital image analysis can also be used to construct more precise maturation curves, implying in a better post-harvest management. This idea already was easily extended to food-dye and meat color analysis, and others minimally processed products (BROSNAN and SUN, 2002).

In post-harvest, the most common systems to describe the color quantitatively are *CIELab* that describe color by using three quantities L^* , a^* , and b^* or *CIELCh* that uses L^* , C^* and h^* coordinates (COMMISSION INTERNATIONALE DE L'ECLAIRAGE, 2007; SCHANDA, 1996; ABBOTT, 1999). The L^* coordinate describes the lightness of a object from black ($L^* = 0$) to white ($L^* = 100$) and coordinates a^* and b^* describe the hue from green to red and from blue

to yellow, respectively. Moreover, it is very common to find a^* and b^* values ranging from -60 to 60 or from -100 to 100 .

The chroma, C^* , on the other hand, can be expressed as a square root of the sum of squared coordinates a^* and b^* ($C^* = \sqrt{a^{*2} + b^{*2}}$). Finally, the hue, h^* is expressed in degrees with 0° being red, then continuing to 90° for yellow, 180° for green, and 270° for blue (see Figure 2.1). Furthermore, it is invariant under the orientation of an object with respect to the lighting (SMEULDERS *et al.*, 2000). Hue variable is especially important because it is frequently used to establish ripening curves for several fruits, such as mango, papayas and bananas (SILVA-AYALA *et al.*, 2005; SANCHO *et al.*, 2010).

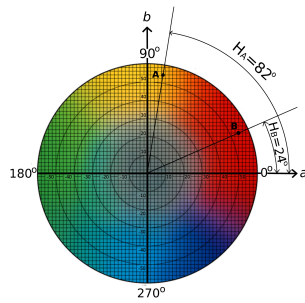


Figure 2.1: CIELab (or CIELCh) color system with two-color representation: **A** as yellow hue, where $a = 8$ and $b = 54$ (or $C = 55$ and $H = 82^\circ$) and **B** as red hue, where $a^* = 50$ and $b^* = 22$ (or $C^* = 55$ and $h^* = 24^\circ$)

Although versatile and simple, this method needs a calibration process because digital devices use a color space that is not standardized. The calibration involves at least the following steps: i) establishing what standard colors represent the color range of the object of interest; ii) measure each standard color with a colorimeter; iii) image acquisition of each standard color with the scanner on a black background, saving this image as a TIFF file; iv) converting the RGB values to *CIELab* or *CIELCh* values according to the type of illuminant (D65 or C) and observation angle; v) determine the relationship between the color data generated from the colorimeter and scanner through, for example, regression procedures. Some studies as YAM and PAPADAKIS (2004); MENDOZA and AGUILERA (2004), DARRIGUES *et al.* (2008), and OLIVEIRA *et al.* (2017) showed that scanner can be used as color measuring device because the correlation coefficient between the values of colorimeter and scanner were greater than 0.9 for L^* , a^* , b^* , C^* , and h^* color components. Besides, color measurement devices based on image analysis have been widely used in determining the color of fruits, vegetables, meats, and others (O'SULLIVAN *et al.*, 2003; MENDOZA and AGUILERA, 2004; DARRIGUES *et al.*, 2008; GUZMÁN *et al.*, 2013; MANNINEN *et al.*, 2015).

Despite of many fruits having characteristic of gradual color changing over time and/or uneven peel color within fruit or among fruits, it is common the use of colorimeter to assess mean color of them (SILVA-AYALA *et al.*, 2005; DA SILVA *et al.*, 2005; KHENG *et al.*, 2011;

CHÁVEZ-SÁNCHEZ *et al.*, 2013; LOVERA *et al.*, 2014; MARTINS *et al.*, 2014). Therefore, it is important to verify the extent of agreement between the digital image analysis and the colorimeter methodologies over time in order to define which method should be used to calculate mean color of these type of fruits.

Initially, we can use the concordance correlation coefficient (CCC) proposed by LIN (1989) to evaluate the agreement between each color component measured by scanner and colorimeter in the same fruit. This coefficient is based on a measure of precision multiplied by a measure of accuracy (C_b) and is defined by the author based on variance components and expected value of the squared difference as

$$\rho_c = \frac{2\sigma_{12}}{\sigma_1^2 + \sigma_2^2 + (\mu_1 - \mu_2)^2} = \rho C_b \quad (2.1)$$

where σ_1^2 is the variance of the first device, σ_2^2 is the variance of the second device, σ_{12} is the covariance among devices, μ_1 is the mean value of the first device and μ_2 is the mean value of the second device. Moreover, $\rho = \sigma_{12}/\sqrt{\sigma_1^2\sigma_2^2}$ is the Pearson correlation coefficient that measures how far each observation deviated from the best-fit line (precision measure) and $C_b = [(v + 1/v + u^2)/2]^{-1}$ is the accuracy, which measures how far the best-fit line deviates from the 45° line through the origin (measure of accuracy), where $v = \sigma_1/\sigma_2$ is the scale shift and $u = (\mu_1 - \mu_2)/\sqrt{\sigma_1\sigma_2}$ is the location shift relative to the scale (LIN, 1989; KING and CHINCHILLI, 2001).

The CCC is the commonly used statistic to assess the degree of agreement among devices when the response variable is continuous and it can assume values ranging from -1 to 1, where -1 represents perfect disagreement, 0 represents no-agreement, and 1 represents perfect agreement (LIN, 1989).

However, when two devices measure a response on N fruits over n times, we need to consider this longitudinal effect in the model. Initially, CHINCHILLI *et al.* (1996) developed a weighted concordance correlation coefficient to analyze repeated measures data based on multivariate linear mixed models. Thereafter, two different approaches were proposed based on the CCC. In the first, BARNHART and WILLIAMSON (2001) proposed the Generalized Estimating Equation (GEE) using three sets of estimating equations in order to model the CCC between two devices. The second approach was established by CARRASCO and JOVER (2003). These authors compared the equivalence between the Intraclass Correlation Coefficient (ICC) and CCC for a two-way linear mixed model as shown below:

$$Y_{ij} = \mu + \phi_i + \zeta_j + \epsilon_{ij}, \quad (2.2)$$

where Y_{ij} is the measurement taken by device j ($j = 1, 2, \dots, m$) on fruit i ($i = 1, 2, \dots, N$); μ is the overall mean over fruits and devices; ϕ_i is the fruit random effect assumed to be distributed as $\phi_i \sim N(0, \sigma_\phi^2)$; ζ_j is the mean deviation of device j from the overall mean; and ϵ_{ij} is the random error assumed to be distributed as $\epsilon_{ij} \sim N(0, \sigma_\epsilon^2)$. Assuming independence of all model

effects, the CCC can be expressed as a function of the variance components:

$$\rho_{ccc} = \frac{\sigma_\phi^2}{\sigma_\phi^2 + S_\zeta + \sigma_\epsilon^2} \quad (2.3)$$

where $S_\zeta = \frac{1}{m-1} \sum_{j=1}^m \zeta_j^2$ accounts for systematic differences between devices. Hence, CARRASCO and JOVER (2003) showed that CCC can be estimated by variance components considering two or more devices.

However, when we work with uneven color fruits, a relevant information to build the model is that ripening process can be very changeable and depends on various interrelated process such as mechanical damage and physiological disorders, which can influence the maturation process differently among fruits (BRON and JACOMINO, 2006). For example, DA SILVA *et al.* (2005) realized that the ethylene biosynthesis of the papaya affects directly the ripening process and it could be different among fruits. Since the stages of ripeness could be different, the individual profiles of fruits assessed by the same device as well as individual profile of the same fruit assessed by distinct device may be strongly different. According to CARRASCO *et al.* (2009), when the devices assess a feature in N subjects over n times, model (2.2) may be modified to account for these replicates:

$$Y_{ijt} = \mu + \phi_i + \zeta_j + \beta_k + \phi\zeta_{ij} + \phi\beta_{ik} + \zeta\beta_{jk} + \epsilon_{ijk} \quad (2.4)$$

where μ is the overall mean, ϕ_i is the fruit random effect ($i = 1, 2, \dots, N$), assumed to be distributed as $\phi_i \sim N(0, \sigma_\phi^2)$; ζ_j is the device fixed effect ($j = 1, 2, \dots, m$), β_k is the time fixed effect ($k = 1, 2, \dots, n$), $\phi\zeta_{ij}$ is the fruit-device random interaction effect, assumed to be distributed as $\phi\zeta_{ij} \sim N(0, \sigma_{\phi\zeta}^2)$, $\phi\beta_{ik}$ is the fruit-time random interaction effect, assumed to be distributed as $\phi\beta_{ik} \sim N(0, \sigma_{\phi\beta}^2)$, $\zeta\beta_{jk}$ is the device-time fixed interaction effect, and ϵ_{ijk} is the random error, assumed to be distributed as $\epsilon_i \sim MVN(\mathbf{0}, \sigma_\epsilon^2 \Sigma_i)$. Assuming independence among all model effects, CARRASCO *et al.* (2009) showed that the CCC for repeated measures ($\rho_{c,rm}$) can be expressed by the variance components as

$$\rho_{c,rm} = \frac{\sigma_\phi^2 + \sigma_{\phi\beta}^2}{\sigma_\phi^2 + \sigma_{\phi\beta}^2 + \sigma_{\phi\zeta}^2 + S_{\zeta\beta} + \sigma_\epsilon^2} \quad (2.5)$$

where a estimator of $S_{\zeta\beta}$ is

$$\widehat{S}_{\zeta\beta} = \frac{1}{nm(m-1)} \sum_{k=1}^n \sum_{j=1}^{m-1} \sum_{j'=j+1}^m (\widehat{\mu}_{jk} - \widehat{\mu}_{j'k})^2 - \frac{\sigma_{\phi\zeta}^2 + \sigma_\epsilon^2}{N}. \quad (2.6)$$

In the case where there are only two devices, the expression (2.6) reduces to

$$\widehat{S}_{\zeta\beta} = \frac{1}{2n} \sum_{k=1}^n (\widehat{\mu}_{1k} - \widehat{\mu}_{2k})^2 - \frac{\sigma_{\phi\zeta}^2 + \sigma_\epsilon^2}{N}. \quad (2.7)$$

According to CARRASCO *et al.* (2009), the $\rho_{c,rm}$ summarizes the interchangeability among devices in relation to all their measures. However, as the colorimeter assesses the equatorial region of the fruit and the scanner assesses the entire peel region, the concordance correlation coefficient can vary over time. In general, papaya fruit changes its color from green to yellow forming yellow stripes which arise initially in the estilar region towards to stem region (DA SILVA *et al.*, 2005; SCHWEIGGERT *et al.*, 2011). In this sense, it can be interesting to check the agreement profile among the devices over time.

We can use regression models to describe how the mean response changes with time as an alternative for models proposed by LIN (1989), KING *et al.* (2007) and CARRASCO *et al.* (2009) to verify the agreement among devices over time. Furthermore, when we modeled the time as a covariate, the concordance correlation will be a function of time and depend on estimation of fixed and random effects of the regression model. According LITTELL *et al.* (2000), the use of a polynomial mixed model can greatly decrease standard errors of estimators when compared with an ANOVA model that accounts the time as factor. Besides, the polynomial mixed-effects model with an autoregressive structure in the conditional covariance can be more efficient in the parameter estimation than other methods which ignore the correlation structure of the data and do not use an autocorrelation structure to modeling the temporal-correlation in the conditional covariance matrix (NI *et al.*, 2010).

2.2 Longitudinal data and mixed effects models

Longitudinal measurements often involve multiples outcomes or covariates that are measured repeatedly within a group of individuals randomly selected from one or more populations. For example, in experiments whose aim is to assess the ripeness process of fruits over time using p explanatory variables, the factor fruit should be treated as random if the sample is representative of the fruit's population. Thus, model building for this experiment should consider fruit's effect as random rather than fixed because it only affect the variance of the response variable distribution.

According to LAIRD and WARE (1982) and VERBEKE and MOLENBERGHS (2009), longitudinal data analysis can be also made by multivariate models with unrestricted or unstructured variance-covariance. However, this approach can become difficult because longitudinal data usually has any type of unbalance over time. The missing values can occur randomly or can be caused by the researcher (not random). Thus, we should consider nature of missing-data mechanism to obtain a valid inference. According to FITZMAURICE *et al.* (2009), the missing-data mechanism in repeated measures describes the probability that a response is observed or missing at any occasion. In this sense, we have a hierarchy of three different types of missing-data mechanism: i) missing completely at random (MCAR), the probability of missing data on a variable Y is unrelated to other observed variables in the data set as well as unrelated to the values of Y itself; ii) missing at random (MAR), the probability of missing data on a variable

Y is related to other observed variables in the data set, but unrelated to the values of Y itself; and iii) missing not at random (MNAR), the probability of missingness on Y depends on unobserved measurements and may be on the observed measurements. Consequently, each type of missing-data mechanism has different assumptions and so can impact differently the validation of research conclusion. Generally, MCAR and MAR mechanisms may be ignorable when one does not require a model for probability of a missing response given the set of observed responses and covariates. Thus, we assume that obtaining a valid likelihood-based analysis does not depend on missing observations, but depends only of the correct model specification (Fitzmaurice *et al.*, 2009).

A common missingness pattern for longitudinal data is due to dropout or attrition, that is, when some individuals can be withdrawn from the experiment before its intended completion due to random factors such as diseases occurrence, days until the harvest, harvest points, etc. Generally, the dropout is treated as ignorable and modeled as MCAR or MAR missing-data mechanism. However, when the individuals may have dropped out at beginning of the experiment or observational study, the dropout mechanism is called “non-ignorable”, consequently we can use a non-MAR mechanism to obtain a valid likelihood-based analysis (Fitzmaurice *et al.*, 2009).

For the likelihood-based estimation, the linear mixed effects (LME) model has a natural application in longitudinal studies because random effects vary among individuals and include within-individual dependence among repeated measurements after conditioning on observed covariates (Pinheiro and Bates, 2000; Fitzmaurice *et al.*, 2009). The linear mixed model assumes that the response vector \mathbf{y}_i for the i th individual satisfy the linear regression model

$$\mathbf{y}_i = \mathbf{X}_i\boldsymbol{\beta} + \mathbf{Z}_i\mathbf{b}_i + \boldsymbol{\epsilon}_i, \quad (2.8)$$

where \mathbf{y}_i is the n_i -dimensional vector of observations for the i -th individual; \mathbf{X}_i is a $n_i \times p$ design matrix, or set of explanatory variable; $\boldsymbol{\beta}$ is a $(p+1)$ -dimensional vector of population-specific parameters (fixed effects) describing the response average trends; \mathbf{Z}_i is a $n_i \times q$ design matrix, or a set of known covariates; \mathbf{b}_i is a q -dimensional vector of individual-specific parameters which affect the variance of marginal distribution of Y_i (random effects) describing how the i th individual deviate from population average; and $\boldsymbol{\epsilon}_i$ is a n_i -dimensional vector of experimental errors assumed to be independent among individuals, and fixed and random effects parameters. Furthermore, we also assumed that $\boldsymbol{\epsilon}_i \sim N(\mathbf{0}, \boldsymbol{\Sigma}_i)$, usually $\boldsymbol{\Sigma}_i$ is assumed to be $\sigma_\epsilon^2 \mathbf{I}_{n_i}$. Generally, the random effects \mathbf{b}_i is assumed to be normally distributed with mean vector $\mathbf{0}$ and variance-covariance matrix \mathbf{G} .

The design matrix \mathbf{X}_i contain values of explanatory variables that may be qualitative or/and quantitative. Thus, it can contain indicator variables (with ones representing presence and zeros absence of determined factor level) that indicate a group membership in the population of interest for an analysis of variance model; and/or it can contain values of continuous variables. We have a regression model when \mathbf{X}_i contains only continuous variables and a model

of covariance analysis when \mathbf{X}_i contains both variables. In the same way, the design matrix \mathbf{Z}_i can also contain values of explanatory variables that may be qualitative or/and quantitative. The main difference between \mathbf{X}_i and \mathbf{Z}_i is that the first one influences only the mean of the response variable distribution while the second one only influences the variance of the response variable distribution.

Considering hierarchical structure of mixed effect model, the general model for the i th individual should be written as

$$\begin{aligned}\mathbf{Y}_i|\mathbf{b}_i &\sim N(\mathbf{X}_i\boldsymbol{\beta} + \mathbf{Z}_i\mathbf{b}_i, \Sigma_i) \\ \mathbf{b}_i &\sim N(\mathbf{0}, \mathbf{G}).\end{aligned}$$

Generally linear regression assumes that ϵ_i and $\epsilon_{i'}$ ($i \neq i' = 1, 2, \dots, N$) are independent, and $\sum_{i=1}^N \mathbf{X}_i^T \mathbf{X}_i$ is non-singular due to identifiability of the fixed effects ($\boldsymbol{\beta}$), besides assumptions of model additivity, homoscedasticity, and normality of errors. However, in the linear mixed effect regression we have additional assumptions besides those already mentioned for linear regression, that are independence between vectors ϵ_i and \mathbf{b}_i ; and $\mathbf{Z}_i^T \mathbf{Z}_i$ should be positive definite matrix (VERBEKE and MOLENBERGHS, 2009).

2.2.1 Estimation methods

To estimate fixed effects and variance components of the linear mixed-effects model we use the restricted maximum likelihood approach (REML). The likelihood function of \mathbf{Y} may be written as the product of marginal function of \mathbf{Y}_i , $i = 1, 2, \dots, N$, because we assume independence among fruits. Then, the likelihood function is expressed as

$$L(\boldsymbol{\theta}; \mathbf{y}) = \frac{1}{\sqrt{2\pi\sigma_\epsilon^2 |\mathbf{V}|}} \exp \left\{ -\frac{1}{2\sigma_\epsilon^2} [(\mathbf{y} - \mathbf{X}\boldsymbol{\beta})^T \mathbf{V}^{-1} (\mathbf{y} - \mathbf{X}\boldsymbol{\beta})] \right\} \quad (2.9)$$

where $\mathbf{V} = \mathbf{Z}\mathbf{G}\mathbf{Z}^T + \sigma_\epsilon^2 \boldsymbol{\Sigma}$, $\boldsymbol{\beta}$ is the vector of fixed effects; $\boldsymbol{\theta} = (\boldsymbol{\beta}^T, \boldsymbol{\theta}_b^T, \boldsymbol{\theta}_\epsilon^T)^T$ and $\boldsymbol{\theta}_b$ and $\boldsymbol{\theta}_\epsilon$ are vectors of variance components associated with variance-covariance matrices \mathbf{G} and $\boldsymbol{\Sigma}$, respectively. Hence, the parametric space is given by

$$\Theta = \left\{ \boldsymbol{\beta} \in \mathbb{R}^{(p+1)} \mid \boldsymbol{\Sigma} \text{ and } \mathbf{G} \text{ are positive definite matrices} \right\}.$$

The derivation of the likelihood may be performed of different forms as showed by PATTERSON and THOMPSON (1971) or HARVILLE (1974). A review of the maximum likelihood (ML) approach for variance parameter estimation including an alternative derivation of the REML approach is presented by HARVILLE (1977) while VERBYLA (1990) presents a clearer derivation of the REML function related to derivation of HARVILLE (1974).

The log-likelihood of \mathbf{Y} is partitioned into a conditional log-likelihood and a marginal log-likelihood, where the conditional log-likelihood maximization results in estimates of fixed effects, which are equivalent to the estimates given by ML estimation (VERBEKE and MOLENBERGHS, 2009). On the other hand, the marginal log-likelihood maximization provides estimates of variance parameters $\boldsymbol{\psi} = (\boldsymbol{\theta}_b^T, \boldsymbol{\theta}_\epsilon^T)^T$ and it is called as residual or REML log-likelihood.

Consider a non-singular matrix $\mathbf{L} = [\mathbf{L}_1 : \mathbf{L}_2]$ where \mathbf{L}_1 and \mathbf{L}_2 are matrices of dimension $N_T \times p$ and $N_T \times (N_T - p - 1)$, respectively, which satisfying the equalities $\mathbf{L}_1^T \mathbf{X} = \mathbf{I}_c$ and $\mathbf{L}_2^T \mathbf{X} = \mathbf{0}$. Therefore, the data is transformed from \mathbf{y} to $\mathbf{L}^T \mathbf{y}$ where $N_T = \sum_{i=1}^N n_i$ is the total number of observations and

$$\mathbf{L}^T \mathbf{y} = \begin{bmatrix} \mathbf{L}_1^T \mathbf{y} \\ \mathbf{L}_2^T \mathbf{y} \end{bmatrix} = \begin{bmatrix} \mathbf{y}_1^* \\ \mathbf{y}_2^* \end{bmatrix}.$$

According to VERBYLA (1990) this transformed data has distribution given by

$$\begin{bmatrix} \mathbf{y}_1^* \\ \mathbf{y}_2^* \end{bmatrix} \sim N \left(\begin{bmatrix} \boldsymbol{\beta} \\ \mathbf{0} \end{bmatrix}, \sigma_\epsilon^2 \begin{bmatrix} \mathbf{L}_1^T \mathbf{V} \mathbf{L}_1 & \mathbf{L}_1^T \mathbf{V} \mathbf{L}_2 \\ \mathbf{L}_2^T \mathbf{V} \mathbf{L}_1 & \mathbf{L}_2^T \mathbf{V} \mathbf{L}_2 \end{bmatrix} \right).$$

Hence, the density function of $\mathbf{L}^T \mathbf{y}$ can be written as the product of the conditional density of \mathbf{y}_1^* given \mathbf{y}_2^* and the marginal density of \mathbf{y}_2^* . The marginal distribution of \mathbf{y}_2^* is given by $\mathbf{y}_2^* \sim N(\mathbf{0}, \sigma_\epsilon^2 \mathbf{L}_2^T \mathbf{V} \mathbf{L}_2)$ and the marginal log-likelihood of \mathbf{y}_2^* using the result presented in Appendix II and omitting constant terms, is given by

$$\begin{aligned} \ell_R(\psi; \mathbf{y}_2^*) &\approx -\frac{1}{2} \left[(N_T - p - 1) \sigma_\epsilon^2 + \ln |\mathbf{L}_2^T \mathbf{V} \mathbf{L}_2| + \frac{1}{\sigma_\epsilon^2} \mathbf{y}_2^{*T} (\mathbf{L}_2^T \mathbf{V} \mathbf{L}_2)^{-1} \mathbf{y}_2^* \right] \\ &= -\frac{1}{2} \left[(N_T - p - 1) \sigma_\epsilon^2 + \ln |\mathbf{L}_2^T \mathbf{V} \mathbf{L}_2| + \frac{1}{\sigma_\epsilon^2} \mathbf{y}_2^{*T} \mathbf{L}_2 (\mathbf{L}_2^T \mathbf{V} \mathbf{L}_2)^{-1} \mathbf{L}_2^T \mathbf{y}_2^* \right] \\ &= -\frac{1}{2} \left[(N_T - p - 1) \sigma_\epsilon^2 + \ln |\mathbf{L}_2^T \mathbf{V} \mathbf{L}_2| + \frac{\mathbf{y}_2^{*T} \mathbf{P} \mathbf{y}_2^*}{\sigma_\epsilon^2} \right]. \end{aligned} \quad (2.10)$$

where $\psi = (\boldsymbol{\theta}_b, \boldsymbol{\theta}_\epsilon)$ is a vector containing all components of variance, and

$$\mathbf{P} = \mathbf{V}^{-1} - \mathbf{V}^{-1} \mathbf{X} (\mathbf{X}^T \mathbf{V}^{-1} \mathbf{X})^{-1} \mathbf{X}^T \mathbf{V}^{-1}.$$

The conditional distribution of \mathbf{y}_1^* given \mathbf{y}_2^* is

$$\mathbf{y}_1^* | \mathbf{y}_2^* \sim N \left(\boldsymbol{\beta} + \mathbf{L}_1^T \mathbf{V} \mathbf{L}_2 (\mathbf{L}_2^T \mathbf{V} \mathbf{L}_2)^{-1} \mathbf{y}_2^*, \sigma_\epsilon^2 \left(\mathbf{L}_1^T \mathbf{V} \mathbf{L}_1 - \mathbf{L}_1^T \mathbf{V} \mathbf{L}_2 (\mathbf{L}_2^T \mathbf{V} \mathbf{L}_2)^{-1} \mathbf{L}_2^T \mathbf{V} \mathbf{L}_1 \right) \right).$$

Using the result presented in Appendix II we can simplify the conditional variance-covariance matrix as following

$$\begin{aligned} &\mathbf{L}_1^T \mathbf{V} \mathbf{L}_1 - \mathbf{L}_1^T \mathbf{V} \mathbf{L}_2 (\mathbf{L}_2^T \mathbf{V} \mathbf{L}_2)^{-1} \mathbf{L}_2^T \mathbf{V} \mathbf{L}_1 \\ &= \mathbf{L}_1^T \left[\mathbf{V} - \mathbf{V} \mathbf{L}_2 (\mathbf{L}_2^T \mathbf{V} \mathbf{L}_2)^{-1} \mathbf{L}_2^T \mathbf{V} \right] \mathbf{L}_1 \\ &= \mathbf{L}_1^T \left\{ \mathbf{V} - \mathbf{V} \left[\mathbf{V}^{-1} - \mathbf{V}^{-1} \mathbf{X} (\mathbf{X}^T \mathbf{V}^{-1} \mathbf{X})^{-1} \mathbf{X}^T \mathbf{V}^{-1} \right] \mathbf{V} \right\} \mathbf{L}_1 \\ &= \mathbf{L}_1^T \mathbf{X} (\mathbf{X}^T \mathbf{V}^{-1} \mathbf{X})^{-1} \mathbf{X}^T \mathbf{L}_1 \\ &= (\mathbf{X}^T \mathbf{V}^{-1} \mathbf{X})^{-1}. \end{aligned}$$

Hence, the conditional distribution of \mathbf{y}_1^* given \mathbf{y}_2^* can be written as

$$\mathbf{y}_1^* | \mathbf{y}_2^* \sim N \left(\boldsymbol{\beta} + \mathbf{L}_1^T \mathbf{V} \mathbf{L}_2 (\mathbf{L}_2^T \mathbf{V} \mathbf{L}_2)^{-1} \mathbf{y}_2^*, \sigma_\epsilon^2 (\mathbf{X}^T \mathbf{V}^{-1} \mathbf{X})^{-1} \right),$$

and the conditional log-likelihood, omitting constant terms, is given by

$$\ell(\boldsymbol{\beta}, \boldsymbol{\psi}; \mathbf{y}_1^* | \mathbf{y}_2^*) = -\frac{1}{2} \left[N_T \ln \sigma_\epsilon^2 + \ln |(\mathbf{X}^T \mathbf{V}^{-1} \mathbf{X})^{-1}| + \frac{1}{\sigma_\epsilon^2} (\mathbf{y}_1^* - \boldsymbol{\beta} - \mathbf{L}_1^T \mathbf{V} \mathbf{L}_2 (\mathbf{L}_2^T \mathbf{V} \mathbf{L}_2)^{-1} \mathbf{y}_2^*)^T (\mathbf{X}^T \mathbf{V}^{-1} \mathbf{X}) (\mathbf{y}_1^* - \boldsymbol{\beta} - \mathbf{L}_1^T \mathbf{V} \mathbf{L}_2 (\mathbf{L}_2^T \mathbf{V} \mathbf{L}_2)^{-1} \mathbf{y}_2^*) \right].$$

As the marginal likelihood for \mathbf{y}_2^* contains no information on $\boldsymbol{\beta}$, so the conditional log-likelihood of \mathbf{y}_1^* given \mathbf{y}_2^* must be used. Thus, the differentiation $\ell(\boldsymbol{\beta}, \boldsymbol{\psi}; \mathbf{y}_1^* | \mathbf{y}_2^*)$ relative to $\boldsymbol{\beta}$ is given by

$$\frac{\partial \ell(\boldsymbol{\beta}, \boldsymbol{\psi}; \mathbf{y}_1^* | \mathbf{y}_2^*)}{\partial \boldsymbol{\beta}} = \frac{\mathbf{X}^T \mathbf{V}^{-1} \mathbf{X} (\mathbf{y}_1^* - \boldsymbol{\beta} - \mathbf{L}_1^T \mathbf{V} \mathbf{L}_2 (\mathbf{L}_2^T \mathbf{V} \mathbf{L}_2)^{-1} \mathbf{y}_2^*)}{\sigma_\epsilon^2}, \quad (2.11)$$

and equate to zero the expression (2.11) to get

$$\begin{aligned} \hat{\boldsymbol{\beta}} &= \mathbf{y}_1^* - \mathbf{L}_1^T \mathbf{V} \mathbf{L}_2 (\mathbf{L}_2^T \mathbf{V} \mathbf{L}_2)^{-1} \mathbf{y}_2^* \\ &= \mathbf{L}_1^T \mathbf{y} - \mathbf{L}_1^T \mathbf{V} \mathbf{L}_2 (\mathbf{L}_2^T \mathbf{V} \mathbf{L}_2)^{-1} \mathbf{L}_2^T \mathbf{y} \\ &= \mathbf{L}_1^T [\mathbf{I} - \mathbf{L}_1^T \mathbf{V} \mathbf{L}_2 (\mathbf{L}_2^T \mathbf{V} \mathbf{L}_2)^{-1} \mathbf{L}_2^T] \mathbf{y} \quad (\text{Using Appendix II}) \\ &= \mathbf{L}_1^T \mathbf{X} (\mathbf{X}^T \mathbf{V}^{-1} \mathbf{X})^{-1} \mathbf{X}^T \mathbf{V}^{-1} \mathbf{y} \\ &= (\mathbf{X}^T \mathbf{V}^{-1} \mathbf{X})^{-1} \mathbf{X}^T \mathbf{V}^{-1} \mathbf{y}, \end{aligned}$$

which is the best linear unbiased estimator (BLUE).

It is noteworthy that the BLUE will not be biased if the variance components were known because the log-likelihood of \mathbf{y}_1^* given \mathbf{y}_2^* is a function of $\boldsymbol{\beta}$ and $\boldsymbol{\psi}$. Therefore, when you have no information about the variance components an iterative process must be used for the joint estimation of the fixed effects and variance components.

To estimate $\boldsymbol{\psi}$, we use the marginal distribution of \mathbf{y}_2^* as given in expression (2.10). Note that as $f(\mathbf{L}^T \mathbf{y}; \boldsymbol{\beta}, \boldsymbol{\psi}) = f(\mathbf{y}_1^* | \mathbf{y}_2^*; \boldsymbol{\beta}, \boldsymbol{\psi}) f(\mathbf{y}_2^*; \boldsymbol{\psi})$, then the log-likelihood of $\mathbf{L}^T \mathbf{y}$ can be written as the sum of the conditional log-likelihood of \mathbf{y}_1^* given \mathbf{y}_2^* and the marginal log-likelihood of \mathbf{y}_2^* , that is

$$\ell(\boldsymbol{\beta}, \boldsymbol{\psi}; \mathbf{L}^T \mathbf{y}) = \ell(\boldsymbol{\beta}, \boldsymbol{\psi}; \mathbf{y}_1^* | \mathbf{y}_2^*) + \ell_R(\boldsymbol{\psi}; \mathbf{y}_2^*).$$

So, it is easy to see the following equality

$$\ln |\mathbf{L}^T \mathbf{V} \mathbf{L}| = \ln |(\mathbf{X}^T \mathbf{V}^{-1} \mathbf{X})^{-1}| + \ln |\mathbf{L}_2^T \mathbf{V} \mathbf{L}_2|$$

and hence

$$\begin{aligned} \ln |\mathbf{L}_2^T \mathbf{V} \mathbf{L}_2| &= \ln |\mathbf{L}^T \mathbf{V} \mathbf{L}| + \ln |\mathbf{X}^T \mathbf{V}^{-1} \mathbf{X}| \quad (\text{Using Theorem 1 of Appendix III}) \\ &= \ln |\mathbf{L}^T \mathbf{L}| + \ln |\mathbf{V}| + \ln |\mathbf{X}^T \mathbf{V}^{-1} \mathbf{X}|. \end{aligned}$$

Therefore, REML log-likelihood presented in expression (2.10), omitting constant terms, can be expressed as

$$\ell_R(\boldsymbol{\psi}; \mathbf{y}_2^*) = -\frac{1}{2} \left[(N_T - p - 1) \ln \sigma_\epsilon^2 + \ln |\mathbf{V}| + \ln |\mathbf{X}^T \mathbf{V}^{-1} \mathbf{X}| + \frac{\mathbf{y}_2^{*T} \mathbf{P} \mathbf{y}_2^*}{\sigma_\epsilon^2} \right]. \quad (2.12)$$

According to MEYER (1989) and KNIGHT (2008) it is computationally convenient to consider the following modification in the REML log-likelihood (2.12)

$$\ln |\mathbf{V}| + \ln |\mathbf{X}^T \mathbf{V}^{-1} \mathbf{X}| = \ln |\mathbf{V}^*| + \ln |\mathbf{G}| + \ln |\boldsymbol{\Sigma}|,$$

where $|\mathbf{V}^*| = |\mathbf{G}^{-1}| |\boldsymbol{\Sigma}^{-1}| |\mathbf{V}| |\mathbf{X}^T \mathbf{V}^{-1} \mathbf{X}|$. So, the REML log-likelihood can be rewritten as

$$\ell_R(\boldsymbol{\psi}; \mathbf{y}_2^*) = -\frac{1}{2} \left[(N_T - p - 1) \ln \sigma_\epsilon^2 + \ln |\mathbf{G}| + \ln |\boldsymbol{\Sigma}| + \ln |\mathbf{V}^*| + \frac{\mathbf{y}_2^{*T} \mathbf{P} \mathbf{y}_2^*}{\sigma_\epsilon^2} \right].$$

The REML estimator of σ_ϵ^2 is given by differentiating the REML log-likelihood in (2.13) with respect to σ_ϵ^2 . The expression of score function for σ_ϵ^2 is, then, given by

$$U(\sigma_\epsilon^2) = \frac{\partial \ell_R}{\partial \sigma_\epsilon^2} = -\frac{1}{2} \left[\frac{N_T - p - 1}{\sigma_\epsilon^2} - \frac{\mathbf{y}^T \mathbf{P} \mathbf{y}}{\sigma_\epsilon^4} \right].$$

Thus, the REML estimator of σ_ϵ^2 is obtained by equating $U(\sigma_\epsilon^2)$ to zero and solving for σ_ϵ^2 , resulting in

$$\hat{\sigma}_\epsilon^2 = \frac{\mathbf{y}^T \mathbf{P} \mathbf{y}}{N_T - p - 1}.$$

On the other hand, REML estimators for $\psi_w = (\theta_{b_1}, \theta_{b_2}, \dots, \theta_{b_{W_1}}, \theta_{\epsilon_{W_1+1}}, \theta_{\epsilon_{W_1+2}}, \dots, \theta_{\epsilon_{W_1+W_2}})$ are given by differentiating the REML log-likelihood in (2.12) with respect to ψ_w and solving for ψ_w . Then, the expression of score function for ψ_w is given by

$$U(\psi_w) = \frac{\partial \ell_R}{\partial \psi_w} = -\frac{1}{2} \left(\frac{\partial \ln |\mathbf{V}|}{\partial \psi_w} + \frac{\partial \ln |\mathbf{X}^T \mathbf{V}^{-1} \mathbf{X}|}{\partial \psi_w} + \frac{1}{\sigma_\epsilon^2} \frac{\partial \mathbf{y}^T \mathbf{P} \mathbf{y}}{\partial \psi_w} \right).$$

Using the Appendix II and definitions 2 and 3 of Appendix III, we can write the following result

$$\begin{aligned} \frac{\partial \ln |\mathbf{V}|}{\partial \psi_w} + \frac{\partial \ln |\mathbf{X}^T \mathbf{V}^{-1} \mathbf{X}|}{\partial \psi_w} &= \text{tr} \left(\mathbf{V}^{-1} \frac{\partial \mathbf{V}}{\partial \psi_w} \right) - \text{tr} \left[(\mathbf{X}^T \mathbf{V}^{-1} \mathbf{X})^{-1} \mathbf{X}^T \mathbf{V}^{-1} \frac{\partial \mathbf{V}}{\partial \psi_w} \mathbf{V}^{-1} \mathbf{X} \right] \\ &= \text{tr} \left(\mathbf{V}^{-1} \frac{\partial \mathbf{V}}{\partial \psi_w} \right) - \text{tr} \left[\mathbf{V}^{-1} \mathbf{X} (\mathbf{X}^T \mathbf{V}^{-1} \mathbf{X})^{-1} \mathbf{X}^T \mathbf{V}^{-1} \frac{\partial \mathbf{V}}{\partial \psi_w} \right] \\ &= \text{tr} \left[\left(\mathbf{V}^{-1} - \mathbf{V}^{-1} \mathbf{X} (\mathbf{X}^T \mathbf{V}^{-1} \mathbf{X})^{-1} \mathbf{X}^T \mathbf{V}^{-1} \right) \frac{\partial \mathbf{V}}{\partial \psi_w} \right] \\ &= \text{tr} \left(\mathbf{P} \frac{\partial \mathbf{V}}{\partial \psi_w} \right). \end{aligned}$$

Finally, using Appendix IV and $\mathbf{V} = \mathbf{Z} \mathbf{G} \mathbf{Z}^T + \boldsymbol{\Sigma}$, we can write the function score of ψ_w ($U(\psi_w)$) as

$$U(\psi_w) = -\frac{1}{2} \left[\text{tr} \left(\mathbf{P} \frac{\partial (\mathbf{Z} \mathbf{G} \mathbf{Z}^T + \boldsymbol{\Sigma})}{\partial \psi_w} \right) - \frac{1}{\sigma_\epsilon^2} \mathbf{y}^T \mathbf{P} \frac{\partial (\mathbf{Z} \mathbf{G} \mathbf{Z}^T + \boldsymbol{\Sigma})}{\partial \psi_w} \mathbf{P} \mathbf{y} \right]. \quad (2.13)$$

Estimators for variance components associated with the \mathbf{G} matrix can be obtained from the partial derivative of $U(\psi_w)$ with respect to $\theta_{b_{w_1}}$, with $w_1 = 1, 2, \dots, W_1$, and solving for $\theta_{b_{w_1}}$. Therefore, the expression (2.13) is reduced to

$$\begin{aligned} U(\theta_{b_{w_1}}) &= -\frac{1}{2} \left[\text{tr} \left(\mathbf{P} \frac{\partial (\mathbf{ZGZ}^T)}{\partial \theta_{b_{w_1}}} \right) - \frac{1}{\sigma_\epsilon^2} \mathbf{y}^T \mathbf{P} \frac{\partial (\mathbf{ZGZ}^T)}{\partial \theta_{b_{w_1}}} \mathbf{P} \mathbf{y} \right] \\ &= -\frac{1}{2} \left[\text{tr} \left(\mathbf{PZ} \frac{\partial \mathbf{G}}{\partial \theta_{b_{w_1}}} \mathbf{Z}^T \right) - \frac{1}{\sigma_\epsilon^2} \mathbf{y}^T \mathbf{PZ} \frac{\partial \mathbf{G}}{\partial \theta_{b_{w_1}}} \mathbf{Z}^T \mathbf{P} \mathbf{y} \right], \end{aligned}$$

using the Lemma 1 (Appendix III).

In the same direction, estimators for variance components associated with the Σ matrix can be obtained from the partial derivative of $U(\psi_w)$ with respect to $\theta_{\epsilon_{w_2}}$, with $w_2 = W_1 + 1, W_1 + 2, \dots, W_1 + W_2$, and solving for $\theta_{\epsilon_{w_2}}$. Then, the expression (2.13) is reduced to

$$U(\theta_{\epsilon_{w_2}}) = -\frac{1}{2} \left[\text{tr} \left(\mathbf{P} \frac{\partial \Sigma}{\partial \theta_{\epsilon_{w_2}}} \right) - \frac{1}{\sigma_\epsilon^2} \mathbf{y}^T \mathbf{P} \frac{\partial \Sigma}{\partial \theta_{\epsilon_{w_2}}} \mathbf{P} \mathbf{y} \right].$$

To estimate $\theta_{b_{w_1}}$ or $\theta_{\epsilon_{w_2}}$ we need to equate respectively $U(\theta_{b_{w_1}}) = 0$ and solve for θ_{b_w} or $U(\theta_{\epsilon_{w_2}}) = 0$ and solve for $\theta_{\epsilon_{w_2}}$. In general this cannot be done directly and an iterative scheme is required.

Several iterative methods for solving ML or REML equations have been proposed. Some of the main iterative methods are Newton-Raphson method which provides fast convergence, but extremely sensitive to initial values (MC LACHLAN and KRISHNAN, 1997), AI algorithm, which is based on average information matrix (\mathcal{I}_A) (GILMOUR, A; THOMSON, R; CULLIS, 1995), EM algorithm, which is very useful for missing, truncated or censored data (MC LACHLAN and KRISHNAN, 1997), PXEM algorithm, which has lower convergence time than EM algorithm (FOULLEY and VAN DYK, 2000) and BOBYQA algorithm, used for bound constrained optimization without derivatives (POWELL, 2009).

2.2.2 Selecting the covariance structure

The first step to select variance-covariance structures for random effects are related to experimental design structure, such as random effect of treatment, blocks etc. In repeated measures analysis, for example, the first step is to accommodate the covariation of measures on the same sampling unit. However, before this selection, fixed effects should be clearly specified (LITTELL *et al.*, 2000). We regard initially a saturated parameter specification for fixed effects considering main and interaction effects. The refinement of fixed effects should only be performed after selecting a satisfactory covariance structure.

Considering the parsimony principle, the covariance structure to representing \mathbf{V}_i matrix must have a relatively small number of parameters.

Parsimony: First, the central objective for parsimony is choosing the simplest possible structure. Thereby, the advantage of this approach is that the covariance structure is easy

to interpret and explain, being specified with a small number of unknown parameters. However, choosing a structure that is too-simple for the dataset may increase Type I error rates, while choosing a too-complex structure for the dataset may decrease the power of the test (increase Type II error) in selecting the fixed effects (MATUSCHEK *et al.*, 2017). On the other hand, a structure that is highly complex and requires estimation of many unknown parameters which could greatly hinder the interpretation of the covariance pattern provide poor predictions (VANDEKERCKHOVE *et al.*, 2014).

As the specification of the covariance structure for mixed model is done through \mathbf{G} and Σ_i , we presented some covariance structures that can be used to fit to the data. Since observations on different fruits are assumed independent, the structure will just take into account for covariance pattern of measurements on the same subject. Besides, as we assumed that repeated measurements are equally spaced, the covariance structure of Σ_i can be characterized in terms of variance and correlations expressed as a function of the time lag.

1. Variance components (VC)

$$\sigma^2 \mathbf{I}_K = \begin{bmatrix} \sigma^2 & 0 & \dots & 0 \\ 0 & \sigma^2 & \dots & 0 \\ \vdots & \vdots & \ddots & \vdots \\ 0 & 0 & \dots & \sigma^2 \end{bmatrix}.$$

The variance component structure (VC) is the simplest, where the correlation of errors within a subject are assumed to be 0. Sometimes, VC is important in the exploration process to get a sense of the effect of fitting more complex structures. Moreover, VC structure can not be realistic for most repeated measures data.

2. Heterogeneous variance components – VC_H :

$$\begin{bmatrix} \sigma_1^2 & 0 & \dots & 0 \\ 0 & \sigma_2^2 & \dots & 0 \\ \vdots & \vdots & \ddots & \vdots \\ 0 & 0 & \dots & \sigma_{n_i}^2 \end{bmatrix}.$$

This matrix has n_i parameters, where n_i denotes the order of the matrix, and it assumes different variances on the diagonal and non-correlated observations.

3. Compound symmetry (CS)

$$\sigma^2 \mathbf{I}_K + \sigma_1^2 \mathbf{J}_K = \begin{bmatrix} \sigma_1^2 + \sigma^2 & \sigma_1^2 & \dots & \sigma_1^2 \\ \sigma_1^2 & \sigma_1^2 + \sigma^2 & \dots & \sigma_1^2 \\ \vdots & \vdots & \ddots & \vdots \\ \sigma_1^2 & \sigma_1^2 & \dots & \sigma_1^2 + \sigma^2 \end{bmatrix}$$

This one is the simplest covariance structure that includes within-subject correlated errors. These correlations are presumed to be the same for each set of observations and may not be realistic for repeated measures data because for most repeated measurements the correlation between observations decreases as the time lag increases. This structure can

be specified in mixed models in terms of \mathbf{G} and $\boldsymbol{\Sigma}_i$ matrices. Besides, the \mathbf{V}_i matrix will have a CS structure when, for example, we specified $\mathbf{G} = \sigma_{\phi_0}^2 \mathbf{I}$ and $\boldsymbol{\Sigma}_i = \sigma_{\epsilon}^2 \mathbf{I}$.

4. Heterogeneous compound symmetry ($\text{CS}_{\mathbf{H}}$)

$$\begin{bmatrix} \sigma_1^2 & \rho\sigma_1\sigma_2 & \dots & \rho\sigma_1\sigma_{n_i} \\ \rho\sigma_1\sigma_2 & \sigma_2^2 & \dots & \rho\sigma_2\sigma_{n_i} \\ \vdots & \vdots & \ddots & \vdots \\ \rho\sigma_1\sigma_{n_i} & \rho\sigma_2\sigma_{n_i} & \dots & \sigma_{n_i}^2 \end{bmatrix}.$$

This matrix has $n_i + 1$ parameters, assuming different variances on the diagonal and including same correlation among them.

5. First order autoregressive structure (AR(1))

$$\sigma^2 \begin{bmatrix} 1 & \rho & \rho^2 & \dots & \rho^{n_i-1} \\ \rho & 1 & \rho & \dots & \rho^{n_i-2} \\ \rho^2 & \rho & 1 & \dots & \rho^{n_i-3} \\ \vdots & \vdots & \vdots & \ddots & \vdots \\ \rho^{n_i-1} & \rho^{n_i-2} & \rho^{n_i-3} & \dots & 1 \end{bmatrix}.$$

This structure considers correlations between observations that decreases systematically with time lag, which can be used when the observations are measured at equally spaced time intervals.

6. Heterogeneous first order autoregressive structure (AR(1) $_{\mathbf{H}}$)

$$\begin{bmatrix} \sigma_1^2 & \rho\sigma_1\sigma_2 & \rho^2\sigma_1\sigma_3 & \dots & \rho^{n_i-1}\sigma_1\sigma_{n_i} \\ \rho\sigma_1\sigma_2 & \sigma_2^2 & \rho\sigma_2\sigma_3 & \dots & \rho^{n_i-2}\sigma_2\sigma_{n_i} \\ \rho^2 & \rho & \sigma_3^2 & \dots & \rho^{n_i-2} \\ \vdots & \vdots & \vdots & \ddots & \vdots \\ \rho^{n_i-1}\sigma_1\sigma_{n_i} & \rho^{n_i-2}\sigma_2\sigma_{n_i} & \rho^{n_i-3}\sigma_3\sigma_{n_i} & \dots & \sigma_{n_i}^2 \end{bmatrix}.$$

This structure considers different variances and correlations between observations that decreases systematically with time lag, which can be used when observations are measured at equally spaced time intervals.

7. ‘Unstructured’ covariance structure (UN)

$$\begin{bmatrix} \sigma_1^2 & \sigma_{12} & \dots & \sigma_{1n_i} \\ \sigma_{12} & \sigma_2^2 & \dots & \sigma_{2n_i} \\ \vdots & \vdots & \ddots & \vdots \\ \sigma_{1n_i} & \sigma_{2n_i} & \dots & \sigma_{n_i}^2 \end{bmatrix}.$$

It is the most complex structure because its specifies no patterns in the covariance matrix, however, this generality introduces a disadvantage due to the large number of parameters.

Selection model procedure can be performed using AIC and BIC criteria when the models are nested or non-nested and by likelihood ratio test when the models are nested. The

AIC and BIC criteria proposed by AKAIKE (1974) and SCHWARZ (1978), respectively, are given by

$$AIC = -2\ell(\hat{\boldsymbol{\theta}}) + 2\omega$$

and

$$BIC = -2\ell(\hat{\boldsymbol{\theta}}) + 2\omega \ln N_T$$

where $\ell(\hat{\boldsymbol{\theta}})$ is the logarithm of likelihood function, N_T is the total number of observations, $N_T = \sum_{i=1}^N n_i$, and ω is the total number of parameter in $\boldsymbol{\theta}$, being $\boldsymbol{\theta} = (\boldsymbol{\beta}^T, \boldsymbol{\theta}_b^T, \boldsymbol{\theta}_\epsilon^T)^T$. These criteria are based on likelihood function and they are used as measure of goodness of fit. Their absolute values have no interpretation, but when we compare AIC or BIC values from different models, smaller values indicate a better fit model. These criteria were proposed to compare regression models which generally includes only the random effect of errors (σ_ϵ^2) and consequently ω is the total number of fixed effect parameters plus one, however, in the linear mixed effects models (LMEM), AIC and BIC criteria can be more complicated. According to VAIDA and BLANCHARD (2005), the marginal AIC criterion for LMEM is given by

$$AIC_m = -2\ell(\hat{\boldsymbol{\theta}}) + 2a_n\omega \quad (2.14)$$

where $a_n = 1$ or $a_n = N_T / (N_T - \omega - 1)$ in the finite sample form. The **lme** function (PINHEIRO *et al.*, 2017) uses AIC_m with $a_n = 1$ while the **SAS Proc Mixed** (SAS INSTITUTE INC., 2011) uses both asymptotic and finite sample forms. On the other hand, the conditional AIC depends on the prediction of \boldsymbol{b} as well as the estimation of $\boldsymbol{\theta}$. When variance components parameters $\boldsymbol{\theta}_b$ and $\boldsymbol{\theta}_\epsilon$ are known, PINHEIRO and BATES (2000) and VERBEKE and MOLENBERGHS (2009) suggest the use of the best linear unbiased predictor (BLUP)

$$\tilde{\boldsymbol{b}}(\boldsymbol{\theta}_b, \boldsymbol{\theta}_\epsilon) = \mathbf{G}\mathbf{Z}^T \mathbf{V}^{-1} [\mathbf{y} - \mathbf{X}\hat{\boldsymbol{\beta}}(\boldsymbol{\theta}_b, \boldsymbol{\theta}_\epsilon)]$$

where $\boldsymbol{\beta}$ is the generalized least squares estimator, defined by VERBEKE and MOLENBERGHS (2009) as

$$\hat{\boldsymbol{\beta}}(\boldsymbol{\theta}_b, \boldsymbol{\theta}_\epsilon) = (\mathbf{X}^T \mathbf{V}^{-1} \mathbf{X})^{-1} \mathbf{X}^T \mathbf{V}^{-1} \mathbf{y}.$$

When $\boldsymbol{\theta}_b$ and $\boldsymbol{\theta}_\epsilon$ are unknown, we use an estimated BLUP (EBLUP) $\tilde{\boldsymbol{b}} = \tilde{\boldsymbol{b}}(\hat{\boldsymbol{\theta}}_b, \hat{\boldsymbol{\theta}}_\epsilon)$. Then, the generalized least squares estimator $\hat{\boldsymbol{\beta}}(\boldsymbol{\theta}_b, \boldsymbol{\theta}_\epsilon)$ and the BLUP $\tilde{\boldsymbol{b}}(\boldsymbol{\theta}_b, \boldsymbol{\theta}_\epsilon)$ can be obtained as the solution of Henderson's mixed model equation (HENDERSON, 1950)

$$\begin{bmatrix} \mathbf{X}^T \boldsymbol{\Sigma}^{-1} \mathbf{X} & \mathbf{X}^T \boldsymbol{\Sigma}^{-1} \mathbf{Z} \\ \mathbf{Z}^T \boldsymbol{\Sigma}^{-1} \mathbf{X} & \mathbf{Z}^T \boldsymbol{\Sigma}^{-1} \mathbf{Z} + \mathbf{G}^{-1} \end{bmatrix} \begin{bmatrix} \hat{\boldsymbol{\beta}}(\boldsymbol{\theta}_b, \boldsymbol{\theta}_\epsilon) \\ \tilde{\boldsymbol{b}}(\boldsymbol{\theta}_b, \boldsymbol{\theta}_\epsilon) \end{bmatrix} = \begin{bmatrix} \mathbf{X}^T \boldsymbol{\Sigma}^{-1} \mathbf{y} \\ \mathbf{Z}^T \boldsymbol{\Sigma}^{-1} \mathbf{y} \end{bmatrix}.$$

Hence, these equations can be rewritten as $\mathbf{X}\hat{\boldsymbol{\beta}}(\boldsymbol{\theta}_b, \boldsymbol{\theta}_\epsilon) + \mathbf{Z}\tilde{\boldsymbol{b}}(\boldsymbol{\theta}_b, \boldsymbol{\theta}_\epsilon) = \mathbf{H}(\boldsymbol{\theta}_b, \boldsymbol{\theta}_\epsilon)\mathbf{y}$, where

$$\mathbf{H}(\boldsymbol{\theta}_b, \boldsymbol{\theta}_\epsilon) = (\mathbf{X}, \mathbf{Z}) \begin{bmatrix} \mathbf{X}^T \boldsymbol{\Sigma}^{-1} \mathbf{X} & \mathbf{X}^T \boldsymbol{\Sigma}^{-1} \mathbf{Z} \\ \mathbf{Z}^T \boldsymbol{\Sigma}^{-1} \mathbf{X} & \mathbf{Z}^T \boldsymbol{\Sigma}^{-1} \mathbf{Z} + \mathbf{G}^{-1} \end{bmatrix}^{-1} \begin{bmatrix} \mathbf{X}^T \boldsymbol{\Sigma}^{-1} \\ \mathbf{Z}^T \boldsymbol{\Sigma}^{-1} \end{bmatrix}$$

is the “hat” matrix. Particularly, when $\boldsymbol{\theta}_b$ and $\boldsymbol{\theta}_\epsilon$ are known, the effective number of degrees of freedom is

$$\begin{aligned} gl(\boldsymbol{\theta}_b, \boldsymbol{\theta}_\epsilon) &= \text{trace}[\mathbf{H}(\boldsymbol{\theta}_b, \boldsymbol{\theta}_\epsilon)] \\ &= \text{trace}\left[(\mathbf{X}^T \mathbf{V}^{-1} \mathbf{X})^{-1} \mathbf{X}^T \mathbf{V}^{-1} \boldsymbol{\Sigma} \mathbf{V}^{-1} \mathbf{X}\right] + N_T - \text{trace}[\boldsymbol{\Sigma} \mathbf{V}^{-1}] \end{aligned}$$

which is used in estimating $\boldsymbol{\beta}$ and predict \mathbf{b} (HODGES and SARGENT, 2001). According to VAIDA and BLANCHARD (2005) and MÜLLER *et al.* (2013) the effective number of degrees of freedom satisfies

$$(p+1) \leq gl(\boldsymbol{\theta}_b, \boldsymbol{\theta}_\epsilon) \leq (p+1) + N(p+1),$$

that is, the $gl(\boldsymbol{\theta}_b, \boldsymbol{\theta}_\epsilon)$ is between the number of degrees of freedom of the regression model without \mathbf{b} and the regression model treating \mathbf{b} as fixed effects.

Thus, we can obtain the conditional AIC criteria as minus twice the conditional log-likelihood plus a penalty and it can be written as

$$AICc = -2\ell(\widehat{\boldsymbol{\theta}}|\widetilde{\mathbf{b}}) + 2\alpha_{re}$$

where α_{re} is the dimension of parameter space to associate with random effects, that is, $\alpha_{re} = \text{trace}[\mathbf{P}^*] + p + 1$, \mathbf{P}^* being the projection matrix given by

$$\mathbf{P}^* = \sigma_\epsilon \mathbf{V}^{-\frac{1}{2}} + (\mathbf{I} - \sigma_\epsilon \mathbf{V}^{\frac{1}{2}}) \mathbf{X} (\mathbf{X}^T \mathbf{V}^{-1} \mathbf{X})^{-1} \mathbf{X}^T \mathbf{V}^{-1}$$

and $p + 1$ was included to accommodate the effect of estimating $\boldsymbol{\theta}_b$ and $\boldsymbol{\theta}_\epsilon$ (BURNHAM and WHITE, 2002). For small samples, BURNHAM and WHITE (2002) proposed a corrected version of $AICc$ as

$$-2\ell(\widehat{\boldsymbol{\theta}}|\widetilde{\mathbf{b}}) + 2\alpha_{re} + 2 \frac{\alpha_{re}(\alpha_{re} + 1)}{N_T + (\alpha_{re} - 1)}.$$

It is noteworthy that $AICc$ is based on maximum likelihood method. Other criteria based on methods of maximum likelihood and restricted maximum likelihood were presented by MÜLLER *et al.* (2013).

When the models are nested, we can use the likelihood ratio test (LRT) to compare a more general model with a more specific model. Suppose that random vector \mathbf{Y} has a probability distribution that is described by an unknown parameter $\boldsymbol{\theta}$, whose probability density function is $f(\mathbf{y}, \boldsymbol{\theta})$. As some of these parameters may be nuisance parameters, the null hypothesis that we wish verify is $H_0 : \boldsymbol{\theta} \in \boldsymbol{\Theta}_0$ and the alternative hypothesis is $H_1 : \boldsymbol{\theta} \in \boldsymbol{\Theta}_0^c$, where $\boldsymbol{\Theta}_0$ is a specified subset of the parameter space $\boldsymbol{\Theta}$. Let $\mathbf{Y}_1, \mathbf{Y}_2, \dots, \mathbf{Y}_N$ be a n_i -dimensional independent continuous random vectors with joint distribution f given by

$$f(\mathbf{y}_1, \mathbf{y}_2, \dots, \mathbf{y}_N; \boldsymbol{\theta}) = f(\mathbf{y}_1, \boldsymbol{\theta}) \times f(\mathbf{y}_2, \boldsymbol{\theta}) \times \dots \times f(\mathbf{y}_N, \boldsymbol{\theta}).$$

Thus, the likelihood function can be written as

$$L(\boldsymbol{\theta}; \mathbf{y}) = \prod_{i=1}^N L(\boldsymbol{\theta}, \mathbf{y}_i).$$

Let $L(\hat{\Theta}_0)$ denote the maximum (actually the supreme) of the likelihood function for all $\theta \in \Theta_0$, that is, $L(\hat{\Theta}_0) = \max_{\theta \in \Theta_0} L(\theta)$ that represents the best explanation for the observed data for all $\theta \in \Theta_0$. Similarly, $L(\hat{\Theta}) = \max_{\theta \in \Theta} L(\theta)$ represents the best explanation for the observed data for all $\theta \in \Theta = \Theta_0 \cup \Theta_0^c$. Then, if $L(\hat{\Theta}_0) = L(\hat{\Theta})$ a best explanation for the observed data can be found inside Θ_0 , that is, we should not reject the null hypothesis H_0 . However, if $L(\hat{\Theta}_0) < L(\hat{\Theta})$ the best explanation for the observed data can be found inside Θ_0^c , that is, we should reject the null hypothesis H_0 . Thus, the likelihood ratio ($LR(\mathbf{y})$), which is a generalization of the optimal test for simple null and alternative hypotheses, developed by NEYMAN and PEARSON (1928), can be defined as

$$LR = \frac{\max_{\theta \in \Theta_0} L(\theta; \mathbf{y})}{\max_{\theta \in \Theta} L(\theta; \mathbf{y})} = \frac{L(\hat{\Theta}_0)}{L(\hat{\Theta})}.$$

According to WACKERLY *et al.* (2008), the likelihood ratio method does not always produce a statistical test with a known probability distribution, however, if the sample size is large, we can obtain an approximation to the distribution of LR if some regularity conditions are satisfied. These regularity conditions mainly involve the existence of derivatives of likelihood function with respect to the parameters θ , and it does not depend on unknown parameter values. Let $\mathbf{Y}_1, \mathbf{Y}_2, \dots, \mathbf{Y}_N$ have joint likelihood function $L(\theta)$.

Let ω_0 denote the number of free parameters that are specified by $H_0 : \theta \in \Theta_0$ and let ω_1 denote the number of free parameters specified by the statement $\theta \in \Theta$ (WACKERLY *et al.*, 2008). Then, for large N_T , $-2\ln(LR)$ has approximately a χ^2 distribution with $\omega_0 - \omega_1$ number of degree of freedom. Therefore, the likelihood ratio statistic is given by

$$\begin{aligned} -2\ln(LR) &= -2 \{ \ln[\max_{\theta \in \Theta_0} L(\theta; \mathbf{y})] - \ln[\max_{\theta \in \Theta} L(\theta; \mathbf{y})] \} \\ &= 2 \{ \ln[\max_{\theta \in \Theta} L(\theta; \mathbf{y})] - \ln[\max_{\theta \in \Theta_0} L(\theta; \mathbf{y})] \}. \end{aligned}$$

As the $-2\ln(LR)$ is a decreasing function of LR , rejection regions (RR) may be written as $RR : \{LR < \omega\}$, taking the logarithm of both sides in this inequality the RR may be rewritten as $RR : \{-2\ln(LR) > -2\ln(\omega) = \omega^*\}$. Therefore, for large sample sizes, $\omega^* \approx \chi_{\omega_0 - \omega_1}^2$ with a significance level of α . That is, the rejection region is given by

$$-2\ln(LR) > \chi_{\omega_0 - \omega_1}^2, \quad \text{with a significance level of } \alpha.$$

2.3 Prediction of random effects

The prediction of random effects are not obtained directly by likelihood estimation, but can be obtained by an extension of Gauss-Markov theorem or by empirical Bayesian methods indicating prior information about the mean and random effects (HARVILLE, 1976; LAIRD and WARE, 1982). Thus, the BLUP is given by

$$\tilde{\mathbf{b}}_i = \mathbf{GZ}_i^T \mathbf{V}_i^{-1} (\mathbf{y}_i - \mathbf{X}_i \hat{\beta}).$$

Since $\hat{\beta}$ and \tilde{b}_i are linear function of \mathbf{y} , LAIRD and WARE (1982) showed that their standard errors are derived as

$$Var(\hat{\beta}) = \left[\sum_{i=1}^N \mathbf{X}_i^T \mathbf{V}_i^{-1} \mathbf{X}_i \right]^{-1}$$

and

$$Var(\tilde{b}_i) = \mathbf{G} \mathbf{Z}_i^T \left\{ \mathbf{V}_i^{-1} - \mathbf{V}_i^{-1} \mathbf{X}_i \left[\sum_{i=1}^N \mathbf{X}_i^T \mathbf{V}_i^{-1} \mathbf{X}_i \right]^{-1} \mathbf{X}_i^T \mathbf{V}_i^{-1} \right\} \mathbf{Z}_i \mathbf{G}. \quad (2.15)$$

When the expression (2.15) is used to assess the error estimation, LAIRD and WARE (1982) suggest the use of

$$Var(\tilde{b}_i - b_i) = \mathbf{G} - \mathbf{G} \mathbf{Z}_i^T \mathbf{V}_i^{-1} \mathbf{Z}_i \mathbf{G} + \mathbf{G} \mathbf{Z}_i^T \mathbf{V}_i^{-1} \mathbf{X}_i \left(\sum_{i=1}^N \mathbf{X}_i^T \mathbf{V}_i \mathbf{X}_i \right)^{-1} \mathbf{X}_i^T \mathbf{V}_i^{-1} \mathbf{Z}_i \mathbf{G}$$

proposed by HARVILLE (1976), because the expression (2.15) ignores the variation of b_i . HARVILLE (1976) also demonstrated that when b_i has multivariate normal distribution, $E[b_i | (\mathbf{y}_i - \mathbf{X}_i \beta)] = E[b_i | \tilde{b}_i] = \tilde{b}_i$ with probability 1, and $Var[b_i | (\mathbf{y}_i - \mathbf{X}_i \beta)] = Var[b_i | \tilde{b}_i] = Var[\tilde{b}_i - b_i]$. Thus, these authors conclude that the distribution of b_i , conditional on the vector of marginal residuals $(\mathbf{y} - \mathbf{X}_i \hat{\beta})$, is the same as the distribution of b_i , conditional on q linear functions of residuals which comprise a BLUE of \tilde{b} .

2.4 Conditional test for fixed effect parameters

After covariance structure is satisfactorily modeled, we perform the fixed effect selection procedure that can be carried using the conditional F -test. The conditional F -test for fixed effect parameters tests the general linear hypothesis given by

$$H_0 : \mathbf{C}\beta = 0 \quad \text{versus} \quad H_1 : \mathbf{C}\beta \neq 0 \quad (2.16)$$

where \mathbf{C} is a known matrix. When we test, for example, $H_0 : \mu = 0$ versus $H_a : \mu \neq 0$, \mathbf{C} matrix has the form $\mathbf{C} = [1, 0, 0, \dots, 0]$. According to VERBEKE and MOLENBERGHS (2009), the F -statistic is defined by

$$F = \frac{\left(\hat{\beta} - \beta \right)^T \mathbf{C}^T \left[\mathbf{C} \left(\sum_{i=1}^N \mathbf{X}_i^T \hat{\mathbf{V}}_i^{-1} \mathbf{X}_i \right)^{-1} \mathbf{C}^T \right]^{-1} \mathbf{C} \left(\hat{\beta} - \beta \right)}{rank(\mathbf{C})}, \quad (2.17)$$

and follows an approximate F distribution, with numerator degrees of freedom equal to the rank of \mathbf{C} matrix and denominator degrees of freedom needs to be estimated from the data. There are several methods for estimating the appropriate number of denominator degrees of freedom as, for example, Satterthwaite approximation.

According to PINHEIRO and BATES (2000), the conditional *F*-test is better than LRT for assessing the significance of fixed effect parameters, since p-values from the *F*-test are more realistic. The conditional *F*-test are implemented in `anova.lme` method of `nlme` package (PINHEIRO and BATES, 2000) available in R environment software (R CORE TEAM, 2017).

2.5 The top-down strategy

The aim of model selection is to find the simplest model with the best fit for the dataset, but there are several ways of fitting a linear mixed model. Thus, we will use, in this thesis, the top-down strategy, as performed in VERBEKE and MOLENBERGHS (2009) and WEST *et al.* (2015). The first step involves starting with a saturated fixed effects model, called the model with the loaded mean structure. The second step involves selecting a structure for random effects in the model by performing REML-based likelihood ratio test for nested models or through AIC or BIC criteria for non-nested models. The third step involves the selection of a covariance structure for residuals in the model by performing REML-based likelihood ratio test for nested models or through the AIC or BIC criteria for non-nested models. This steps can be performed using the `anova.lme` (PINHEIRO and BATES, 2000).

After selecting the structure for Σ_i , it can be performed a new selection for \mathbf{G} matrix to simplify the previously selected structure. Finally, the last step involves using appropriate statistical tests to determine whether certain fixed-effect parameters are needed in the model. Moreover, to determine whether each of the fixed effect should be included in the model it can use the conditional F-test made available in `anova.lme` (PINHEIRO and BATES, 2000).

References

- ABBOTT, J. A., 1999 Quality measurement of fruits and vegetables. Postharvest Biology and Technology **15**: 207–225.
- AKAIKE, H., 1974 A New Look at the Statistical Model Identification. IEEE Transactions on automatic control **19**: 716—723.
- AVILA, F., M. MORA, M. OYARCE, A. ZUÑIGA, and C. FREDES, 2015 A method to construct fruit maturity color scales based on support machines for regression: Application to olives and grape seeds. Journal of Food Engineering **162**: 9–17.
- BARNHART, H. X. and J. M. WILLIAMSON, 2001 Modeling concordance correlation via GEE to evaluate reproducibility. Biometrics **57**: 931–940.
- BRON, I. U. and A. P. JACOMINO, 2006 Ripening and quality of ‘Golden’ papaya fruit harvested at different maturity stages. Brazilian Journal of Plant Physiology **18**: 389–396.
- BROSNAN, T. and D.-W. SUN, 2002 Inspection and grading of agricultural and food products by computer vision systemsa review. Computers and Electronics in Agriculture **36**: 193–213.

- BURNHAM, K. P. and G. C. WHITE, 2002 Evaluation of some random effects methodology applicable to bird ringing data. *Journal of Applied Statistics* **29**: 245–264.
- CARRASCO, J. L. and L. JOVER, 2003 Estimating the Generalized Concordance Correlation Coefficient through Variance Components. *Biometrics* **59**: 849–858.
- CARRASCO, J. L., T. S. KING, and V. M. CHINCHILLI, 2009 The concordance correlation coefficient for repeated measures estimated by variance components. *Journal of biopharmaceutical statistics* **19**: 90–105.
- CHÁVEZ-SÁNCHEZ, I., A. CARRILLO-LÓPEZ, M. VEGA-GARCÍA, and E. M. YAHIA, 2013 The effect of antifungal hot-water treatments on papaya postharvest quality and activity of pectinmethyl esterase and polygalacturonase. *Journal of Food Science and Technology* **50**: 101–107.
- CHINCHILLI, V. M., J. K. MARTEL, S. KUMANYIKA, and T. LLOYD, 1996 A Weighted Concordance Correlation Coefficient for Repeated Measurement Designs. *Biometrics* **52**: 341–353.
- CHITARRA, M. I. F. and A. D. CHITARRA, 2005 *Pós-colheita de frutos e hortaliças - Fisiologia e Manuseio*. Universidade Federal de Lavras, Lavras, second edition.
- COMMISSION INTERNATIONALE DE L'ECLAIRAGE, 2007 Colorimetry - Part 4 : CIE 1976 L * a * b * colour space. Technical report, Commission Internationale de l'Eclairage, Vienna.
- DA SILVA, M. G., J. G. OLIVEIRA, A. P. VITORIA, S. F. CORRÊA, M. G. PEREIRA, E. CAMPOSTRINI, E. O. SANTOS, A. CAVALLI, and H. VARGAS, 2005 Correlation between ethylene emission and skin colour changes during papaya (*Carica papaya* L.) fruit ripening. *Journal de Physique IV* **125**: 877–879.
- DARRIGUES, A., J. HALL, E. V. D. KNAAP, D. M. FRANCIS, N. DUJMOVIC, and S. GRAY, 2008 Tomato Analyzer-color Test : A New Tool for Efficient Digital Phenotyping. *Journal of the American Society for Horticultural Science* **133**: 579–586.
- EMBRAPA, 2012 Produção brasileira de mamão em 2012. Technical report, Empresa Brasileira de Pesquisa Agropecuária, Brasília.
- FIORAVANÇO, J. C., M. C. PAIVA, R. I. N. DE. CARVALHO, and I. MANICA, 1994 Características do mamão Formosa comercializado em Porto Alegre de outubro/91 a junho/92. *Ciência Rural* **24**: 519–522.
- FITZMAURICE, G., M. DAVIDIAN, G. VERBEKE, and G. MOLENBERGHS, 2009 *Longitudinal data analysis*. Chapman & Hall/CRC, New York, first edition.
- FONSECA, M. J. O., N. R. LEAL, S. A. CENCI, P. R. CECON, R. E. BRESSAN-SMITH, and J. M. S. BALBINO, 2007 Evolução dos pigmentos durante o amadurecimento de mamão “sunrise solo” e “golden”. *Revista Brasileira de Fruticultura* **29**: 451–455.

- FOULLEY, J.-L. and D. A. VAN DYK, 2000 The PX-EM algorithm for fast stable fitting of Henderson's mixed model. *Genetics, selection, evolution : GSE* **32**: 143–163.
- GILMOUR, A; THOMSON, R; CULLIS, B., 1995 Average Information REML: An efficient algorithm for variance estimation in linear mixed models. *Biometrics* **20**: 1440–1450.
- GUZMÁN, E., V. BAETEN, J. A. F. PIERNA, and J. A. GARCÍA-MESA, 2013 Determination of the olive maturity index of intact fruits using image analysis. *Journal of Food Science and Technology* **52**: 1–9.
- HARVILLE, D., 1976 Extension of the Gauss-Markov Theorem to Include the Estimation of Random Effects. In *The Annals of Statistics*, volume 4, pp. 384–395, Rockville, Institute of Mathematical Statistics.
- HARVILLE, D. A., 1974 Bayesian inference for variance components using only error contrasts. *Biometrika* **61**: 383–385.
- HARVILLE, D. A., 1977 Maximum Likelihood Approaches to Variance Component Estimation and to Related Problems. *Journal of the American Statistical Association* **72**: 320–338.
- HENDERSON, C. R., 1950 Estimation of genetic parameters. In *Ann. Math. Statist.* **21**, pp. 309–310.
- HODGES, J. S. and D. J. SARGENT, 2001 Counting degrees of freedom in hierarchical and other richly-parameterised models. *Biometrika* **88**: 367–379.
- KHENG, T. Y., P. DING, and N. A. A. RAHMAN, 2011 Physical and cellular structure changes of Rastali banana (*Musa AAB*) during growth and development. *Scientia Horticulturae* **129**: 382–389.
- KING, T. S. and V. M. CHINCHILLI, 2001 A generalized concordance correlation coefficient for continuous and categorical data. *Statistics in Medicine* **20**: 2131–2147.
- KING, T. S., V. M. CHINCHILLI, K.-L. WANG, and J. L. CARRASCO, 2007 A class of repeated measures concordance correlation coefficients. *Journal of biopharmaceutical statistics* **17**: 653–672.
- KNIGHT, E., 2008 *Improved iterative schemes for REML estimation of variance parameters in linear mixed models..* Ph.D. thesis, The University of Adelaide.
- LAIRD, N. M. and J. H. WARE, 1982 Random-effects models for longitudinal data. *Biometrics* **38**: 963–974.
- LIN, L. I., 1989 A Concordance Correlation Coefficient to Evaluate Reproducibility. *Biometrics* **45**: 255–268.

- LITTELL, R. C., J. PENDERGAST, and R. NATARAJAN, 2000 Modelling covariance structure in the analysis of repeated measures data. *Statistics in Medicine* **19**: 1793–1819.
- LOVERA, N., L. RAMALLO, and V. SALVADORI, 2014 Effect of Processing Conditions on Calcium Content, Firmness, and Color of Papaya in Syrup. *Journal of Food Processing* **2014**: 8.
- MANNINEN, H., M. PAAKKI, A. HOPIA, and R. FRANZÉN, 2015 Measuring the green color of vegetables from digital images using image analysis. *LWT - Food Science and Technology* **63**: 1184–1190.
- MARTINS, D. R., N. C. BARBOSA, and E. D. D. RESENDE, 2014 Respiration rate of Golden papaya stored under refrigeration and with different controlled atmospheres. *Scientia Agricola* **71**: 345–355.
- MATUSCHEK, H., R. KLIegl, S. VASISHTH, H. BAAYEN, and D. BATES, 2017 Balancing Type I Error and Power in Linear Mixed Models. *Journal of Memory and Language* **94**: 305–315.
- McLACHLAN, G. J. and T. KRISHNAN, 1997 *The EM Algorithm and Extensions*, volume 274. John Wiley & Sons, New York, first edition.
- MENDOZA, F. and J. M. AGUILERA, 2004 Application of image analysis for classification of ripening bananas. *Journal of food science* **69**: 471–477.
- MEYER, K., 1989 Restricted maximum likelihood to estimate variance components for animal models with several random effects using a derivative-free algorithm. *Genetics Selection Evolution* **21**: 317–340.
- MINOLTA, 1991 *Chroma meter instruction manual*. Minolta Company, Japan.
- MÜLLER, S., J. L. SCEALY, and A. H. WELSH, 2013 Model Selection in Linear Mixed Models. *Statistical Science* **28**: 135–167.
- MUNSELL COLOR COMPANY, 1952 *Munsell color charts for plant tissues*. Munsell Color Company, Baltimore.
- NEYMAN, J. and E. S. PEARSON, 1928 On the Use and Interpretation of Certain Test Criteria for Purposes of Statistical Inference: Part I. *Biometrika* **20A**: 175–240.
- NI, X., D. ZHANG, and H. H. ZHANG, 2010 Variable Selection for Semiparametric Mixed Models in Longitudinal Studies. *Biometrics* **66**: 79–88.
- OLIVEIRA, M. A. B., R. VIANNI, G. SOUZA, and T. M. R. ARAÚJO, 2002 Caracterização do estádio de maturação do papaia ‘Golden’. *Revista Brasileira de Fruticultura* **24**: 559–561.
- OLIVEIRA, T. P., S. S. ZOCCHI, and A. P. JACOMINO, 2017 Measuring color hue in Sunrise Solo’ papaya using a flatbed scanner. *Revista Brasileira de Fruticultura* **39**.

- O'SULLIVAN, M. G., D. V. BYRNE, H. MARTENS, L. H. GIDSKEHAUG, H. J. ANDERSEN, and M. MARTENS, 2003 Evaluation of pork colour: Prediction of visual sensory quality of meat from instrumental and computer vision methods of colour analysis. *Meat Science* **65**: 909–918.
- PATTERSON, H. D. and R. THOMPSON, 1971 Recovery of inter-block information when block sizes are unequal. *Biometrika* **58**: 545–554.
- PINHEIRO, J., D. BATES, S. DEBROY, D. SARKAR, and R CORE TEAM, 2017 nlme: linear and nonlinear mixed effects models.
- PINHEIRO, J. C. and D. M. BATES, 2000 *Mixed-Effects Models in S and S-PLUS*. Springer, New York.
- POWELL, M., 2009 The BOBYQA algorithm for bound constrained optimization without derivatives. Technical report, Centre for Mathematical Sciences, Cambridge.
- R CORE TEAM, 2017 The R environment.
- SANCHO, L. E. G., E. M. YAHIA, M. A. MARTÍNEZ-TÉLLEZ, and G. A. GONZÁLEZ-AGUILAR, 2010 Effect of Maturity Stage of Papaya Maradol on Physiological and Biochemical Parameters. *American Journal of Agricultural and Biological Science* **5**: 194–203.
- SAS INSTITUTE INC., 2011 Base SAS 9.3 procedures guide.
- SCHANDA, J., 1996 Cie colorimetry and colour displays. In *Color and Imaging Conference*, pp. 230–234, Society for Imaging Science and Technology.
- SCHWARZ, G., 1978 Estimating the dimension of a model. *The Annals of Statistics* **2**: 461—464.
- SCHWEIGGERT, R. M., C. B. STEINGASS, A. HELLER, P. ESQUIVEL, and R. CARLE, 2011 Characterization of chromoplasts and carotenoids of red- and yellow-fleshed papaya (*Carica papaya* L.). *Planta* **234**: 1031–1044.
- SECRETARIA DA AGRICULTURA, PECUÁRIA, IRRIGAÇÃO, PESCA E AQUICULTURA, 2014 Exportações brasileiras de mamão registram crescimento em setembro. Technical report.
- SILVA-AYALA, T., R. J. SCHNELL, A. W. MEEROW, M. WINTERSTEIN, C. CERVANTES, and J. S. BROWN, 2005 Determination of Color and Fruit Traits of Half-Sib Families of Mango (*Mangifera Indica* L.). *Proceedings of the Florida State Horticultural Society* **118**: 253–257.
- SINGH, N., M. J. DELWICHE, and R. JOHNSON, 1993 Image analysis methods for real-time color grading of stonefruit. *Computers and Electronics in Agriculture* **9**: 71–84.
- SMEULDERS, A. W. M., M. WORRING, S. SANTINI, A. GUPTA, and R. JAIN, 2000 Content-based image retrieval at the end of the early years. *IEEE Transactions in Pattern Analysis and Machine Intelligence* **22**: 1349–1380.

- VAIDA, F. and S. BLANCHARD, 2005 Conditional Akaike information for mixed-effects models. *Biometrika* **92**: 351–370.
- VANDEKERCKHOVE, J., D. MATZKE, and E.-J. WAGENMAKERS, 2014 Model comparison and the principle of parsimony. *Oxford Handbook of pp. 1–29*.
- VERBEKE, G. and G. MOLENBERGHS, 2009 *Linear mixed models for longitudinal data*. Springer Verlag, Nova York.
- VERBYLA, A., 1990 A conditional derivation of residual maximum likelihood. *Austalian Journal of Statistics* **32**: 227–230.
- WACKERLY, D. D., W. MENDENHALL III, and R. L. SCHEAFFER, 2008 *Mathematical statistics with applications*. Thomson Brooks/Cole, Belmont, 7th edition.
- WEST, B., K. B. WELCH, and A. T. GALECKI, 2015 *Linear Mixed Models: A Practical Guide Using Statistical Software*. CRC Press, New York, second edition.
- WU, D. and D. W. SUN, 2013 Colour measurements by computer vision for food quality control - A review. *Trends in Food Science and Technology* **29**: 5–20.
- YAM, K. L. and S. E. PAPADAKIS, 2004 A simple digital imaging method for measuring and analyzing color of food surfaces. *Journal of Food Engineering* **61**: 137–142.

3 LONGITUDINAL CONCORDANCE CORRELATION FUNCTION BASED ON VARIANCE COMPONENTS: AN APPLICATION IN FRUIT COLOR ANALYSIS

Abstract: The maturity stages of papaya fruit based on peel color is frequently characterized from a sample of four points on the equatorial region measured by a colorimeter. However, this procedure may not be suitable for assessing the papaya's overall mean color and an alternative proposal is to use image acquisition of the whole fruit's peel. Questions of interest are whether a sample on the equatorial region can reproduce a sample over the whole peel region and if the colorimeter can compete with a scanner, or digital camera, in measuring the mean hue over time. The reproducibility can be verified by using the concordance correlation for responses measured on a continuous scale. Thus, in this work we propose a longitudinal concordance correlation (LCC), based on a mixed-effects regression model, to estimate agreement over time among pairs of observations obtained from different combinations between measurement method and sampled peel region. The results show that the papaya's equatorial region is not representative of the whole peel region, suggesting the use of image analysis rather than a colorimeter to measure the mean hue. Moreover, in longitudinal studies the LCC can suggest over which period the two methods are likely to be in agreement and where the simpler colorimeter method could be used. The performance of the LCC is evaluated using a small simulation study.

KEYWORDS: Colorimeter, digital image analysis, longitudinal data, mixed-effects model, postharvest

3.1 Introduction

Papaya (*Carica papaya* L.) is a tropical and climacteric fruit with antioxidant, anti-carcinogenic and anti-mutagenic properties, containing carotenoids and with nutritionally valuable accumulations of lycopene (Sancho et al., 2010). Brazil is ranked second in the world for papaya production with 1.6 million tons cultivated annually, which is equivalent to 17.5% of global production, and is also the second major papaya exporting country, accounting for 11.2% of the global trade (Evans and Ballen, 2015). Nevertheless, for expanding its internal and external market, Brazil still needs to improve its papaya postharvest quality, which will also bring added economic value to the product. Consumers purchase papaya based on color (yellow-orange papayas), freshness, taste, and size (Bron and Jacomino, 2006; Sivakumar and Wall, 2013).

Many studies, such as Silva-Ayala et al. (2005), Schweiggert et al. (2011), and Sivakumar and Wall (2013) have been conducted to understand how some variables may influence the papaya's quality in the postharvest period. One of the most important variables is the peel color, a criterion used for determination of the ripeness stage and fruit classification based on maturation scales (Mendoza and Aguilera, 2004). Moreover, the color is highly correlated with acidity, firmness, and ethylene emission, which are used as physical, chemical, and sensory indicators of product quality (Bron and Jacomino, 2006). Color is traditionally measured by a colorimeter at various points on the fruit's surface, but this can lead to bias in the determination of the mean color depending on the number and location of sampled points (Mendoza and Aguilera, 2004; Oliveira et al., 2017). For example, it is common to sample only four equidistant points on the equatorial region of the papaya fruit (Chávez-Sánchez et al., 2013; Martins et al., 2014).

A possible alternative to measure color, suggested by Mendoza and Aguilera (2004) and Darrigues et al. (2008), is the use of image analysis. This involves using a digital camera, or a scanner, for acquisition of an image or video under standard lighting conditions that can be processed using image analysis software. An image or video offers advantages in providing pixel-by-pixel information on the fruit's peel along with other associated data, such as the fruit's shape (Wu and Sun, 2013). Not surprisingly the colorimeter approach is faster and easier than image analysis, however as noted by Oliveira et al. (2017) it may not be suitable for assessing the overall mean color of the papaya's peel and its performance will depend on the number of measured points and choice of sampled region. Therefore, other studies are still needed to assess if a sample on the equatorial region can reproduce a sample over the whole region, and if the colorimeter can compete with a scanner or digital camera in measuring the mean hue of papaya peel over time. Hence, it is important to know about the magnitude of agreement over time between values observed by both approaches.

The bivariate agreement coefficient was introduced by Krippendorff (1970) to assess the agreement between two independent observers, or methods, based on nominal, ordinal, or

interval measurement scales. Later, Lin (1989) proposed the concordance correlation coefficient (CCC) to evaluate the agreement between observations measured by two methods when responses are measured on a continuous scale (King et al., 2007b). The reproducibility between the two methods is calculated by measuring the variation of the linear relationship between each pair of observations from the 45° line through the origin. The main advantages of CCC are that it measures how far each observation deviates from the best-fit line (measure of precision) and how far the best-fit line deviates from the 45° line through the origin (measure of accuracy) (Lin, 1989).

A weighted CCC for repeated measurements was proposed by Chinchilli et al. (1996), allowing for within-unit variances to vary across experimental units using a random coefficients model. King and Chinchilli (2001) proposed a generalized CCC for categorical data, allowing for the calculation of the agreement between two or more methods. Another relevant extension was proposed by King et al. (2007a,b), which focused on the estimation of a CCC for repeated measures incorporating a non-negative definite matrix of weights across different repeated measurements. Soon after, Carrasco et al. (2009) proposed the estimation of a CCC for repeated measures (CCC_{rm}) based on variance components (VC) from a mixed-effects model summarizing the agreement among methods over all measurements. These authors considered that individual effects impact the variance of distribution of the responses, including this as random effect in the model. Consequently, the interaction between individual and method, or time, are also random, allowing the estimation of individual-specific variances for method and/or at repeated measurements over time. Another relevant agreement index was proposed by Hirioite and Chinchilli (2011), who introduced a repeated measures CCC from a matrix that characterizes the overall agreement between two vectors of random variables. Recently, Rathnayake and Choudhary (2017) proposed a time-dependent CCC for multiple methods based on semiparametric models, using penalized regression splines for modeling longitudinal data.

An advantage of the VC approach is that the covariance structure of linear mixed effects models is flexible and allows for constant, or non-constant, correlation between the observations and can handle unbalanced data (Lindstrom and Bates, 1990). Restricted maximum likelihood (REML) can be used to obtain the estimates of variance components, since it is less biased and more accurate than standard maximum likelihood (Carrasco et al., 2009). This is a popular framework for analysing repeated measures data and, in particular, longitudinal data. However, if the model is incorrectly, or incompletely, specified then the REML estimates may also be biased. Additionally, mixed-effects regression models can be used to describe the CCC as a function of time, rather than summarizing it in a single coefficient as proposed by Carrasco et al. (2009). This approach may give improved statistical power in the presence of missing data (Pinheiro and Bates, 2000), decreasing the standard errors of estimators, and allows the assumption of different forms for random effects, such as constant or non-constant over time (Fitzmaurice et al., 2009). Moreover, standard repeated-measures ANOVA cannot be applied to longitudinal data when observations are irregularly spaced or when we need to include quan-

titative covariates in the model. In this work we propose an extension of the ideas presented by Lin (1989) and Carrasco et al. (2009) based on the mixed-effects regression model rather than a mixed-effects ANOVA approach. This allows us to estimate the longitudinal agreement over time among pairs of observations obtained from different methods and from different sampled regions on the papaya peel.

The remainder of the paper is organized as follows. The experimental data and descriptive analysis are introduced in Section 3.2. Section 3.3 presents the definition of the longitudinal concordance correlation (LCC) based on fixed effects and variance components in a multiple mixed-effects regression model. Section 3.4 considers the estimation of LCC from the fixed effects and variance components estimates. Section 3.5 presents bootstrap confidence intervals for the LCC and the performance of the approach is considered in a small simulation study in Section 3.6. Section 3.7 illustrates the application of this LCC methodology to the papaya hue color example, considering fruit classification and maturation studies in the postharvest phase. Section 4.7 presents a discussion on the advantages of the LCC, and some caveats on using this methodology and associated bootstrap confidence intervals. Finally, Section 4.9 gives some concluding remarks. All statistical computing and graphics have been performed using the free software environment R (R core Team, 2015).

3.2 Experimental data and descriptive analysis

An observational study was conducted in the Vegetable Production Department at “Luiz de Queiroz” College of Agriculture/Universiy of São Paulo in 2010/2011 to evaluate the peel color of 20 papaya cv. ‘Sunrise Solo’ over time. The fruits were harvested on the same day and all of them presented up to 10% yellow peel color. They were labelled and stored in a cool chamber at 18°C and 80% \pm 5% relative humidity.

A flat-bed scanner (HP Scanjet G2410) with 200 pixels per inch resolution and a tristimulus colorimeter Minolta CR-300 (Konica Minolta, 2003) were used to measure the fruits’ peel color. In order to minimize the effects of shade and provide a dark background for the image, the scanner was covered with a cardboard box coated with black colour fabric before the digitalization. The colorimeter was calibrated daily before the assessments, following the procedures in the manual (Minolta, 1991), and the *CIELCh* color space was used to describe the luminosity (L^*), chroma (C^*), and hue (h^*). Each day, after calibration, four predetermined equidistant points on the papaya’s equatorial region were observed with the colorimeter and then both sides of the fruit (labelled sides A and B) were scanned, which provided information on the whole peel region.

The processing of these images used the GNU Image Manipulation Program (GIMP) (Kimball et al., 2014) for two main aspects: i) the fruit’s equatorial region was obtained from a longitudinal slice of the original images from both sides, A and B, and these were stacked and saved as a single image (Figure 3.1(a)); ii) sides A and B of the whole region were stacked and

saved as a single image to represent the whole peel region (Figure 3.1(b)). Consequently, the equatorial region obtained from the original scanned images is a subset of the total. Afterwards, the separation of fruit peel from the black background was made using the `autoThreshold` function of the `rtiff` in R (R core Team, 2015). The `autoThreshold` uses a simple and automatic method proposed by Ridler and Calvard (1978) for identifying equatorial and whole regions of the peel, as shown in Figures 3.1(a) and 3.1(c), respectively. We observed approximately 1,000 pixels on the equatorial region and 10,000 pixels over the whole region of the fruit’s peel using both scanned sides.

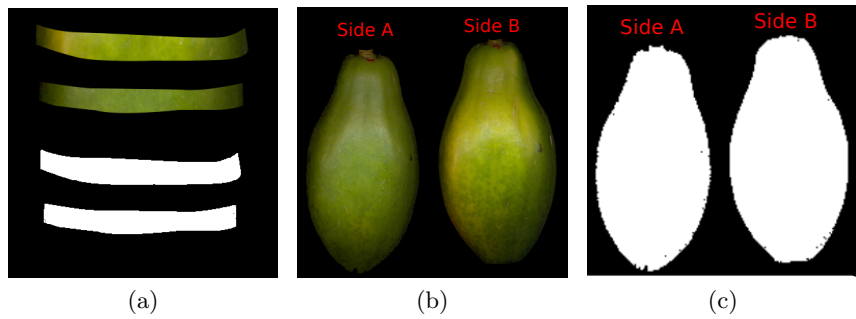


Figure 3.1: Equatorial region of both sides of one fruit (above) and separation of the equatorial region (in blank) of the black background using the `autoThreshold` function (a), both sides of one fruit stacked in one image (b) and separation of fruit’s peel of the black background through the `autoThreshold` function as well (c)

In the following, as the scanner uses the standard *RGB* (*sRGB*) rather than *CIELCh* color space, the pixels of each image need to be converted from *RGB* to *CIELCh* color space. This is done by using specific functions available in the `colorspace` package (Ihaka et al., 2015) of R. Oliveira et al. (2017) undertook a calibration study using 297 different color standards of Munsell’s color charts for vegetable tissues (Munsell Color Company, 1952) in order to correct the values of L^* , C^* , and h^* obtained by the scanner.

Here, the hue variable will be used to illustrate the statistical methodology since this is frequently used in classification procedures and to establish ripening curves for various fruits, such as mango, papayas, and bananas (Silva-Ayala et al., 2005; Sancho et al., 2010). As the hue variable is an angle it needs to be treated as a circular variable and the circular mean should be used to summarize the data (Figure 3.2) (Fisher, 1993; Mardia and Jupp, 2000). Thus, the circular mean hue (\bar{h}^*) was calculated for the i th fruit, $i = 1, 2, \dots, N$, measured by the j -method, $j = 1, 2, \dots, m$, on the l th region, $l = 1, 2, \dots, r$, at time t_{ik} , $k = 1, 2, \dots, n_i$. Besides, as the multivariate von Mises distribution of \bar{h}^* is concentrated around the vector mean $\mu_{\bar{h}^*}$, the distribution of \bar{h}^* could be treated as a normal distribution with mean $\mu_{\bar{h}^*}$ and covariance matrix \mathbf{R} (Mardia et al., 2008).

Note that because of some problems with fungal diseases, such as anthracnose (*Colletotrichum gloeosporioides* Penz.), and stem-end rot (*Mycosphaerella sp.*) on the fruit’s peel

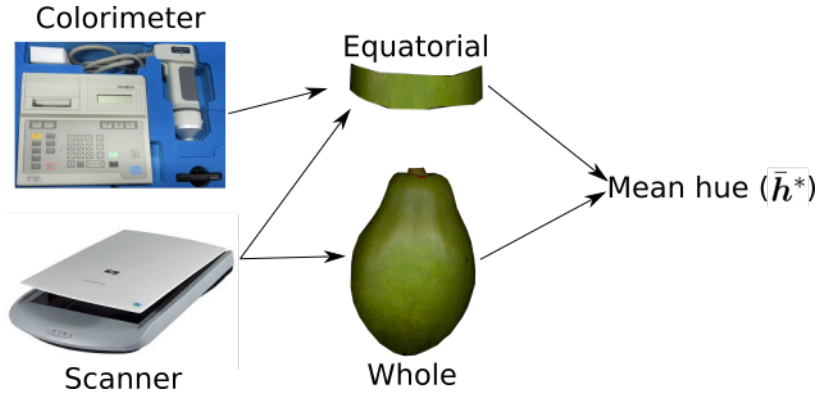


Figure 3.2: Vector of mean hue obtained from observed points on equatorial region by the colorimeter and scanner, and whole region by the scanner

during the conduct of the experiment, some fruits did not have a complete set of responses, see Figure 3.3 where some profiles terminate before day 14 and correspond to dropout. The form of missingness in this experiment is classified as missing at random (MAR), because the probability of dropout may depend on the observed responses, but, given the observed responses, is conditionally independent of the missing data . Therefore, here the MAR mechanism can be treated as ignorable, because the probability that Y_{ijkl} is observed does not depend on missing observations.

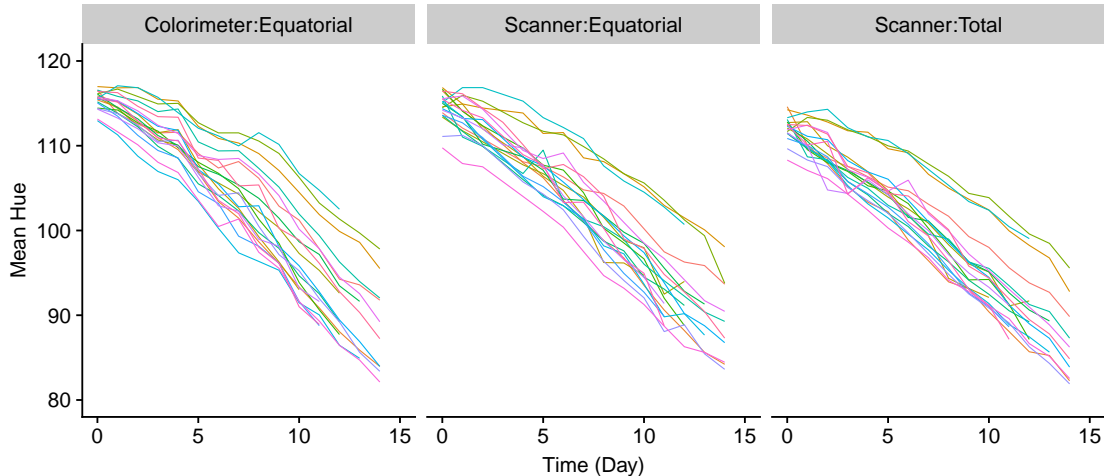


Figure 3.3: Individual profiles of 20 fruits assessed on the equatorial region by the scanner and colorimeter, and whole region by the scanner over time

In general, the papaya fruits showed a gradual and non-uniform color change over time from green ($\bar{h}^* \approx 115$), with some yellow bands at the style region, to yellowish orange ($\bar{h}^* \approx 85$) (Figure 3.3). This is in line with the experiences of Sancho et al. (2010) and Martins et al. (2014), who have also studied the peel color of papaya fruit.

3.3 Definition of the longitudinal concordance correlation (LCC)

3.3.1 The multiple mixed effects regression model for longitudinal data

Let y_{ijkl} be a realization of random variable Y_{ijkl} measured on the i th fruit ($i = 1, 2, \dots, N$) by the j th method ($j = 1, 2, \dots, m$) on the l th region ($l = 1, 2, \dots, r$) at time t_{ik} ($k = 1, 2, \dots, n_i$), where n_i is the total number of observations taken on the i th fruit over time. As an initial model we can consider a linear regression

$$Y_{ijkl} = \sum_{h=0}^p \beta_{hjl} t_{ik}^h + \varepsilon_{ijkl}, \quad (3.1)$$

which represents a polynomial regression of degree p over time. Generally, the maximum value considered for p is 4, because the use of high order polynomials ($p > 4$) may lead to over-fitting. The time variable, t , is assumed to be on a predetermined scale, such as, week, day, month, year, etc. In this simplest case, the errors ε_{ijkl} are assumed to be independent and normally distributed with mean zero and variance σ_ε^2 . However, this independence assumption may not be reasonable for longitudinal repeated measures data.

An alternative is to include in the model a random variable that indicates the influence of repeated measurements on individual i , that is, we assume that observations from the same individual are correlated. This variable is called a random effect and its population distribution is assumed to be normal with mean $\mathbf{0}$ and covariance matrix \mathbf{G} . Thus, the linear mixed effects model, including an unstructured covariance matrix for the random effects, is given by

$$Y_{ijkl} = \sum_{h=0}^p \beta_{hjl} t_{ik}^h + \sum_{h=0}^q b_{hi} t_{ik}^h + \epsilon_{ijkl} \quad (3.2)$$

$$\mathbf{b}_i \sim MVN(\mathbf{0}, \mathbf{G}) \quad \text{and} \quad \boldsymbol{\epsilon}_i \sim MVN(\mathbf{0}, \mathbf{R}_i)$$

where $h = 1, 2, \dots, q, q+1, \dots, p$ is an index identifying the degree of the linear mixed effects polynomial model, with $q \leq p$; y_{ijkl} is the response of i th fruit measured by the j th method on region l at time k ; t_{ik} is the time, in days since harvesting, at which the i th individual is observed; $\beta_{jl} = [\beta_{0jl}, \beta_{1jl}, \dots, \beta_{pj}]^T$ is a $(p+1)$ -dimensional vector of fixed effects for the j th method on the l th region; $\mathbf{b}_i = [b_{0i}, b_{1i}, \dots, b_{qi}]^T$ is a $(q+1)$ -dimensional vector of random effects with mean vector $\mathbf{0}$ and covariance matrix \mathbf{G} ; $\boldsymbol{\epsilon}_i$ is a (mrn_i) -dimensional vector assumed to be independent for different i, j, l and k and independent of the random effects \mathbf{b}_i with mean vector $\mathbf{0}$ and (diagonal) covariance matrix \mathbf{R}_i . In this case, the independence among errors is much more reasonable because the individual longitudinal dependence is accounted for by the random effects.

Under model (3.2), we can assume two different forms for the random effects: i) constant over time, or ii) non-constant over time. An example of constant random effects over time is the random-intercept model ($q = 0$) with $Cov(Y_{ijkl}, Y_{ijkl'}) = \sigma_{b_0}^2 + \sigma_\epsilon^2$; while an example of

time-dependence is the random-intercept-slope model ($q = 1$) with $Cov(Y_{ijkl}, Y_{ijkl'}) = \sigma_{b_0}^2 + \sigma_{b_1}^2 t_{ik} t_{ik'} + \sigma_{b_{01}} (t_{ik} + t_{ik'}) + \sigma_\epsilon^2$.

Sometimes, even when assuming non-constant random effects over time, it is necessary to include a time-dependent variance function in the model. As in Pinheiro and Bates (2000), we can generalize the variance function to

$$Var(\epsilon_{ijkl}) = \sigma_\epsilon^2 g(t_{ik}, \boldsymbol{\delta}_{jl}), \quad (3.3)$$

where $g(\cdot)$ is a variance function assumed continuous in $\boldsymbol{\delta}$; t_{ik} is the time covariate and $\boldsymbol{\delta}_{jl}$ is a vector of variance parameters for observations measured by the j th method on the l th region. Further details on the possible forms of variance functions can be seen in Pinheiro and Bates (2000).

The assumption of heteroscedasticity between different combinations of method and region is necessary in this context because there are subpopulation differences (equatorial and whole regions) as well as different numbers of raw observations for calculating the mean hue (four points for colorimeter; 1000 for the scanner on the equatorial region; and 10,000 for the scanner over the whole region).

The intercepts, time effects, and interactions that are related to the method and region under the model (3.2) are given by $\beta_{hjl} = \beta_h + \varphi_{hj} + \gamma_{hl} + \lambda_{hjl}$, where β_h is the overall polynomial coefficient; φ_{hj} , γ_{hl} , and λ_{hjl} are the method-time, region-time, and method-region-time interactions, respectively. Note that when $h = 0$, φ_{0j} and γ_{0l} are the main effects of method and region, respectively. To ensure identifiability of the fixed effects, it is assumed that $\varphi_{h1} = \gamma_{h1} = \lambda_{h1l} = \lambda_{hj1} = 0$, for $j = 1, 2, \dots, m$, $l = 1, 2, \dots, r$.

3.3.2 Model extensions

The hue change in papaya fruit depends on several variables that were not measured before the beginning of experiment described in section 3.2, such as fruit position on the plant, temperature and relative humidity, time until harvest of fruit, plant and/or fruit diseases, sun exposure time, etc. These unobserved variables can influence directly, or indirectly, the physiological processes of the fruit and consequently its initial hue, justifying the inclusion of a random intercept in the model. Furthermore, as we take measurements on different fruit regions, it is reasonable that we assume these unobserved variables can differentially affect the response variable given the locality of the observed point on the peel. In particular, this assumption is necessary because papaya has an uneven ripening process, starting at the style and moving towards the peduncle insertion regions, forming yellowish-hue bands.

To estimate this additional variability associated with the interaction between method and region, we create a new variable A with mr categories given by the combination of fruit, region and method levels. Then the $mr - 1$ associated dummy variables for fruit i at time k are

defined as follows:

$$d_{ick} = \begin{cases} 1, & \text{for category } c \text{ of variable } A \\ 0, & \text{otherwise} \end{cases} .$$

with $c = 1, 2, \dots, mr-1$ and associated vector $\mathbf{d}_{ik} = (d_{i1k}, d_{i2k}, \dots, d_{i(mr-1)k})$, with the reference category mr corresponding to $d_{i1k} = d_{i2k} = \dots = d_{i(mr-1)k} = 0$. In this way, we can extend model (3.2) to

$$\begin{aligned} Y_{ijkl} &= \sum_{h=0}^p \beta_{hjlt_{ik}^h} + \sum_{h=0}^q b_{hit_{ik}^h} + \sum_{c=1}^{mr-1} \alpha_{ci} d_{ick} + \epsilon_{ijkl} \\ \mathbf{u}_i &= \begin{bmatrix} \mathbf{b}_i \\ \boldsymbol{\alpha}_i \end{bmatrix} \sim MVN \left(\begin{bmatrix} \mathbf{0} \\ \mathbf{0} \end{bmatrix}, \mathbf{D} = \begin{bmatrix} \mathbf{G} & \boldsymbol{\Phi} \\ \boldsymbol{\Phi} & \mathbf{G}_\alpha \end{bmatrix} \right) \quad \text{and} \quad \boldsymbol{\epsilon}_i \sim MVN(\mathbf{0}, \mathbf{R}_i), \end{aligned} \quad (3.4)$$

where $\boldsymbol{\alpha}_i$ is a $(mr - 1)$ -dimensional vector of random effects; \mathbf{G}_α is an $(mr - 1) \times (mr - 1)$ matrix of covariances; $\mathbf{u}_i = [\mathbf{b}_i^T, \boldsymbol{\alpha}_i^T]^T$ is $(q + mr)$ -dimensional vector of random effects with mean vector $\mathbf{0}$ and covariance matrix \mathbf{D} ; and $\boldsymbol{\Phi}$ is a matrix of zeros. Model (3.4) may be much more reasonable than model (3.2) because the individual influence on the intercept due to the interaction of method and region is also removed from the error term.

Model (3.4) is equivalent to a general linear mixed model defined by Verbeke and Molenberghs (2000) as

$$\begin{aligned} \mathbf{Y}_i &= \mathbf{X}_i(t_{ik}) \boldsymbol{\beta} + \mathbf{Z}_i(t_{ik}) \mathbf{u}_i + \boldsymbol{\epsilon}_i \\ \mathbf{u}_i &\sim MVN(\mathbf{0}, \mathbf{D}) \quad \text{and} \quad \boldsymbol{\epsilon}_i \sim MVN(\mathbf{0}, \mathbf{R}_i) \end{aligned} . \quad (3.5)$$

where $\mathbf{Y}_i = (\mathbf{Y}_{i1}^T, \mathbf{Y}_{i2}^T, \dots, \mathbf{Y}_{in_i}^T)^T$ is the associated vector of measurements for fruit i , $\mathbf{X}_i(t_{ik})$ and $\mathbf{Z}_i(t_{ik})$ are design matrices with $(p+1)mr$ and $q+mr$ covariates for fruit i at time t_{ik} with dimensions $mrn_i \times (p+1)mr$ and $mrn_i \times (q+mr)$, respectively. Hence, under model (3.5), $\mathbf{X}_i(t_{ik})$ is the design matrix associated with fixed effects $\boldsymbol{\beta} = [\boldsymbol{\beta}_0^T, \boldsymbol{\beta}_1^T, \dots, \boldsymbol{\beta}_p^T]^T$, and $\mathbf{Z}_i(t_{ik})$ includes random coefficients of the model such as random intercept, or random intercept and slope, etc. Marginally, the vector \mathbf{Y}_i is normally distributed with mean $\mathbf{X}_i(t_{ik}) \boldsymbol{\beta}$ and covariance matrix $Var(\mathbf{Y}_i) = \mathbf{Z}_i(t_{ik}) \mathbf{D} \mathbf{Z}_i^T(t_{ik}) + \mathbf{R}_i = \mathbf{V}_i$.

3.3.3 The longitudinal concordance correlation

Let Y_1 and Y_2 be random variables independently selected from a bivariate population with means μ_1 and μ_2 , $Var(Y_1) = \sigma_1^2$, $Var(Y_2) = \sigma_2^2$ and $Cov(Y_1, Y_2) = \sigma_{12}$. The concordance correlation coefficient (CCC) introduced by Lin (1989) is defined as

$$\rho_c = 1 - \frac{E \left[(Y_1 - Y_2)^2 \right]}{E_I \left[(Y_1 - Y_2)^2 \right]} = \frac{2\sigma_{12}}{\sigma_1^2 + \sigma_2^2 + (\mu_1 - \mu_2)^2} = \rho_p C_b \quad (3.6)$$

where $|\rho_c| \leq 1$, E_I is the expectation assuming that Y_1 and Y_2 are uncorrelated. ρ_p is the Pearson correlation coefficient ($|\rho_p| \leq 1$) that measures how far each observation deviated from the best-fit line (precision measure), and C_b is the accuracy ($0 < C_b \leq 1$) that measures how far the best-fit line deviates from the 45° line through the origin. Lin (1989) defined $C_b = 2(v + v^{-1} + u^2)^{-1}$, where $v = \sigma_1/\sigma_2$ is a scale shift, while $u = (\mu_1 - \mu_2)/\sqrt{\sigma_1\sigma_2}$ is a location shift relative to the scale.

Now suppose that the i th fruit is measured n_i times by each of m methods on r regions and that the researcher wants to investigate the agreement between observations measured by different methods on the same region, by different methods and regions, and by the same method on distinct regions of the fruit's peel. Here we denote y_{ijlk} and $y_{ij'l'k}$ as general realizations of random variables Y_{ijlk} and $Y_{ij'l'k}$ measured from different unique combination of two factors (method and region) at time t_{ik} , with $j > j' = 1, 2, \dots, m$, and $l > l' = 1, 2, \dots, r$. Thus, under the model (3.4), we can define the LCC based on variance components for observations measured from different unique combinations of two factors at time t_{ik} as

$$\rho_{jl, j'l'}(t_{ik}) = \frac{2Cov(Y_{ijlk}, Y_{ij'l'k})}{Var(Y_{ijlk}) + Var(Y_{ij'l'k}) + [E(Y_{ijlk}) - E(Y_{ij'l'k})]^2}. \quad (3.7)$$

Let \mathbf{z}_{ijlk} and $\mathbf{z}_{ij'l'k}$ be, respectively, rows of $\mathbf{Z}_i(t_{ik})$ matrix such that $\mathbf{z}_{ijlk} = (\mathbf{t}_{ik}, \mathbf{d}_{ik})$ and $\mathbf{z}_{ij'l'k} = (\mathbf{t}_{ik}, \mathbf{d}'_{ik})$, where $\mathbf{t}_{ik} = (t_{ik}^0, t_{ik}^1, \dots, t_{ik}^q)$ and \mathbf{d}_{ik} and \mathbf{d}'_{ik} are the dummy variables for the two method-region combinations (jl and $j'l'$). Thus, the covariance between Y_{ijlk} and $Y_{ij'l'k}$ is given by

$$Cov(Y_{ijlk}, Y_{ij'l'k}) = \mathbf{z}_{ijlk} \mathbf{D} \mathbf{z}_{ij'l'k}^T = \mathbf{t}_{ik} \mathbf{G} \mathbf{t}_{ik}^T + \mathbf{d}_{ik} \mathbf{G}_\alpha \mathbf{d}_{ik}^T. \quad (3.8)$$

If we assume different variances for each unique combination between method and region, the variances of Y_{ijlk} and $Y_{ij'l'k}$ can be expressed as

$$\begin{cases} Var(Y_{ijlk}) = \mathbf{t}_{ik} \mathbf{G} \mathbf{t}_{ik}^T + \mathbf{d}_{ik} \mathbf{G}_\alpha \mathbf{d}_{ik}^T + \sigma_\epsilon^2 g(t_{ik}, \delta_{jl}) \\ Var(Y_{ij'l'k}) = \mathbf{t}_{ik} \mathbf{G} \mathbf{t}_{ik}^T + \mathbf{d}'_{ik} \mathbf{G}_\alpha \mathbf{d}'_{ik}^T + \sigma_\epsilon^2 g(t_{ik}, \delta_{j'l'}) \end{cases}. \quad (3.9)$$

On the other hand, the systematic difference between the mean responses for Y_{ijlk} and $Y_{ij'l'k}$ given by $S_{jl, j'l'}(t_{ik}) = E(Y_{ijlk}) - E(Y_{ij'l'k}) = \mu_{jl}(t_{ik}) - \mu_{j'l'}(t_{ik})$ reduces to

$$S_{jl, j'l'}(t_{ik}) = \mathbf{t}_{ik}(\beta_{jl} - \beta_{j'l'}), \text{ with } h = 1, 2, \dots, p \text{ and } jl \neq j'l'. \quad (3.10)$$

Thus, replacing the expressions (3.8), (3.9), and (3.10) in (3.7) and considering all individual fruits that were assessed at time t_k , we have that the LCC is given by

$$\begin{aligned} \rho_{jl, j'l'}(t_k) &= \frac{\mathbf{t}_k \mathbf{G} \mathbf{t}_k^T + \mathbf{d}_k \mathbf{G}_\alpha \mathbf{d}_k^T}{\mathbf{t}_k \mathbf{G} \mathbf{t}_k^T + \frac{1}{2} \{ \mathbf{d}_k \mathbf{G}_\alpha \mathbf{d}_k^T + \mathbf{d}'_k \mathbf{G}_\alpha \mathbf{d}'_k^T + \sigma_\epsilon^2 [g(t_k, \delta_{jl}) + g(t_k, \delta_{j'l'})] + S_{jl, j'l'}^2(t_k) \}} \\ &= \rho_{jl, j'l'}^{(p)}(t_k) C_{jl, j'l'}(t_k) \end{aligned} \quad (3.11)$$

where $\mathbf{t}_k = \frac{1}{N_k} \sum_{i=1}^{N_k} \mathbf{t}_{ik}$ and $\mathbf{d}_k = \frac{1}{N_k} \sum_{i=1}^{N_k} \mathbf{d}_{ik}$. $\rho_{jl, j'l'}^{(p)}(t_k)$ and $C_{jl, j'l'}(t_k)$ are, respectively, the longitudinal Pearson correlation and longitudinal accuracy based on variance components for each unique combination of two factors, $j > j' = 1, 2, \dots, m$ and $l > l' = 1, 2, \dots, r$.

The $\rho_{jl, j'l'}^{(p)}(t_k)$ measures how far each observation deviated from the best-fit line at a fixed time $t_k = t$ and is given by

$$\rho_{jl, j'l'}^{(p)}(t_k) = \frac{\mathbf{t}_k \mathbf{G} \mathbf{t}_k^T + \mathbf{d}_k \mathbf{G}_\alpha \mathbf{d}_k^T}{\sqrt{[\mathbf{t}_k \mathbf{G} \mathbf{t}_k^T + \mathbf{d}_k \mathbf{G}_\alpha \mathbf{d}_k^T + \sigma_\epsilon^2 g(t_k, \delta_{jl})] [\mathbf{t}_k \mathbf{G} \mathbf{t}_k^T + \mathbf{d}'_k \mathbf{G}_\alpha \mathbf{d}'_k^T + \sigma_\epsilon^2 g(t_k, \delta_{j'l'})]}}.$$

The accuracy $C_{jl, j'l'}(t_k)$ is a longitudinal bias correction factor that measures how far the best-fit line deviates from the 45° line at a fixed time $t_k = t$ and is given by

$$C_{jl, j'l'}(t_k) = \frac{2}{v_{jl, j'l'}(t_k) + [v_{jl, j'l'}(t_k)]^{-1} + u_{jl, j'l'}^2(t_k)}$$

where

$$v_{jl, j'l'}(t_k) = \sqrt{\frac{Var(Y_{ijlk})}{Var(Y_{ij'l'k})}} = \sqrt{\frac{\mathbf{t}_k \mathbf{G} \mathbf{t}_k^T + \mathbf{d}_k \mathbf{G}_\alpha \mathbf{d}_k^T + \sigma_\epsilon^2 g(t_k, \delta_{jl})}{\mathbf{t}_k \mathbf{G} \mathbf{t}_k^T + \mathbf{d}'_k \mathbf{G}_\alpha \mathbf{d}'_k^T + \sigma_\epsilon^2 g(t_k, \delta_{j'l'})}}$$

denotes the scale shift and

$$\begin{aligned} u_{jl, j'l'}(t_k) &= \frac{E(Y_{ijlk}) - E(Y_{ij'l'k})}{[Var(Y_{ijlk}) Var(Y_{ij'l'k})]^{\frac{1}{4}}} \\ &= \frac{\mathbf{t}_k (\beta_{jl} - \beta_{j'l'})}{\{[\mathbf{t}_k \mathbf{G} \mathbf{t}_k^T + \mathbf{d}_k \mathbf{G}_\alpha \mathbf{d}_k^T + \sigma_\epsilon^2 g(t_k, \delta_{jl})] [\mathbf{t}_k \mathbf{G} \mathbf{t}_k^T + \mathbf{d}'_k \mathbf{G}_\alpha \mathbf{d}'_k^T + \sigma_\epsilon^2 g(t_k, \delta_{j'l'})]\}^{\frac{1}{4}}} \end{aligned}$$

denotes the location shift relative to the scale (Lin, 1989). When $Var(Y_{ijlk}) = Var(Y_{ij'l'k})$ and $E(Y_{ijlk}) = E(Y_{ij'l'k})$ there is no deviation from the 45° line.

It is worth noting that, as often studies will use two or more methods to measure a characteristic on the same group of subjects, these measurements will tend to be positively correlated (Barnhart and Williamson, 2001; King et al., 2007b). Here we may expect similar positive association between measurement methods and hue color (ripeness) at different regions of the fruit. Thus, it is plausible to assume that in most situations $0 \leq \rho_{jl, j'l'}(t) \leq 1$.

3.4 Estimation of the LCC using variance components

To estimate the fixed effects and variance components of the linear mixed-effects model we use the restricted maximum likelihood approach. The log-likelihood function to maximize is proportional to

$$l_R(\boldsymbol{\beta}, \boldsymbol{\psi}_u, \boldsymbol{\psi}_\epsilon; \mathbf{y}) \propto -\frac{1}{2} \left\{ \log |\mathbf{V}| + |\mathbf{X}(t_{ik})^T \mathbf{V}^{-1} \mathbf{X}(t_{ik})| + \mathbf{r}^T \mathbf{V}^{-1} \mathbf{r} \right\},$$

where $\boldsymbol{\psi}_u$ and $\boldsymbol{\psi}_\epsilon$ denote, respectively, vectors of variance components of the \mathbf{D} and \mathbf{R}_i matrices; and $\mathbf{r} = (\mathbf{y} - \mathbf{X}(t_{ik}) \boldsymbol{\beta})$ is a residual. It is worth noting that when the data are missing at

random, or missing completely at random, the missing-data mechanism may be ignored and the resulting likelihood function remains valid (Fitzmaurice et al., 2009).

Since $\rho_{jl,j'l'}(t_{ik})$ is a function of the fixed effects (β) and variance components (ψ_u, ψ_ϵ) it can be estimated by replacing β , ψ_u , and ψ_ϵ by their REML estimates.

3.5 Non-parametric bootstrap confidence intervals

Let \widehat{F}_1 and \widehat{F}_2 be the empirical distributions of ϵ and u which are defined to be discrete distributions with probabilities $1/n$ on each value of ϵ and $1/N$ on each group of random effects associated with the i th fruit, u_i , respectively. Then, B pseudo-samples of size n and N are drawn with replacement from ϵ and u , respectively, to give the bootstrap resamples. This process is called the nonparametric bootstrap coupled with a global residual bootstrap, which consists of the sampling of entire subjects with replacement and of sampling residuals with replacement globally (Thai et al., 2013).

The nonparametric bootstrap approach depends on the fixed effects and variance-covariance matrix structure of the model to calculate the raw random effects or residuals, but it does not require a particular assumption about the distribution of the estimator (Thai et al., 2013). Some steps are needed to build the $100(1 - \alpha)\%$ bootstrap CI for the LCC.

Initially, we generate B pseudo-samples by resampling from the data then refit the model in order to obtain B sets of estimates for all parameters of the LCC. Then for each pseudo-sample, for a specific time $t_k = t$ we use the estimated values to obtain $\rho_{jl,j'l'}^{(b)}(t)$ and apply the Fisher Z-transformation $\left(\frac{1}{2} \log\left(\frac{1+\rho}{1-\rho}\right)\right)$ to provide values that may be approximately normally distributed. The expected value of the Z-transformed bootstrap estimator is calculated from the B bootstrap samples at time t as

$$\widehat{\rho}_{jl,j'l'}^*(t) = \frac{1}{2B} \sum_{b=1}^B \log \left[\frac{1 + \rho_{jl,j'l'}^{(b)}(t)}{1 - \rho_{jl,j'l'}^{(b)}(t)} \right].$$

and the standard deviation of the bootstrap distribution of $\widehat{\rho}_{jl,j'l'}^*(t)$ is given by

$$\widehat{SE}_{jl,j'l'}^*(t) = \sqrt{\frac{1}{B-1} \sum_{b=1}^B \left[\frac{1}{2} \log \left(\frac{1 + \rho_{jl,j'l'}^{(b)}(t)}{1 - \rho_{jl,j'l'}^{(b)}(t)} \right) - \widehat{\rho}_{jl,j'l'}^*(t) \right]^2}.$$

An approximate level $1 - \alpha$ bootstrap confidence interval for the LCC $\widehat{\rho}_{jl,j'l'}$ on the original scale is $[LB, UB]$, where

$$LB = \frac{\exp \left\{ 2 \left[\widehat{\rho}_{jl,j'l'}^*(t) - z_{(1-\frac{\alpha}{2})} \widehat{SE}_{jl,j'l'}^*(t) \right] \right\} - 1}{\exp \left\{ 2 \left[\widehat{\rho}_{jl,j'l'}^*(t) - z_{(1-\frac{\alpha}{2})} \widehat{SE}_{jl,j'l'}^*(t) \right] \right\} + 1}$$

and

$$UB = \frac{\exp \left\{ 2 \left[\widehat{\rho}_{jl,j'l'}^*(t) - z_{\frac{\alpha}{2}} \widehat{SE}_{jl,j'l'}^*(t) \right] \right\} - 1}{\exp \left\{ 2 \left[\widehat{\rho}_{jl,j'l'}^*(t) - z_{\frac{\alpha}{2}} \widehat{SE}_{jl,j'l'}^*(t) \right] \right\} + 1}.$$

with $z_{\frac{\alpha}{2}}$ and $z_{(1-\frac{\alpha}{2})}$ denoting the $\frac{\alpha}{2}$ and $1 - \frac{\alpha}{2}$ quantiles of the standard normal distribution.

When N is small the shape of the sampling distribution of $\hat{\rho}_{jl,j'l'}^*$ may look non-normal, then a more appropriate bootstrap CI approach should be based on the percentile method because the discrepancy between the CI based on $\widehat{SE}_{jl,j'l'}^*$ and CI based on percentiles increases with decreasing N (Thai et al., 2013).

The inference about $\hat{\rho}_{jl,j'l'}^{(p)}$ can be performed in a similar way as presented for LCC. However, the inference about $C_{jl,j'l'}$ is a little different because it belongs to the interval $[0, 1]$, consequently we can use the logit transformation $\log\left(\frac{C_{jl,j'l'}(t_k=t)}{1-C_{jl,j'l'}(t_k=t)}\right)$ instead of Fisher Z-transformation to approximate the distribution of $C_{jl,j'l'}(t_k = t)$ to the normal distribution.

Here we consider a simple case-resampling bootstrap, an alternative would be to use a model-based residual resampling approach.

3.6 Simulation study

To evaluate the LCC approach, we conducted a simulation study to investigate its estimation performance under variance components approaches for papaya ripeness over different scenarios. We are specifically interested in examining the scaled mean error (SME), as a bias measure, root mean square error (RMSE), as an accuracy measure, for LCC. We also examined the accuracy of simultaneous confidence intervals for $S_{jl,j'l'}(t_k) = \mu_{jl}(t_k) - \mu_{j'l'}(t_k)$ and LCC(t_k). To simplify the study, we restrict attention to $m = 2$ methods, $r = 2$ regions, and $k = 16$ repeated measures (days) and we evaluate the LCC for the same methods over different fruit regions, as well as among methods on the same regions of the fruit; we label these cases as Examples 1 (whole versus equatorial region measured by colorimeter), 2 (whole versus equatorial region measured by scanner), 3 (colorimeter versus scanner on equatorial region), and 4 (colorimeter versus scanner on whole region).

The data are simulated from a particular case of model (3.4) with $p = 1$ and $q = 1$, resulting in the following model

$$\begin{aligned} Y_{ijkl} &= \beta_{0jl} + b_{0i} + (\beta_{1jl} + b_{1i})t_{ik} + \epsilon_{ijkl}, \\ \mathbf{b}_i &\sim N_2(\mathbf{0}, \mathbf{G}) \quad \text{and} \quad \boldsymbol{\epsilon}_i \sim MVN(\mathbf{0}, \mathbf{I}\sigma_\epsilon^2). \end{aligned} \quad (3.12)$$

Specifically, we take mean functions $\mu_{11}(t_k) = 114 - 2.5k$, $\mu_{12}(t_k) = \mu_{22}(t_k) = 105 - 2.0t_k$, and $\mu_{21}(t_k) = 115 - 2.2t_k$; and variance components $(\sigma_{b_0}^2, \sigma_{b_1}^2, \sigma_{b_{01}}^2, \sigma_\epsilon^2) = (4.3, 0.2, -0.5, 0.3)$. Thus, we generate a response vector \mathbf{y} from a multivariate normal distribution with mean $\mathbf{X}\boldsymbol{\beta}$, and variance-covariance matrix $\mathbf{ZGZ}^T + \mathbf{I}\sigma_\epsilon^2$.

We also consider two trajectories per fruit for $N \in \{20, 50, 100\}$ fruits using both balanced and unbalanced designs, where the missing value pattern used was (monotone) dropout. The data for unbalanced designs are initially simulated as in a balanced design and then we create an indicator variable (I_{rm}) for the total number of repeated measures on the i -th fruit. We suppose that this variable has a Poisson distribution with mean and variance equal 11, subject to a maximum of 16 repeated measurements. The individual observations up until observation

Table 3.1: Overall mean of simulated scaled mean error (SME), in absolute values, and root mean square error (RMSE) for four examples of longitudinal concordance correlation based on 2.000 Monte Carlo samples for 20, 50 and 100 fruits in the balanced and unbalanced design cases

Design	N	SME $\times 10^2$				RMSE			
		Ex. 1	Ex. 2	Ex. 3	Ex. 4	Ex. 1	Ex. 2	Ex. 3	Ex. 4
Balanced	20	0.798	0.198	0.466	0.502	0.024	0.032	0.035	0.044
	50	0.396	0.111	0.274	0.450	0.015	0.020	0.022	0.028
	100	0.336	0.091	0.151	0.169	0.011	0.014	0.015	0.020
Unbalanced	20	1.692	1.088	0.914	1.509	0.038	0.047	0.051	0.065
	50	0.648	0.580	0.396	0.483	0.024	0.029	0.032	0.040
	100	0.328	0.278	0.177	0.265	0.016	0.021	0.023	0.029

$n_i = I_{rm_i} \sim \text{Poisson}(11)$ are kept in the data, while the remainder are treated as missing values. Note that, the number of repeated measurements taken on the i -th fruit does not depend on method nor sampled region. A similar approach to generating unbalanced datasets was used by Rathnayake and Choudhary (2017).

We use the methodology of Section 3.5 with $B=2.000$ bootstrap replications to compute the simultaneous confidence intervals with $1 - \alpha = 0.95$ based on the Fisher Z-transformation to approximate the distribution of $\rho_{jl,j'l'}(t_k)$ by the normal distribution. The process of simulating data and constructing confidence intervals is repeated 2.000 times, and we computed the coverage probability for each interval.

Table 3.1 presents the overall mean of estimated SME and RMSE for the LCC in examples 1, 2, 3, and 4 for balanced and unbalanced designs. We see a small SME under both designs for $N = 20, 50$, or 100 for all examples, however as would be expected the estimator of $\rho_{jl,j'l'}(t_k)$ is more biased in the unbalanced design than in the balanced one. Furthermore, the RMSE indicates that the estimator of LCC is close to the true value as the number of individuals (N) increases, demonstrating a satisfactory performance even in conditions of unbalance and a low number of individuals.

The estimated coverage rate for the simultaneous confidence intervals around $\rho_{jl,j'l'}(t_k)$ and $S_{jl,j'l'}(t_k)$ at a fixed time $t_k = t$ are graphically summarize for both experimental designs in Figure 3.4. In the balanced case, we see that LCC bands still have a slight tendency over time to stay below the nominal coverage for $N = 20$, however, this phenomenon disappears as the sample size is increased. Interestingly, even in a severe unbalance condition there is no considerable difference in the coverage rate between balanced and unbalanced cases for LCC. This indicates that the methodology is robust to the unbalance conditions in the data. On the other hand, in both experiment designs the estimated coverage rate for systematic differences ($S_{jl,j'l'}(t_k)$) appear decreases a little as we increase the number of fruits. In general, the coverage rate is acceptable for the sample size of 20 and appropriate for 100 subjects.

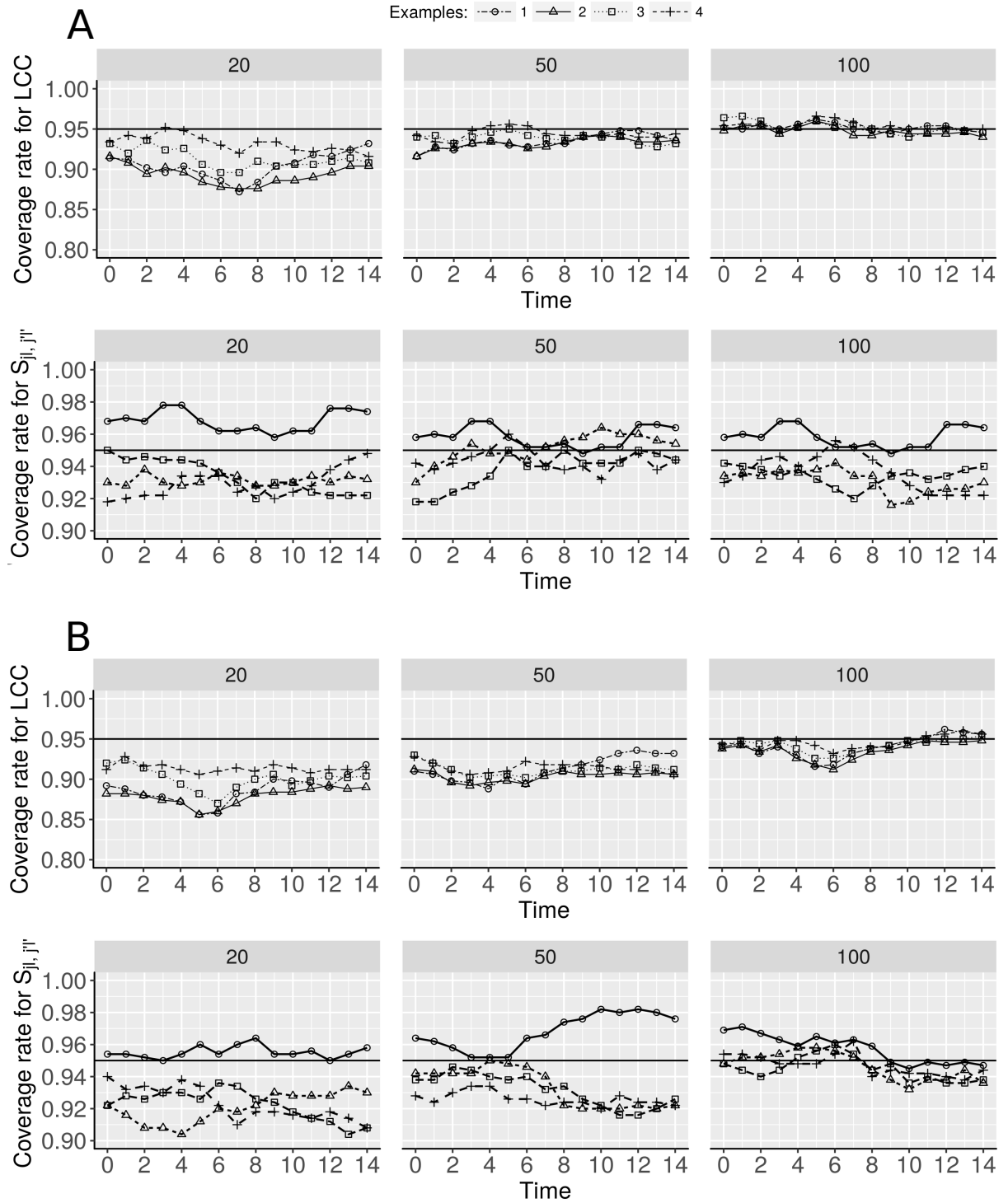


Figure 3.4: Estimated simultaneous coverage rate based on 95% confidence intervals for $S_{jl,j'l'}(t_k)$ and $LCC(t_k)$, both considering $N \in \{20, 50, 100\}$ fruits in the balanced (A) and unbalanced (B) designs

3.7 Papaya's peel hue data analysis

Initially, a quadratic growth model with a random effect of fruit was fitted for each combination between method ($j = 1, 2$) and region ($l = 1, 2$), where $j = 1$ refers to the colorimeter while $j = 2$ to the scanner, while $l = 1$ refers to the equatorial region and $l = 2$ to the whole region. However, for computational reasons time was transformed to a log scale, $\tau_{ik} = \log(t_{ik} + 1)$.

In sequence, a model selection procedure was performed from the model of expression (3.4), resulting in the following model:

$$y_{ijkl} = \beta_{0jl} + b_{0i} + (\beta_{1jl} + b_{1i})\tau_{ik} + (\beta_{2jl} + b_{2i})\tau_{ik}^2 + \beta_3\tau_{ik}^3 + \alpha_{1i}d_{i1k} + \alpha_{2i}d_{i2k} + \epsilon_{ijkl}$$

$$\begin{bmatrix} b_{0i} \\ b_{1i} \\ b_{2i} \\ \alpha_{(21)i} \\ \alpha_{(22)i} \end{bmatrix} \sim MVN \left(\begin{bmatrix} 0 \\ 0 \\ 0 \\ 0 \\ 0 \end{bmatrix}, \mathbf{D} = \begin{bmatrix} \sigma_{b_0}^2 & 0 & 0 & 0 & 0 \\ 0 & \sigma_{b_1}^2 & \sigma_{b_{12}} & 0 & 0 \\ 0 & \sigma_{b_{12}} & \sigma_{b_2}^2 & 0 & 0 \\ 0 & 0 & 0 & \sigma_\alpha^2 & \sigma_{\alpha_{12}} \\ 0 & 0 & 0 & \sigma_{\alpha_{12}} & \sigma_\alpha^2 \end{bmatrix} \right) \quad \text{and} \quad \boldsymbol{\epsilon}_i \sim MVN(\mathbf{0}, \mathbf{R}_i), \quad (3.13)$$

where d_{i1k} and d_{i2k} are dummy variables equal to 1 for observations measured by the scanner on equatorial region and whole region, respectively, and zero otherwise, as described in Subsection 3.3.2.

In this model, the conditional residuals were assumed to be independent (see Appendix VI) with constant variance over time and we checked this assumption from a variogram constructed using these residuals, suggesting that it was adequate for the whole region. On the other hand, the variability of observations measured on the equatorial region increased faster over time than observations measured on the whole region of the fruit. To solve this, a variance function using time as covariate was included in the model, which can be represented by $\text{Var}(\epsilon_{ijkl}) = \sigma_\epsilon^2 \exp(2\delta_{jl}\tau_{ik})$ for observations measured by the j th method on l th region, where the parameter δ_{jl} is unrestricted enabling the variance to increase or decrease over time (Pinheiro and Bates, 2000). As variances remained constant over time for observations measured on the whole region, we fixed $\delta_{22} = 0$, which represents the scanner on the whole region.

The parameter point estimates and respective 95% confidence intervals are presented in Table 3.2. The intercept as well as linear and quadratic coefficients were different between methods and sampled regions, which indicates that the colorimeter and scanner, as well as the equatorial and whole regions, differed in mean hue quantification. As $E[Y_{ijkl}] = \beta_{0jl} + \beta_{1jl}\tau_{ik} + \beta_{2jl}\tau_{ik}^2 + \beta_3\tau_{ik}^3 \neq E[Y_{j'l'k}]$ for $j > j' = 1, 2, \dots, m$, and $l > l' = 1, 2, \dots, r$, the systematic differences ($S_{j,l,j',l'}^2(t_{ik})$) between methods by region were different from zero and vary over time t_{ik} . This difference was smallest between observations measured by the colorimeter and by the scanner on the equatorial region (Figure 3.5), indicating greater accuracy between these compared to other combinations.

Table 3.2: Coefficients, parameter estimates by REML and their 95% confidence interval obtained by the non-parametric bootstrap method

Coefficient	Value	Parameter	Lower	Estimate	Upper
Intercepts		β_0	114.792	115.342	116.063
$\beta_{011} = \beta_0$	115.342	φ_{02}	-1.4205	-0.6554	-0.0846
$\beta_{021} = \beta_0 + \varphi_{02}$	114.687	γ_{02}	-2.9306	-2.4255	-1.9753
$\beta_{022} = \beta_0 + \varphi_{02} + \gamma_{02}$	111.940	β_1	-4.0129	-2.7467	-2.1555
Linear effect		φ_{12}	-1.7603	-1.4721	-0.4275
$\beta_{111} = \beta_1$	-2.7467	γ_{12}	-1.4507	-0.9158	0.1909
$\beta_{121} = \beta_1 + \varphi_{12}$	-4.2188	β_2	3.0049	3.5877	4.3571
$\beta_{122} = \beta_1 + \varphi_{12} + \gamma_{12}$	-5.1346	φ_{22}	0.2313	0.6632	0.7351
Quadratic effect		γ_{22}	0.1228	0.3990	0.5837
$\beta_{211} = \beta_2$	3.5877	β_3	-2.4569	-2.3437	-2.1567
$\beta_{221} = \beta_2 + \varphi_{22}$	4.2509	σ_{b_0}	0.7885	1.4219	1.7726
$\beta_{221} = \beta_2 + \varphi_{22} + \gamma_{22}$	4.6499	σ_{b_1}	1.0929	1.6339	1.8261
Cubic effect		σ_{b_2}	0.5443	0.8259	0.9450
$\beta_{3jl} = \beta_3$	-2.3437	ρ_{b_1, b_2}	-0.8908	-0.6650	-0.2276
		σ_α	0.5147	1.1975	1.5942
		ρ_α	0.6351	0.8592	0.9846
		δ_{j1}	0.0622	0.1210	0.1974
		σ_ϵ	0.6380	0.7759	0.8025

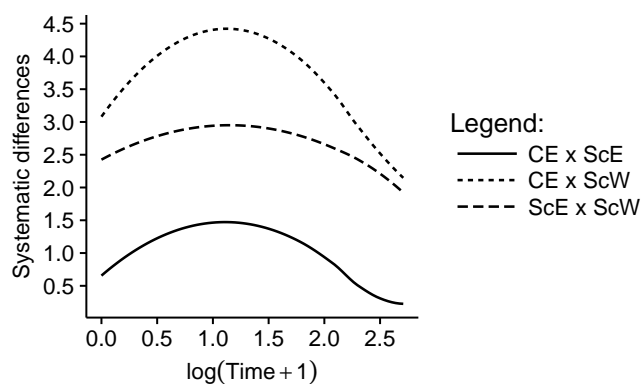


Figure 3.5: Systematic differences between CE and ScE; CE and ScW; and ScE and ScW over the time, where CE and ScE indicate, respectively, observations measured by the colorimeter and scanner on the equatorial region while ScW indicates observations measured by the scanner on the whole region

Variance components as well as their 95% confidence intervals presented in Table 3.2 show that the variability of observations measured on papaya skin at the beginning of the experiment by the colorimeter was less than that by the scanner, with variances $Var(Y_{11l1}) = \sigma_{b_0}^2$ for the colorimeter and $Var(Y_{2l1}) = \sigma_{b_0}^2 + \sigma_\alpha^2$ for the scanner. This showed that a sample of four points on the equatorial region for the colorimeter was not representative of this region at the beginning of the experiment. At this point the papaya's ripening process has led to larger proportions of green hues than yellowish-green or yellow hues on the equatorial region, resulting in a distribution more concentrated around the mean hue when the fruit was assessed by the colorimeter in relation to scanner. Similar results can be verified in studies conducted by Bron and Jacomino (2006), Schweiggert et al. (2011) and Chávez-Sánchez et al. (2013), who also showed a low variability among fruits measured by the colorimeter on the equatorial region at start of experiments. Therefore, it is necessary that a greater number of points be sampled in this region with the colorimeter in order to obtain a representative sample, especially at initial ripeness stages.

The correlation parameter $\rho_\alpha = \sigma_{\alpha_{12}}/\sigma_\alpha^2$ included in the model to quantify the relationship between observations measured by the scanner on the equatorial and whole regions showed a positive and high correlation ($\rho_\alpha=0.85$). It was a indicative of high precision among these measurements and makes sense because the equatorial region was represented by a percentage of pixels belonging to the whole region, in such a way that, as we increase this percentage, the Pearson correlation will tend to 1.

Under the fixed effects and variance components of the model described in (3.13), the longitudinal concordance correlation (LCC), longitudinal Pearson correlation (LPC), and longitudinal accuracy (LA) were estimated for each pair of unique combinations among levels of method and region, as well as their 95% bootstrap confidence intervals. Here we assumed that the scanner was the standard methodology because from it one we captured images that provided information on the whole region of the fruit's peel. We graphically summarize these functions and their respective confidence intervals for each case as follows:

- i) Case 1 (Figure 3.6): agreement among observations measured on the equatorial region by the scanner and colorimeter;
- ii) Case 2 (Figure 3.7): agreement among observations measured on the equatorial region by the colorimeter and on the whole region by the scanner;
- iii) Case 3 (Figure 3.8): agreement among observations measured on the equatorial and whole regions by the scanner.

Figure 3.6 shows that the LCC and LPC between observations measured on the equatorial region by the scanner and colorimeter were smallest at the beginning (0.57 and 0.62 respectively) increasing over time to approximately 0.92. On the other hand, the LA always had estimated values above 0.78 over time, therefore, the only moderate agreement at the beginning

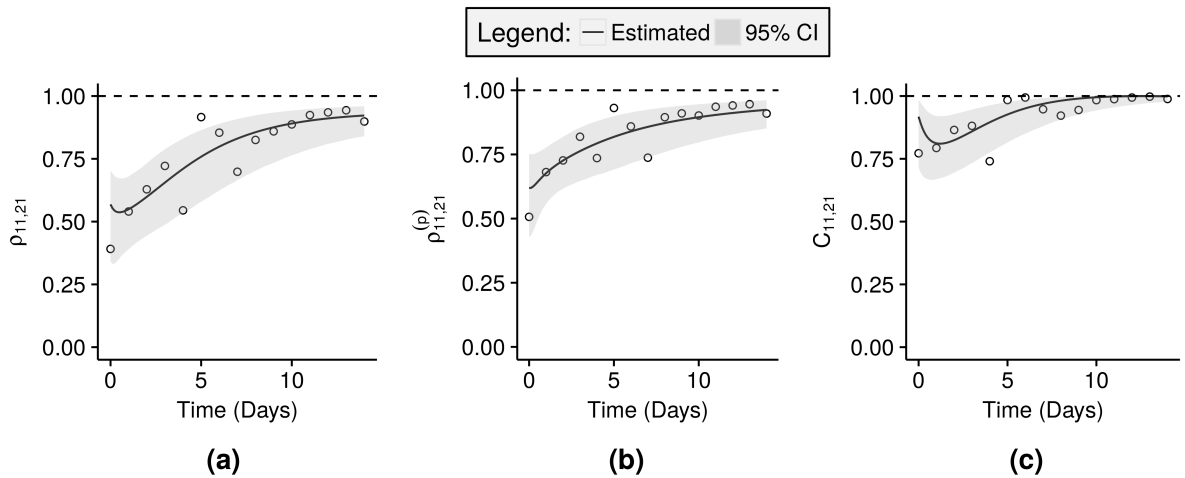


Figure 3.6: Estimate and 95% confidence interval (CI) for the longitudinal concordance correlation (a); longitudinal Pearson correlation (b); and longitudinal accuracy (c) between observations measured on the equatorial region by the scanner and colorimeter with addition of points that represent the concordance correlation coefficient considering independent measurements taken over time

was caused by a lower precision. Consequently, despite the lower precision between them, we can conclude that values of mean hue obtained by the colorimeter were close to those obtained by the scanner on the equatorial region. Moreover, it also indicated that the topography and curved surface of the papaya fruit did not affect, or only slightly affected, the hue measurements taken on its peel by the scanner. Similar results were observed by Mendoza et al. (2006), who verified that the hue color was not affected by the topography and curved surface of green and yellow bananas, or red peppers, when measured by a digital camera.

Although confidence intervals for the LPC for Cases 1 (Figure 3.6) and 2 (Figure 3.7) are similar, the confidence intervals for LA between them over time were different, indicating that the mean hue calculated from observed values by the scanner over the whole region was not close to the observed values from the colorimeter on the equatorial region, especially over the period 0 to 7 days after start of the experiment.

Similar results were also observed between Cases 2 and 3 (Figure 3.8) where the equatorial and whole regions were obtained by the scanner from a common image of both sides of the fruit's peel, reinforcing the conclusion that the whole region of the fruit's peel cannot be represented by sampling only on the equatorial region. Therefore, ideally image analysis of whole fruit's region should be used to compute the mean hue.

Another important characteristic observed from Figures 3.6, 3.7, and 3.8 was that the LCC increased with time, showing a non-uniform ripening process, even when observed only on the equatorial region (Figure 3.6). Many studies such as Bron and Jacomino (2006), Sancho et al. (2010), and Schweiggert et al. (2011) observed that the color changes were non-

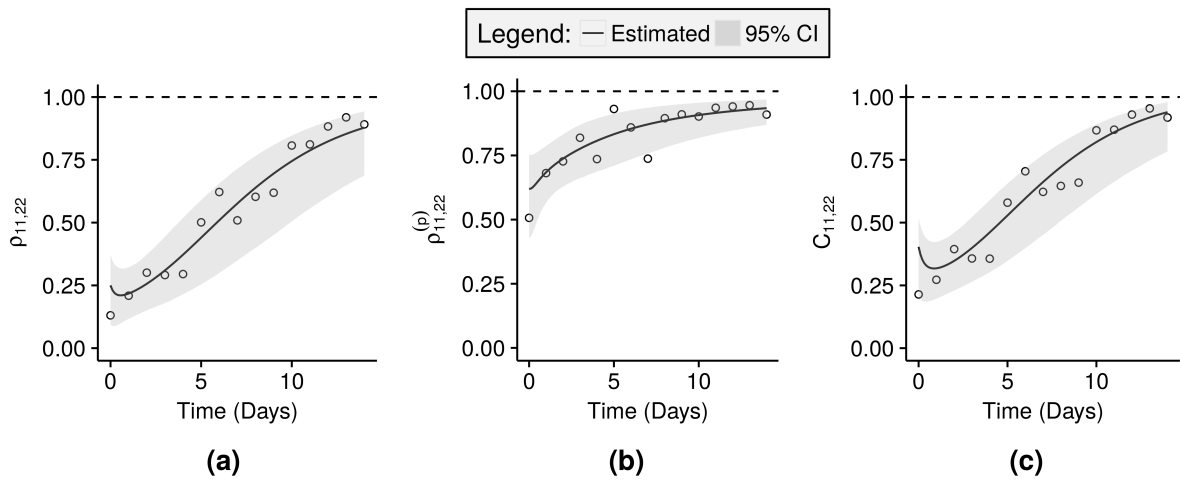


Figure 3.7: Estimate and 95% confidence interval (CI) for the longitudinal concordance correlation (a); longitudinal Pearson correlation (b); and longitudinal accuracy (c) between observations measured on the equatorial region by the colorimeter and whole region by the scanner with addition of respective observed values considering independent measurements taken over time (points)

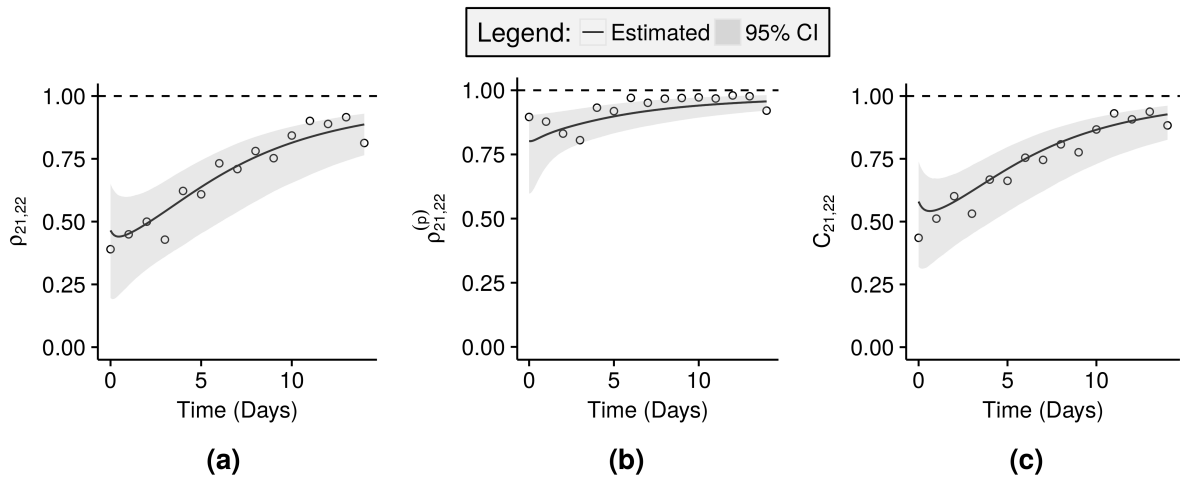


Figure 3.8: Estimate and 95% confidence interval (CI) for the longitudinal concordance correlation (a); longitudinal Pearson correlation (b); and longitudinal accuracy (c) between observations measured on the equatorial and whole regions by the scanner with addition of respective observed values considering independent measurements taken over time (points)

uniform from green to yellow/orange, as the yellow and orange colors on the peel are directly associated with production of carotenoids such as β -cryptoxanthin, β -carotene, and lycopene. Thus, it is plausible to assume that the chlorophyll degradation as well as the production of these carotenoids are also non-uniform over the peel surface.

3.8 Discussion

Our main motivations for this study were to verify if a colorimeter reproduces a scanner and if a sample on the equatorial region can reproduce observation of the whole region in measuring the mean hue on papaya peel. For this, we proposed a LCC for assessing the agreement of paired continuous measurements over time associated with different level combinations of two factors (method and region) based on a mixed-effects regression model. Thus, the main contribution of this paper was describing the longitudinal agreement profile considering different forms for random effects rather than summarizing it in a single coefficient, as proposed by Carrasco et al. (2009).

Evaluating the longitudinal agreement profile can help the researcher to decide in which period the new method reproduces the observed values by the standard method. In Figure 3.6, for example, if we consider that the ideal agreement is given by a lower band of a confidence interval higher than 0.80, then the colorimeter methodology may be used on the equatorial region from the 12th day after harvest. On the other hand, when we used the methodology proposed by Carrasco et al. (2013), we obtained a 95% confidence interval for the CCCrm between 0.7069 and 0.9041, consequently the conclusion would be that the colorimeter may not be used to calculate the mean hue on the fruit's equatorial region, when in fact we demonstrated that it could be used in a specific period.

Clearly the experimental design and study objectives should be taken into account before choosing which method we should use to calculate the agreement between pairs of observations over time. Furthermore, in longitudinal designs, the number and spacing of measurements and missing data mechanisms should also be taken into account. In this way, in further studies we intend to extend this methodology to other forms of missingness. Also, the minimum number of time points that are necessary to use this LCC methodology should not be two, or even three, because this number depends on the change pattern of the response variable over time. Increasing the number of time points, provided that they are not concentrated near a specific time, allows us to use different types of polynomial growth curve models, which can directly influence the calculation of LCC.

Here we treated method and region as fixed effects, however it is possible to extend this methodology to consider the method, region, or both, as random effects. Chen and Barnhart (2013), for example, have already proposed extensions to CCC and the intraclass correlation coefficient based on three-way random-effects ANOVA, discussing about when the observer (or method), time, or both, should be treated as fixed or random effects. Furthermore, as we con-

sider that conditional errors are independent, a possible extension to this methodology could be to include a more complex structure in the error variance-covariance matrix, such as autocorrelation functions. This procedure has been discussed by Rathnayake and Choudhary (2017), who compared independent errors, a first order autoregressive process, a first order moving average process and a compound symmetry model.

Model selection was made from the likelihood ratio test for nested models, and AIC or BIC for non-nested models, to get a more parsimonious description for the data and, consequently, more reliable inference for the LCC. The LCC estimation was based on the REML approach, while $100(1-\alpha)\%$ confidence intervals were obtained using a nonparametric bootstrap approach with case resampling (10,000 bootstrap replicates), as described in section 3.5. The amount of CPU time required to produce these samples was approximately 3,5 hours on a laptop computer with an Intel® Core™ 2.40GHz i7 processor and 4GB of RAM. Moreover, only two convergence problems were encountered. However, note that if the model assumptions are not fulfilled, or if they are not correctly specified, the estimates of LCC as well as its bootstrap confidence intervals may be biased.

The simulations indicated a satisfactory performance of LCC for 20 or more individuals, with robustness to problems caused by dropouts. Although the proposed simulation model assumed independent errors, it can be extended to include a serially autocorrelated error term. In this sense, Rathnayake and Choudhary (2017) proposed a longitudinal concordance correlation based on a semi-parametric model under various autocorrelation function assumptions.

3.9 Conclusions

In this article, we developed a longitudinal concordance correlation as well as its $100(1-\alpha)\%$ bootstrap confidence interval based on the fixed effects and variance components estimates from a multiple mixed-effects polynomial regression model. Its performance was satisfactory as was demonstrated based on simulation study. Further work will focus on developing a LCC for other combinations of random or fixed effects for method, region, or both.

In the substantive application the use of LCC, as well as LPC and LA, showed that sample points only on the equatorial region were not representative of the whole peel region, suggesting that image analysis of the whole peel region should be used to compute the mean hue. Moreover, the LA between observations measured by the colorimeter and scanner on the equatorial region suggested that the topography and curved surface of papaya fruit did not affect the mean hue obtained by the scanner.

Acknowledgments

The authors are grateful to FAPESP (grants #2010/16955-1, São Paulo Research Foundation-FAPESP), CNPq (National Counsel of Technological and Scientific Development), University of São Paulo, and National University of Ireland, that supported this research project.

In addition, we would like to thank the professors Clarice Garcia Borges Demétrio and Renata Alcarde Sermarini for their important contributions on this research.

References

- Barnhart, H. X. and Williamson, J. M. Modeling concordance correlation via GEE to evaluate reproducibility. *Biometrics*, 57(3):931–940, 2001.
- Bron, I. U. and Jacomino, A. P. Ripening and quality of 'Golden' papaya fruit harvested at different maturity stages. *Brazilian Journal of Plant Physiology*, 18(3):389–396, 2006.
- Carrasco, J. L., King, T. S., and Chinchilli, V. M. The concordance correlation coefficient for repeated measures estimated by variance components. *Journal of biopharmaceutical statistics*, 19(1):90–105, 2009.
- Carrasco, J. L., Phillips, B. R., Puig-Martinez, J., King, T. S., and Chinchilli, V. M. Estimation of the concordance correlation coefficient for repeated measures using SAS and R. *Computer Methods and Programs in Biomedicine*, 109:293–304, 2013.
- Chávez-Sánchez, I., Carrillo-López, A., Vega-García, M., and Yahia, E. M. The effect of anti-fungal hot-water treatments on papaya postharvest quality and activity of pectinmethyl esterase and polygalacturonase. *Journal of Food Science and Technology*, 50(1):101–107, 2013.
- Chen, C. C. and Barnhart, H. X. Assessing agreement with intraclass correlation coefficient and concordance correlation coefficient for data with repeated measures. *Computational Statistics and Data Analysis*, 60:132–145, 2013.
- Chinchilli, V. M., Martel, J. K., Kumanyika, S., and Lloyd, T. A Weighted Concordance Correlation Coefficient for Repeated Measurement Designs. *Biometrics*, 52(1):341–353, 1996.
- Darrigues, A., Hall, J., Knaap, E. V. D., Francis, D. M., Dujmovic, N., and Gray, S. Tomato Analyzer-color Test : A New Tool for Efficient Digital Phenotyping. *Journal of the American Society for Horticultural Science*, 133(4):579–586, 2008.
- Evans, E. A. and Ballen, F. H. An Overview of Global Papaya Production , Trade , and. Technical report, University of Florida, Florida, 2015.
- Fisher, N. I. *Statistical analysis of circular data*. Cambridge University Press, New York, 1 edition, 1993.
- Fitzmaurice, G., Davidian, M., Verbeke, G., and Molenberghs, G. *Longitudinal data analysis*. Chapman & Hall/CRC, New York, 1 edition, 2009.
- Hiriote, S. and Chinchilli, V. M. Matrix-based Concordance Correlation Coefficient for Repeated Measures. *Biometrics*, 67:1007–1016, 2011.

- Ihaka, R., Murrell, P., Hornik, K., Fisher, J. C., and Zeileis, A. Color Space Manipulation, 2015.
- Kimball, S., Mattis, P., and The GIMP Development Team. GNU Image Manipulation Program, 2014. URL <http://www.gimp.org/>.
- King, T. S. and Chinchilli, V. M. A generalized concordance correlation coefficient for continuous and categorical data. *Statistics in Medicine*, 20(14):2131–2147, 2001.
- King, T. S., Chinchilli, V. M., and Carrasco, J. L. A repeated measures concordance correlation coefficient. *Statistics in medicine*, 26:3095–3113, 2007a.
- King, T. S., Chinchilli, V. M., Wang, K.-L., and Carrasco, J. L. A class of repeated measures concordance correlation coefficients. *Journal of biopharmaceutical statistics*, 17:653–672, 2007b.
- Konica Minolta. *Precise colour communication, colour control from perception to instrumentation*. Konica Minolta Sensing, 2003.
- Krippendorff, K. Bivariate Agreement Coefficients for Reliability of Data. *Sociological Methodology*, 2:139–150, 1970. ISSN 07591063.
- Lin, L. I. A Concordance Correlation Coefficient to Evaluate Reproducibility. *Biometrics*, 45(1):255–268, 1989.
- Lindstrom, M. J. and Bates, D. M. Nonlinear Mixed Effects Models for Repeated Measures Data. *Biometrics*, 46(3):673–687, 1990.
- Mardia, K. V., Hughes, G., Taylor, C. C., and Singh, H. A Multivariate Von Mises Distribution with Applications to Bioinformatics. *The Canadian Journal of Statistics*, 36(1):99–109, 2008.
- Mardia, K. V. and Jupp, P. E. *Directional Statistics*. John Wiley & Sons, New York, 2000.
- Martins, D. R., Barbosa, N. C., and Resende, E. D. D. Respiration rate of Golden papaya stored under refrigeration and with different controlled atmospheres. *Scientia Agricola*, 71(5):345–355, 2014.
- Mendoza, F. and Aguilera, J. M. Application of image analysis for classification of ripening bananas. *Journal of food science*, 69(9):471–477, 2004.
- Mendoza, F., Dejmek, P., and Aguilera, J. M. Calibrated color measurements of agricultural foods using image analysis. *Postharvest Biology and Technology*, 41(3):285–295, 2006.
- Minolta. *Chroma meter instruction manual*. Minolta Company, Japan, 1991.
- Munsell Color Company. *Munsell color charts for plant tissues*. Munsell Color Company, Baltimore, 1952.

- Oliveira, T. P., Zocchi, S. S., and Jacobino, A. P. Measuring color hue in 'Sunrise Solo' papaya using a flatbed scanner. *Revista Brasileira de Fruticultura*, 2017.
- Pinheiro, J. C. and Bates, D. M. *Mixed-Effects Models in S and S-PLUS*. Springer, New York, 2000.
- R core Team. The R environment, 2015. URL <https://www.r-project.org/>.
- Rathnayake, L. N. and Choudhary, P. K. Semiparametric modeling and analysis of longitudinal method comparison data. *Statistics in Medicine*, 36(13):2003–2015, 2017.
- Ridler, T. and Calvard, S. Picture Thresholding Using an Iterative Selection Method. *IEEE Transactions on Systems, Man and Cybernetics*, 8(8):630–632, 1978.
- Sancho, L. E. G., Yahia, E. M., Martínez-Téllez, M. A., and González-Aguilar, G. A. Effect of Maturity Stage of Papaya Maradol on Physiological and Biochemical Parameters. *American Journal of Agricultural and Biological Science*, 5(2):194–203, 2010.
- Schweiggert, R. M., Steingass, C. B., Mora, E., Esquivel, P., and Carle, R. Carotenogenesis and physico-chemical characteristics during maturation of red fleshed papaya fruit (*Carica papaya* L.). *Food Research International*, 44(5):1373–1380, 2011.
- Silva-Ayala, T., Schnell, R. J., Meerow, A. W., Winterstein, M., Cervantes, C., and Brown, J. S. Determination of Color and Fruit Traits of Half-Sib Families of Mango (*Mangifera Indica* L .). *Proceedings of the Florida State Horticultural Society*, 118:253–257, 2005.
- Sivakumar, D. and Wall, M. M. Papaya Fruit Quality Management during the Postharvest Supply Chain. *Food Reviews International*, 29:24–48, 2013. ISSN 87559129.
- Thai, H. T., Mentré, F., Holford, N. H. G., Veyrat-Follet, C., and Comets, E. A comparison of bootstrap approaches for estimating uncertainty of parameters in linear mixed-effects models. *Pharmaceutical Statistics*, 12(3):129–140, 2013.
- Verbeke, G. and Molenberghs, G. *Linear mixed models for longitudinal data*. Springer, New York, 2000.
- Wu, D. and Sun, D. W. Colour measurements by computer vision for food quality control - A review. *Trends in Food Science and Technology*, 29(1):5–20, 2013.

4 ESTIMATION OF THE LONGITUDINAL CONCORDANCE CORRELATION FUNCTION IN R: THE LCC PACKAGE

Abstract: Suppose a longitudinal study where two or more methods are used to quantify a continuous measurement at same individual and the researcher goal is describe the extent of agreement among them. This agreement can be performed using the longitudinal concordance correlation, which are functions of parameters of the assumed model. In this sense, we present the `lcc` package under development for publication in the comprehensive R archive network (CRAN) with two applications involving papaya hue color in post-harvest, and cortisol concentrations from blood draw samples in the medical area. The package implements estimation procedures for longitudinal concordance correlation, longitudinal Pearson correlation, and longitudinal accuracy through fixed effects and variance components of polynomial mixed-effect regression model. The main features of the package are its ability to perform inference about the extent of agreement and use a numerical and graphical to summary the fitted values, sampled values, and confidence intervals. Moreover, our approach accommodate balanced or unbalanced experimental design, allows to model heteroscedasticity among within-group errors using or not the time as variance covariate, and also allows for inclusion of covariates in the linear predictor to control systematic variations in the response variable.

KEYWORDS: Extent of agreement, Polynomial mixed-effects regression model, Bootstrap procedures, Heteroscedasticity, R

4.1 Introduction

Agreement indexes are generally used when the same experimental unit is assessed by at least two methods or observers. The concordance correlation coefficient (CCC) introduced by Lin (1989) is a common statistic used to measure the agreement between methods when data are continuous. Let Y_1 and Y_2 be two random variables with joint distribution

$$\begin{bmatrix} Y_1 \\ Y_2 \end{bmatrix} \sim N_2 \left(\begin{bmatrix} \mu_1 \\ \mu_2 \end{bmatrix}, \Sigma = \begin{bmatrix} \sigma_1^2 & \sigma_{12} \\ \sigma_{12} & \sigma_2^2 \end{bmatrix} \right).$$

Here the expected value of the squared difference between Y_1 and Y_2 can be used as a agreement value. However, it ranges from 0 (perfect agreement) to infinity, which makes its interpretation more laborious. Lin (1989) proposed a transformation to this agreement index so that the values lie between -1 and 1:

$$\rho_{CCC} = 1 - \frac{E[(Y_1 - Y_2)^2]}{\sigma_1^2 + \sigma_2^2 + (\mu_1 - \mu_2)^2} = \frac{2\sigma_{12}}{\sigma_1^2 + \sigma_2^2 + (\mu_1 - \mu_2)^2} = \rho C_b,$$

where $\mu_1 = E(Y_1)$, $\mu_2 = E(Y_2)$, $\sigma_1^2 = Var(Y_1)$, $\sigma_2^2 = Var(Y_2)$, $\sigma_{12} = Cov(Y_1, Y_2)$. This makes the coefficient -1 when perfect disagreement, zero when no agreement, and 1 when perfect agreement. Moreover, ρ is the Pearson correlation coefficient ($|\rho| \leq 1$) that measures how far each observation deviated from the best-fit line (precision measure), and C_b is the accuracy ($0 < C_b \leq 1$) that measures how far the best-fit line deviates from the 45° line through the origin. The last component is defined as $C_b = 2(v + v^{-1} + u^2)^{-1}$, where $v = \sigma_1^2/\sigma_2^2$ is a scale shift and $u = (\mu_1 - \mu_2)/\sqrt{\sigma_1\sigma_2}$ is a location shift relative to the scale.

When the pair of samples (Y_{i1k}, Y_{i2k}) , $k = 1, 2, \dots, K$, is measured together on the same subject or experimental unit over time, the use of generalized multivariate analysis of variance to compute a weighted version of CCC for repeated measurement is recommended (Chinchilli *et al.*, 1996). Moreover, this coefficient has also been expanded to assess the agreement among more than two methods (King and Chinchilli, 2001).

When it is necessary to include a random variability due to subject and/or covariates in the model, the CCC can be estimated through the variance components (VC) of a mixed-effects model (Carrasco *et al.*, 2009). The advantages is that mixed-effects model represent an alternative to analyze repeated measures and unbalanced data; they allow for the inclusion of different variance-covariance structures for the random effects or error matrices; and the restricted maximum likelihood (REML) approach is used to obtain the estimates of VC.

Nevertheless, sometimes the researcher is not interested in summarizing the CCC for repeated measurements in a single coefficient, as proposed by Carrasco *et al.* (2009) and Carrasco *et al.* (2013), but in describing the extent of agreement between methods over time. To do this, we can consider a linear or non-linear function of the time and/or covariates in the model to describe the response variable, as proposed in the Chapter 3 and by Rathnayake and Choudhary (2017). Thus, in this chapter we proposed the development of R (R core Team, 2017) package

called `lcc`, which provides functions for estimating the longitudinal concordance correlation (LCC) among methods based on variance components and fixed effects of polynomial mixed-effects model. It also computes estimates of the longitudinal Pearson correlation (LPC), a precision measure, and the longitudinal bias corrector factor (LA), a accuracy measure.

The `lcc()` function gives fitted values and non-parametric bootstrap confidence intervals for the LCC, LPC, and LA statistics. Moreover, they can be estimated using different structures for variance-covariance matrices of random effects and variance functions to model heteroscedasticity among within-group errors using or not the time as variance covariate.

The remainder of the paper is organized as follows: Section 4.2 introduces the theoretical definition of LCC as well as its point estimation, and the computation of simultaneous confidence intervals is briefly summarized with references for more details. Section 4.3 introduces the input and output of the `lcc` function, describing in detail the arguments as well as the generic function summary applied to the `lcc()` function. On Section 4.5, we illustrates the usage of the package with a real data example. Section 4.6 reviews the `cccrm` R package which is capable to estimate the CCC for longitudinal data and compares it with our package. Section 4.7 presents a discussion on advantages of the LCC, and some caveats on using this methodology and associated bootstrap confidence intervals. Section 4.8 gives an outlook on possible future extensions of our package. Finally, Section 4.9 presents some final considerations about our package.

4.2 The longitudinal concordance correlation (LCC)

We assume that the researcher is interested in investigating the extent of agreement between two or more methods, indexed as $j = 1, 2, \dots, J$. Suppose there are N subjects in the experiment or observational study, indexed as $i = 1, 2, \dots, N$, and each subject is observed n_i times (visits). Let y_{ijk} be a realization of random variable Y_{ijk} measured on the i th subject by the j th method at time t_k , $k = 1, 2, \dots, n_i$. Here t_k assumes values of the time covariate $t \in \mathcal{T}$. Thus, the linear mixed effects model considering a polynomial function of the time, the fixed effect of method as well as their interactions and by-subject random polynomial coefficient are given by

$$y_{ijk} = \sum_{h=0}^p \beta_{hj} t_{ik}^h + \sum_{h=0}^q b_{hi} t_{ik}^h + \epsilon_{ijk} \quad (4.1)$$

$$\boldsymbol{b}_i \sim N_q(\mathbf{0}, \boldsymbol{G}) \quad \text{and} \quad \boldsymbol{\epsilon}_i \sim N_{Jn_i}(\mathbf{0}, \boldsymbol{R}_i)$$

where $h = 1, 2, \dots, q, q+1, \dots, p$ is an index identifying the degree of linear mixed effects polynomial model, with $q \leq p$; y_{ijk} is the response measured on the of i th subject measured by the j th method at time t_{ik} ; t_{ik} represent the time (seconds, minutes, weeks, days, years...) at which the i th individual was observed; $\boldsymbol{\beta}_j = [\beta_{0j}, \beta_{1j}, \dots, \beta_{pj}]^T$ is a $(p+1)$ -dimensional vector of fixed effects for the j th method; $\boldsymbol{b}_i = [b_{0i}, b_{1i}, \dots, b_{qi}]^T$ is a $(q+1)$ -dimensional vector of random

effects with mean vector $\mathbf{0}$ and variance-covariance matrix \mathbf{G} ; $\boldsymbol{\epsilon}_i$ is a (Jn_i) -dimensional vector assumed to be independent for different i, j and k , and independent of random effects, with mean vector $\mathbf{0}$ and covariance matrix \mathbf{R}_i , and \mathbf{R}_i is a $Jn_i \times Jn_i$ matrix of variance-covariance for errors, which depends on i only through its dimension n_i and is assumed to be positive-definite. Here we define $\mathbf{R}_i = \sigma_\epsilon^2 \boldsymbol{\Sigma}_i(\boldsymbol{\delta})$, where $\boldsymbol{\delta}$ are ratios relative to σ_ϵ^2 .

Under the model (4.1), the longitudinal concordance correlation (LCC) is given by

$$\rho_{jj'}(t_k) = \frac{\mathbf{t}_k \mathbf{G} \mathbf{t}_k^T}{\mathbf{t}_k \mathbf{G} \mathbf{t}_k^T + \frac{1}{2} \{ \sigma_\epsilon^2 [g(t_k, \boldsymbol{\delta}_j) + g(t_k, \boldsymbol{\delta}_{j'})] + S_{jj'}^2(t_k) \}} = \rho_{jj'}^{(p)}(t_k) C_{jj'}(t_k) \quad (4.2)$$

where $S_{jj'}(t_k) = \mathbf{t}_k (\boldsymbol{\beta}_j - \boldsymbol{\beta}_{j'})$ is the systematic difference between methods j and j' ; $\mathbf{t}_k^T = (t_k^0, t_k^1, \dots, t_k^q)^T$; $g(\cdot)$ is a variance function assumed continuous in $\boldsymbol{\delta}$; $\boldsymbol{\delta}_j$ is a vector of variance components for observations measured by the j th method or observer; $\rho_{jj'}^{(p)}(t_k)$ is the longitudinal Pearson correlation (LPC) that measures how far each observation deviated from the best-fit line at a fixed time $t_k = t$ and is given by

$$\rho_{jj'}^{(p)}(t_k) = \frac{\mathbf{t}_k \mathbf{G} \mathbf{t}_k^T}{\sqrt{[\mathbf{t}_k \mathbf{G} \mathbf{t}_k^T + \sigma_\epsilon^2 g(t_k, \boldsymbol{\delta}_j)] [\mathbf{t}_k \mathbf{G} \mathbf{t}_k^T + \sigma_\epsilon^2 g(t_k, \boldsymbol{\delta}_{j'})]}}$$

and $C_{jj'}(t_k)$ is the longitudinal accuracy (LA) that measures how far the best-fit line deviates from the 45° line at a fixed time $t_k = t$ and is given by

$$C_{jj'}(t_k) = \frac{2}{v_{jj'}(t_k) + [v_{jj'}(t_k)]^{-1} + u_{jj'}^2(t_k)}$$

where

$$v_{jj'}(t_k) = \sqrt{\frac{Var(Y_{ijk})}{Var(Y_{ij'k})}} = \sqrt{\frac{\mathbf{t}_k \mathbf{G} \mathbf{t}_k^T + \sigma_\epsilon^2 g(t_k, \boldsymbol{\delta}_{jl})}{\mathbf{t}_k \mathbf{G} \mathbf{t}_k^T + \sigma_\epsilon^2 g(t_k, \boldsymbol{\delta}_{j'l'})}}$$

denotes the scale shift at time $t_k = t$ and

$$\begin{aligned} u_{jj'}(t_k) &= \frac{E(Y_{ijk}) - E(Y_{ij'k})}{[Var(Y_{ijk}) Var(Y_{ij'k})]^{\frac{1}{4}}} \\ &= \frac{\mathbf{t}_k (\boldsymbol{\beta}_j - \boldsymbol{\beta}_{j'})}{\{[\mathbf{t}_k \mathbf{G} \mathbf{t}_k^T + \sigma_\epsilon^2 g(t_k, \boldsymbol{\delta}_j)] [\mathbf{t}_k \mathbf{G} \mathbf{t}_k^T + \sigma_\epsilon^2 g(t_k, \boldsymbol{\delta}_{j'})]\}^{\frac{1}{4}}} \end{aligned}$$

denotes the location shift at time t_k relative to the scale (see Chapter 3). Moreover, when $Var(Y_{ijkl}) = Var(Y_{ij'l'k})$ and $E(Y_{ijkl}) = E(Y_{ij'l'k})$ there is no deviation from the 45° line.

4.2.1 Estimation

The point estimation and statistical inference of LCC has been proposed in Chapter 3. $\rho_{jj'}^{(p)}$ is estimated by replacing the $\boldsymbol{\beta}$, and variance components by their REML estimates:

$$\hat{\rho}_{jj'}(t_k) = \frac{\mathbf{t}_k \hat{\mathbf{G}} \mathbf{t}_k^T}{\mathbf{t}_k \hat{\mathbf{G}} \mathbf{t}_k^T + \frac{1}{2} \{ \hat{\sigma}_\epsilon^2 [\hat{g}(t_k, \hat{\boldsymbol{\delta}}_j) + \hat{g}(t_k, \hat{\boldsymbol{\delta}}_{j'})] + \hat{S}_{jj'}^2(t_k) \}}.$$

Because the variance components are estimated using REML approach, their estimates have asymptotically normal distribution as well as it is less biased than using maximum likelihood (ML) approach. Moreover, we demonstrated in Chapter 3 a satisfactory performance of the LCC even under severe conditions of unbalance and for low number of subjects (N=20).

For constructing a confidence interval for $\rho_{j,j'}(t_k)$, we use a nonparametric bootstrap percentile method for $N \leq 30$ or, otherwise, a normal approximation confidence intervals considering B bootstrap samples, as described in Chapter 3.

When we use a normal approximation CI, the Fisher Z-transformation given by

$$\rho_{j,j'}^*(t_k) = \frac{1}{2} \ln \left(\frac{1 + \rho_{j,j'}(t_k)}{1 - \rho_{j,j'}(t_k)} \right)$$

should be used to approximate the empirical distribution of $\rho_{j,j'}(t_k)$ using the normal distribution (Lin, 1989). Consequently, for inference on $\rho_{j,j'}(t_k)$ confidence limits can be estimated using the bootstrap estimator of $\rho_{j,j'}^*(t_k)$ for a fixed time $t_k = t$ given by

$$\widehat{\rho}_{j,j'}^*(t_k = t) = \frac{1}{2B} \sum_{b=1}^B \ln \left[\frac{1 + \rho_{j,j'}^{(b)}(t)}{1 - \rho_{j,j'}^{(b)}(t)} \right], \quad b = 1, 2, \dots, B,$$

and standard deviation of the bootstrap distribution of $\widehat{\rho}_{j,j'}^*(t_k)$ for a fixed time $t_k = t$ given by

$$\widehat{SE}_{j,j'}^*(t_k = t) = \sqrt{\frac{1}{B-1} \sum_{b=1}^B \left[\frac{1}{2} \ln \left(\frac{1 + \rho_{j,j'}^{(b)}(t)}{1 - \rho_{j,j'}^{(b)}(t)} \right) - \widehat{\rho}_{j,j'}^*(t) \right]^2}.$$

Thus, an approximate bootstrap confidence interval of level $1 - \alpha$ for $\widehat{\rho}_{j,j'}$ is $[LB, UB]$, where

$$LB = \frac{\exp \left\{ 2 \left[\widehat{\rho}_{j,j'}^*(t_k = t) - z_{(1-\frac{\alpha}{2})} \widehat{SE}_{j,j'}^*(t_k = t) \right] \right\} - 1}{\exp \left\{ 2 \left[\widehat{\rho}_{j,j'}^*(t_k = t) - z_{(\frac{\alpha}{2})} \widehat{SE}_{j,j'}^*(t_k = t) \right] \right\} + 1}$$

and

$$UB = \frac{\exp \left\{ 2 \left[\widehat{\rho}_{j,j'}^*(t_k = t) - z_{\frac{\alpha}{2}} \widehat{SE}_{j,j'}^*(t_k = t) \right] \right\} - 1}{\exp \left\{ 2 \left[\widehat{\rho}_{j,j'}^*(t_k = t) - z_{\frac{\alpha}{2}} \widehat{SE}_{j,j'}^*(t_k = t) \right] \right\} + 1}.$$

where $z_{\frac{\alpha}{2}}$ and $z_{(1-\frac{\alpha}{2})}$ are the $\frac{\alpha}{2}$ and $1 - \frac{\alpha}{2}$ quantiles of the standard normal distribution.

On the other hand, CI based on the percentile method uses the percentiles of bootstrap distribution of $\widehat{\rho}_{j,j'}(t_k = t)$, and is given by

$$\left(\widehat{\rho}_{j,j'(\alpha/2)}(t_k = t), \widehat{\rho}_{(j,j')(1-\alpha/2)}(t_k = t) \right) \approx \left(\widehat{\rho}_{j,j'(\alpha/2)}^{*(B)}(t_k = t), \widehat{\rho}_{(j,j')(1-\alpha/2)}^{*(B)}(t_k = t) \right),$$

where $\widehat{\rho}_{(j,j')(\alpha/2)}^{*(B)}(t_k = t)$ and $\widehat{\rho}_{(j,j')(1-\alpha/2)}^{*(B)}(t_k = t)$ are the $100 \times \frac{\alpha}{2}$ th and $100 \times 1 - \frac{\alpha}{2}$ th empirical percentiles of the $\widehat{\rho}_{j,j'}^{*(b)}(t_k = t)$ values, $b = 1, 2, \dots, B$. If the bootstrap distribution of

$\rho_{j,j'}^*(t_k = t)$ is approximately normal, then both methods proposed to compute the CI will be very similar as N increase.

Furthermore, the inference about $\hat{\rho}_{jj'}^{(p)}(t_k)$ can be performed in a similar way as presented for LCC. Since $C_{(j,j')(1-\alpha/2)}(t_k = t)$ belong to the $[0, 1]$ interval, we can use the logit transformation

$$C_{(j,j')(1-\alpha/2)}^*(t_k = t) = \log \left(\frac{C_{(j,j')(1-\alpha/2)}(t_k = t)}{1 - C_{(j,j')(1-\alpha/2)}(t_k = t)} \right)$$

instead of the Fisher Z-transformation to approximate the distribution of $C_{(j,j')(1-\alpha/2)}(t_k = t)$ to the normal distribution. Thus, the confidence limits can be estimated using the bootstrap estimator of $C_{j,j'}^*(t_k)$ for a fixed time $t_k = t$ given by

$$\hat{C}_{j,j'}^*(t_k = t) = \frac{1}{B} \sum_{b=1}^B \log \left[\frac{C_{j,j'}^{(b)}(t)}{1 - C_{j,j'}^{(b)}(t)} \right], \quad b = 1, 2, \dots, B,$$

and standard deviation of the bootstrap distribution of $\hat{C}_{j,j'}^*(t_k)$ for a fixed time $t_k = t$ given by

$$\widehat{SE}_{C_{j,j'}}^*(t_k = t) = \sqrt{\frac{1}{B-1} \sum_{b=1}^B \left[\log \left(\frac{C_{j,j'}^{(b)}(t)}{1 - C_{j,j'}^{(b)}(t)} \right) - \hat{C}_{j,j'}^*(t) \right]^2}.$$

Therefore, an approximate bootstrap confidence interval of level $1 - \alpha$ for $\hat{C}_{j,j'}$ is $[LB_C, UB_C]$, where

$$LB_C = \frac{\exp \left[\hat{C}_{j,j'}^*(t_k = t) - z_{(1-\frac{\alpha}{2})} \widehat{SE}_{C_{j,j'}}^*(t_k = t) \right]}{\exp \left[\hat{C}_{j,j'}^*(t_k = t) - z_{(1-\frac{\alpha}{2})} \widehat{SE}_{C_{j,j'}}^*(t_k = t) \right] + 1}$$

and

$$UB_C = \frac{\exp \left[\hat{C}_{j,j'}^*(t_k = t) - z_{\frac{\alpha}{2}} \widehat{SE}_{C_{j,j'}}^*(t_k = t) \right]}{\exp \left[\hat{C}_{j,j'}^*(t_k = t) - z_{\frac{\alpha}{2}} \widehat{SE}_{C_{j,j'}}^*(t_k = t) \right] + 1}.$$

where $z_{\frac{\alpha}{2}}$ and $z_{(1-\frac{\alpha}{2})}$ denoting $\frac{\alpha}{2}$ and $1 - \frac{\alpha}{2}$ quantiles of the standard normal distribution.

4.3 Overview of the package **lcc** and R syntax

This section provide some details on the implementation of the **lcc** function and explain its technical arguments, whose default settings were chosen carefully. We use the **nlme** package to formulate the polynomial mixed effects model and from their fixed effects and variance components there are functions to estimate the LCC, LPC, and LA statistics.

The **lcc** package has 21 arguments that are briefly summarized in Table 4.1. Note that through the arguments **qf** and **qr** users can decide the degree of the polynomial regression model, and by-subject random effect, respectively.

Table 4.1: Input arguments for LCC package

Argument	Type	Description	Required
<code>dataset</code>	An object of class <code>data.frame</code>	Specifies the input dataset	Yes
<code>subject</code>	Character string	Name of the subject variable	Yes
<code>resp</code>	Character string	Name of the response variable	Yes
<code>factorA</code>	Character string	Name of the method variable	Yes
<code>time</code>	Character string	Name of the time variable	Yes
<code>qf</code>	Value	Polynomial degree for fixed part	Yes
<code>qr</code>	Value	Polynomial degree for by-subject random effect	Yes
<code>time.lcc</code>	List	Specifying control arguments to generate regular sequences for time variable to compute the LCC. Default is <code>NULL</code>	No
<code>ci</code>	TRUE/FALSE	Bootstrap confidence interval. Default is FALSE.	No
<code>alpha</code>	Value	Confidence level. Default is 0.05.	No ¹
<code>percentile.ci</code>	TRUE/FALSE	Method of bootstrap confidence intervals (CI). If FALSE, the default, normal approximation method is used to compute CI. If TRUE, the percentile method is used.	No ¹
<code>nboot</code>	Value	Number of bootstrap samples. Default is 5.000.	No ¹
<code>pdmat</code>	Function	Standard classes of positive-definite matrices structures available in the <code>nlme</code> package. Default is <code>pdSymm</code>	No
<code>covar</code>	Character vector	Name of covariates to include in the model as fixed effects. Default is <code>NULL</code> .	No
<code>var.class</code>	Function	Standard classes of variance function structures available in the <code>nlme</code> package. Default is <code>NULL</code>	No

Continued on next page

¹It can only be specified when `ci=TRUE`

Table 4.1 – continued from previous page

Argument	Type	Description	Required
<code>weights.form</code>	Character string	An one-sided formula specifying a variance covariate and, optionally, a grouping factor for the variance parameters in the <code>var.class</code> . If <code>var.class = varIdent</code> , the form “method”, $\sim 1 \text{factorA}$ must be used. If <code>var.class = varExp</code> , the form “time”, $\sim \text{time}$, or “both”, $\sim \text{time} \text{factorA}$, must be used.	No ²
<code>show.warnings</code>	TRUE/FALSE	If FALSE, the default, shows the number of convergence error in the bootstrap samples. If TRUE shows in which bootstrap sample the error occurred.	No
<code>components</code>	TRUE/FALSE	If FALSE, the default, provides only the LCC. If TRUE, the function provides the LCC, LPC, and LA components.	No
<code>plot</code>	List	A list of control values or character string applicable to ggplot for graphics control that replace the default values returned by the <code>plot.control</code> function. Defaults to an empty list.	No
<code>lme.control</code>	List	Specifying control values for lme fit by the function <code>lmeControl</code> . Defaults to an empty list.	No
<code>REML</code>	TRUE/FALSE	If TRUE, the default, the restricted log-likelihood is maximized to fit the model. If FALSE the log-likelihood (ML) is maximized.	No

A more detailed description of some arguments is as follows:

1. **dataset**: specifies the input dataset, whose form must be of a data frame containing the response variable, subject identification, method, and the time that indicates the moment, in seconds, minutes, hours, days etc., at which each observation was measured;
2. **factorA**: name of method/observer variable in the dataset, the LCC package recognizes the first level of variable associated with this argument as the gold-standard method and then compares it with all other levels;

²Required when `var.class` is specified.

3. **time.lcc**: specifies a list with settings (values for arguments **from**, **to**, and **n**) used in the **time.lcc()** function to generate a regular sequence for predictions from the results of LCC, LPC and LA estimating functions. Arguments **from** and **to** are used to define, respectively, the starting and end values of the time variable, and **n** is used to specify the desired length of the sequence. We recommend a grid $\mathbf{t} = (t_1, t_2, \dots, t_{n^*})^T$ of n^* points in \mathcal{T} to constructed the agreement curve and simultaneous confidence intervals. In practice, n^* between 30 and 50 in generally adequate. Example:

```
R> lcc(..., time.lcc=list(from=0, to=10, n=40))
```

4. **ppmat**: the **lcc** package provides six standard classes of positive-definite matrices structures available in the **nlme** package. They are **pdSymm**, **pdLogChol**, **pdDiag**, **pdIdent**, **pdCompSymm** and **pdNatural**. More information about these classes are available in Pinheiro and Bates (2000).
5. **var.class**: a class of variance functions that are used to model the variance structure of within-group errors using covariates (Pinheiro and Bates, 2000). We generalize this class as

$$\text{Var}(\epsilon_{ijk}) = \sigma_\epsilon^2 g(t_k, \boldsymbol{\delta}), \quad (4.3)$$

where $g(\cdot)$ is the variance function assumed continuous in $\boldsymbol{\delta}$; t_k is the covariate time and $\boldsymbol{\delta}$ is a vector of variance parameters. The **LCC** package provides two different standard variance functions classes that are included in the **nlme** library (Pinheiro *et al.*, 2017).

The first one is the **varIdent** class that represents a variance model with different variances for each level of a stratification variable s , $s = 1, 2, \dots, S$, given by

$$\text{Var}(\epsilon_{ijk}) = \sigma_\epsilon^2 \delta_{s_{ijk}}^2.$$

As we have $S+1$ parameters to represent S variances, we need to impose the restriction $\delta_1 = 1$, consequently $\delta_l = \delta_{s^*}/\delta_1$, $s^* = 2, 3, \dots, S$ and $\delta_l > 0$, $l = 2, 3, \dots, S$. Here each level of method/observer or time represents a stratum of a homogeneous subgroup.

The second variance function is an exponential function of the variance covariate, **varExp** class, represented as

$$\text{Var}(\epsilon_{ijk}) = \sigma_\epsilon^2 \exp(2\delta_{s_{ijk}} t_k)$$

where $\delta_{s_{ijk}}$ is unrestricted, so the variance model (4.4) allows to $\text{Var}(\epsilon_{ijk})$ increases or decreases over time.

6. **weights.form**: represents a constructor to the **form** argument in the standard **varFunc** classes included in the **nlme** library. **weights.form** is a one-sided formula specifying a variance covariate and, optionally, a grouping factor for the variance parameters. Moreover, this argument must be specified only when **var.class** is specified as well.

The first class **varIdent** represents a variance model with different variances for each level of grouping factor, whose **weights.form** in the LCC package is as follows:

- a) “method”: specifies a variance model with different variances for each level of factor method/observer and is given by

$$\text{Var}(\epsilon_{ijk}) = \sigma_\epsilon^2 \delta_{\text{method}_j}^2, \quad j = 1, 2, \dots, J,$$

where $g(\text{method}_j, \delta_j) = \delta_{\text{method}_j}^2$ is the variance function, and δ_{method_j} is the variance parameter for observations measured by the j th method. The form argument in the **varFunc** is **form = ~ 1 | method;**

The class **varExp** represents a variance model whose variance function $g()$ is an exponential function of the variance covariate. This class has also two options of **weights.form** in the LCC package as follows:

- a) “time”: specifies a variance model given by

$$\text{Var}(\epsilon_{ijk}) = \sigma_\epsilon^2 \exp(2\delta t_k),$$

where the variance function $g(t_k, \delta) = \exp(2\delta t_k)$ is an exponential function of the time $t_k = t$; and δ is the variance parameter. The form argument in **varFunc** class is **form = ~ time;**

- b) “both”: specifies a variance model for each level of factor method given by

$$\text{Var}(\epsilon_{ijk}) = \sigma_\epsilon^2 \exp\left(2\delta_{\text{method}_j} t_k\right), \quad j = 1, 2, \dots, J,$$

where the variance function $g(t_k, \text{method}_j, \delta) = \exp\left(2\delta_{\text{method}_j} t_k\right)$ is an exponential function of the time $t_k = t$ for each level of method; and δ_{method_j} is the variance parameter for the j th level of method. The form argument in the **varFunc** is **form = ~ time | method;**

7. **plot**: A list of control values or character string applicable to **ggplot** (Wickham, 2009) for graphics control that replace the default values returned by the function **plot.control**. Provides plots for model estimates and their 95% simultaneous confidence intervals based on bootstrap techniques. This function has 10 additional arguments that possibility changes in shape, size, color, axis labels and limits. Furthermore, when the argument **plot=TRUE**, the default, returns a **ggplot** object with an initial plot for LCC class. If the number of method levels is greater than 2, the argument **all.plot=TRUE**, the default, returns an object created by the **viewport** function with multiple plots in a single one page, otherwise, if **all.plot=False**, the function returns a single **ggplot** object by page.

Table 4.2: Observations (*Obs*) from 1 to 4 and 278 to 281 of the hue color dataset. The response variable is *H_mean*, *Method* represents the method/observer variable, *Time* represents the time variable, and *Fruit* shows the subject identification variable

Obs	H_mean	Method	Time	Fruit
1	116.54	Colorimeter	0	1
2	115.41	Colorimeter	0	2
3	116.98	Colorimeter	0	3
4	115.88	Colorimeter	0	4
:	:	:	:	:
278	106.32	Scanner	6	1
279	103.53	Scanner	6	2
280	111.55	Scanner	6	3
281	104.73	Scanner	6	4

As an example of the appropriate hierarchical structure of the dataset, Table 4.2 shows the observations from 1 to 4 and 278 to 281 of hue color dataset, which will be analyzed in the next section.

Furthermore, the package depends on the `nlme`, `gdata` (Warnes *et al.*, 2017), and `ggplot2` packages, which must be previously loaded.

4.3.1 Output of the `lcc` function

Numerical and graphical summaries for the fitted model and confidence intervals of the LCC can be obtained by using the `summary` and `plot` methods implemented for class 'lcc'. The generic function `summary` applied to an object of class 'lcc' must be specified as `summary(obj, type)`, where `obj` is a object of class "lcc" and `type` is a character string defining the LCC components, which are of 'model' or 'fitted'. When `type = "model"`, the summary function gives the model used in the `lcc()` function whereas `type = "lcc"` gives the fitted and sampled values for the LCC component, its 95% bootstrap confidence intervals, and the CCC between fitted and sampled values as a goodness-of-fit statistic.

The output of the `summary` method depends on whether components was set as TRUE or FALSE in the 'lcc' object. Thus, if the `components` argument is TRUE, the generic function `summary` with `type = "lcc"` gives a list containing the following components: the fitted values of i) LCC, the longitudinal concordance correlation; ii) LPC, the longitudinal Pearson correlation; and iii) LA, the longitudinal accuracy; their lower and upper limits of 95% bootstrap confidence intervals; iv) the sample values for CCC, Pearson correlation coefficient and accuracy measure C_b (Lin, 1989); and v) CCC between the fitted and sampled values as goodness of fit statistic.

The fitted LCC, LPC, and LA and their confidence intervals can be again visualized thought the generic function `plot.lcc`, as we will be show in the hue data example.

4.4 Specifying models in the lcc

In the `lcc` package, to describe the LCC we need to specify the subject, response, method, time, a polynomial mixed-effect model, and the dataset. These arguments are specified through easy-to-use syntax. Consider a first degree polynomial model with by-subjects random intercept for a continuous dependent variable y observed on i th fruit ($i = 1, 2, \dots, N$) by J methods at time t_k ($k = 1, 2, \dots, n_i$):

$$\begin{aligned} y_{ijk} &= \beta_{0j} + b_{0i} + \beta_{1j}t_k + \epsilon_{ijk}, \quad \text{with} \\ b_{0i} &\sim N(0, \sigma_{b_0}^2) \quad \text{and} \quad \epsilon_{ijk} \sim N(0, \sigma_\epsilon^2) \end{aligned}$$

Thus, the LCC based on the fixed effects and variance components at time t_k is given by

$$\rho_{jj'}(t_k) = \frac{\sigma_{b_0}^2}{\sigma_{b_0}^2 + \sigma_\epsilon^2 + \frac{1}{2} [\beta_{01} - \beta_{02} + (\beta_{11} - \beta_{12}) t_k]^2}$$

and the syntax to specify this model in the `lcc()` function:

```
R> fit1 <- lcc(dataset = data, subject = "Subject", resp = "y",
  factorA = "Method", time = "Time", qf = 1, qr = 0)
```

where `qf=1` represents the polynomial degree for fixed part, `qr=0` an by-subjects random intercept. Suppose that the experimental design in previous example was randomized block designs, so the fixed effect of blocks can be included in that model as

```
R> fit2 <- lcc(dataset = data, subject = "Subject", resp = "y", covar = "Block",
  factorA = "Method", time = "Time", qf = 1, qr = 0)
```

Additionally, suppose that the within-group variability increases or decreases with time, thus the corresponding model including a variance function $g(t_k, \delta) = \exp(t_k \delta)$ is given by:

```
R> fit3 <- lcc(dataset = data, subject = "Subject", resp = "y", covar = "Block",
  factorA = "Method", time = "Time", qf = 1, qr = 0,
  var.class = varExp, weights.form = "time").
```

Many other possible models can be built to estimate the LCC through the function `lcc()`, see Section 4.3. The model selection can be done using the likelihood ratio test for nested models or by using the AIC or BIC criteria.

```
R> mod1 <- summary(fit2, type = "model")
R> mod2 <- summary(fit3, type = "model")
R> anova(mod1, mod2)
```

4.5 The papaya's peel hue dataset

Papaya is a tropical and climacteric fruit with high nutritional values, and antioxidant, anti-carcinogenic and anti-mutagenic properties (Sancho *et al.*, 2010). Its production in Brazil is responsible for about 11.2% of global trade, making Brazil by the second major papaya exporting country (Evans and Ballen, 2015). Papaya plantations, produces annually approximately 1.900 thousand tons annually, covering some 36 thousand hectares, are mainly located in the states of Bahia (~ 900 thousand tons) and Espírito Santo (~ 600 thousand tons), where the environment and climate provide ideal growing conditions (Evans and Ballen, 2015). In the fruit classification process, one of the most important variables is the hue color, because it is used to determine the ripeness stage (Mendoza and Aguilera, 2004; Oliveira *et al.*, 2017).

In an experiment described in Chapter 3, the hue color component was measured in a sample of 20 papaya fruits using a flat-bed scanner (HP Scanjet G2410) and a colorimeter Minolta CR-300 (Konica Minolta, 2003). This variable was measured on the equatorial region of the fruit by using both devices over 15 days. The mean hue was calculated based on four equidistant observations with the colorimeter and 1,000 observations obtained from images of the equatorial region digitalized by the scanner. The aim of the agreement study is to determine whether the colorimeter can compete with the scanner in measuring the mean hue of papaya peel over time. It is important to know about the magnitude of agreement because the colorimeter is faster and easier use than a flatbed scanner. Moreover, for the latter, each image needs to processed by an image manipulation program to select the object and extract its pixel-by-pixel information.

The individual profiles grouped by measurement device, scatter plot of hue data, and individual confidence intervals for second degree polynomial coefficients are showed in Figure 4.1. Apparently, we have a moderate agreement between scanner and colorimeter, which increases as the mean hue decreases (Figure 4.1a). On the other hand, Figures 4.1b and 4.1c may be useful to make a decision about the initial model. They show that we can begin by fitting a second degree polynomial mixed-effect model with random effect of fruit in the intercept, linear and quadratic coefficients:

$$Y_{ijk} = \beta_{0j} + b_{0i} + (\beta_{1j} + b_{1i}) t_k + (\beta_{2j} + b_{2i}) t_k^2 + \epsilon_{ijk}, \quad (4.4)$$

$$\mathbf{b} = [b_{0i}, b_{1i}, b_{2i}]^T \sim N_3(\mathbf{0}, \mathbf{G}) \quad \text{and} \quad \epsilon_{ijk} \sim N(0, \sigma_\epsilon^2),$$

where $\text{vech}(\mathbf{G}) = [\sigma_{b_0}^2, \sigma_{b_{01}}, \sigma_{b_{02}}, \sigma_{b_1}^2, \sigma_{b_{12}}, \sigma_{b_2}^2]^T$, and $\text{vech}(.)$ is the half-vectorization of \mathbf{G} . Consequently, under the model (4.4), the LCC is given by

$$\rho_{jj'}(t_k) = \frac{\mathbf{t}_k \mathbf{G} \mathbf{t}_k^T}{\mathbf{t}_k \mathbf{G} \mathbf{t}_k^T + \sigma_\epsilon^2 + \frac{1}{2} S_{jj'}^2(t_k)}.$$

We can fit this model, estimate the LCC, LPC and LA statistics, and compute their 95% bootstrap confidence intervals based on 8.000 bootstrap samples using the `lcc()` function directly:

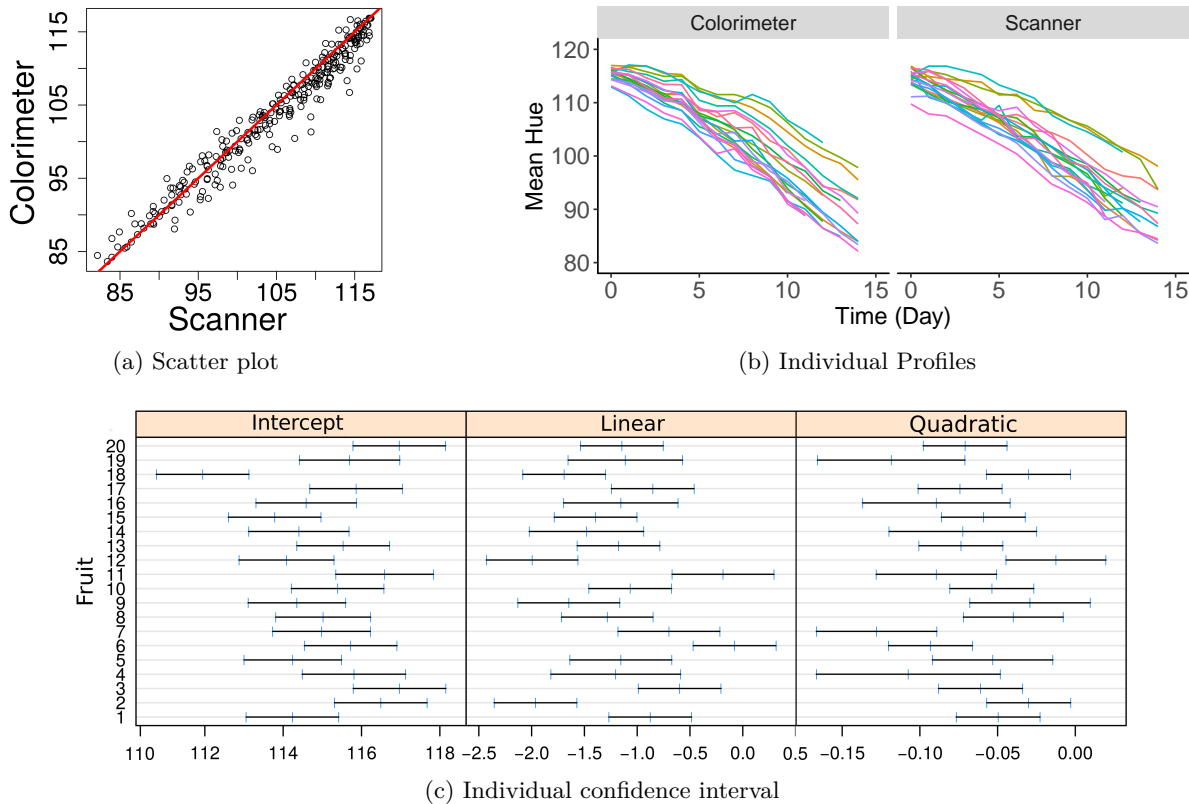


Figure 4.1: (a) Individual profiles of 20 fruits assessed on the equatorial region by colorimeter and scanner, (b) scatter plot of hue data considering all repeated measurements, and (c) individual 95% confidence intervals for second degree polynomial coefficients

```
R> fit1 <- lcc(dataset = hue, subject = "Fruit", resp = "H_mean",
  factorA = "Method", time = "Time", qf = 2, qr = 2,
  ci=TRUE, nboot=8000, components=TRUE)
```

The model used to estimate $\rho_{jj'}(t_k)$ as well as its sampled and fitted values can be extracted by using `summary(fit1, type = "model")` and `summary(fit1, type = "lcc")`, respectively. Moreover, the graphical representation of fitted values and confidence intervals for LCC, LPC and LA is obtained using the `plot.lcc` function, as shown in Figure 4.2. Apparently, the LCC did not fit well to the sampled values (Figure 4.2a), consequently it is necessary to check whether the model assumptions were met because the estimates for the LCC and its bootstrap confidence intervals may be biased under a misspecified model. Hence, we checked: i) the normality of error by producing the normal plot of within-group standardized residuals (Figure 4.3a), which indicates that this assumption for the within-group errors is plausible; ii) the homoscedasticity over time via standardized residuals versus time plot (Figure 4.3b), which indicates an apparently smaller variability for fruits measured by colorimeter than by the scanner; and iii) the CCC between fitted and sampled values as a goodness of fit, whose estimated value was 0.761

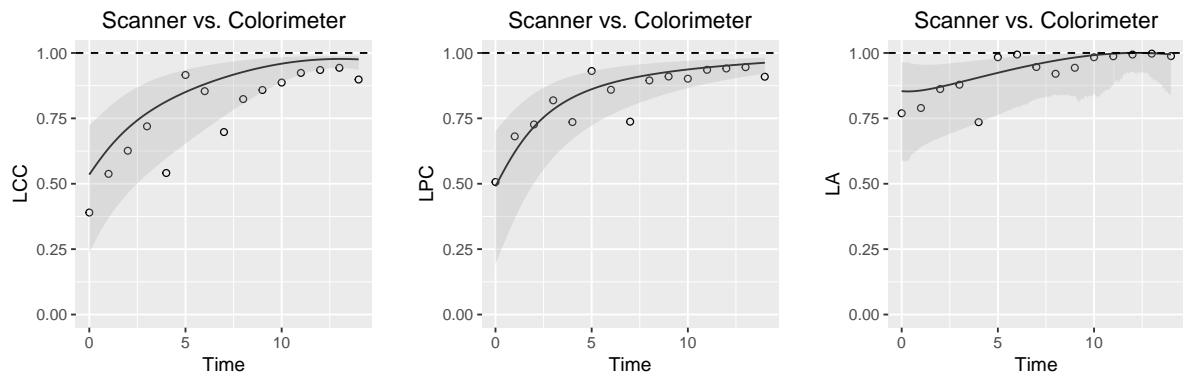


Figure 4.2: Estimate and 95% bootstrap confidence interval for the (a) longitudinal concordance correlation (LCC); (b) longitudinal Pearson correlation; and (c) longitudinal accuracy between observations measured on the equatorial region by the scanner and colorimeter with addition of points that represent the sample CCC, sample Pearson correlation coefficient, and sample accuracy, respectively

indicating an reasonable fit to the data.

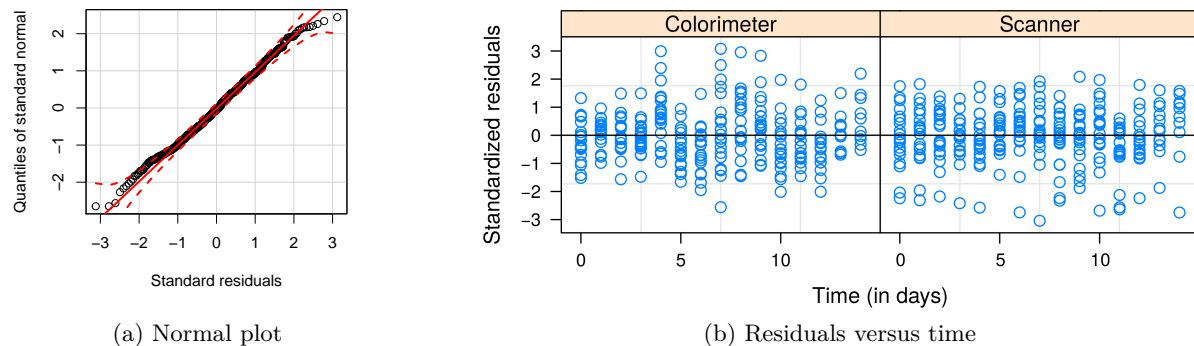


Figure 4.3: (a) Normal plot of within-group standardized residuals, (b) scatter plots of standardized residuals versus fitted values for the homoscedastic fitted, and (c) plot of standardized residuals versus time for `m1` fitted object

```
R> m1 <- summary(fit1, type = "model")
R> qqnorm(residuals(m1), ylab="Quantiles of standard normal",
xlab="Standard residuals")
R> qline(residuals(m1))
R> plot(m1, resid(., type = "p") ~ time | FacA, abline = 0)
R> summary(fit1, type = "lcc")$gof
[1] 0.7606758
```

Thus we update the model `fit1` to estimate different variances for each level of the factor “method”:

```
R > fit2<-lcc(dataset = hue, subject = "Fruit", resp = "H_mean", factorA = "Method",
  time = "Time", qf = 2, qr = 2, components = TRUE, var.class = varIdent,
  weights.form = "method", ci=TRUE, nboot = 8000, lme.control =
  lmeControl(opt="optim"))
```

Because models `fit1` and `fit2` are nested, we can use the likelihood ratio to test the hypothesis $H_0 : \delta^2 = 1$ versus $H_a : \delta^2 \neq 1$:

```
R> m2 <- summary(fit2, type = "model")
R> anova(m1,m2)
```

Model	df	AIC	BIC	logLik	Test	L.Ratio	p-value
m1	1	13	1938.125	1994.107	-956.0625		
m2	2	14	1934.920	1995.207	-953.4598	1 vs 2	5.205332 0.0225

```
R> summary(fit2, type = "lcc")$gof
[1] 0.8873875
```

The result shows that we can reject H_0 in favor of H_a considering a significance level $\alpha = 0.05$, that is, the variance associated with fruits measured by the colorimeter is different from when the scanner was used. Moreover, the LCC between fitted and sampled values also shows that model `fit2` fits the data better than model `fit1`, with values 0.887 and 0.761, respectively.

Figure 4.4 shows that the agreement profile changes over time, being smaller at the beginning of the experiment and increasing over time to values close to 1. If we consider values above 0.80 for the lower bound of the CI as an indicative for interchangeability between them to measure papaya’s peel color, the colorimeter could be used from the 12th day onwards.

4.6 Comparison with `cccrm` package

In this section we review the `cccrm` R package proposed by Carrasco *et al.* (2013) to estimate the CCC for repeated or non-repeated measures data and we discuss how this package differ from our package `lcc`. The `cccrm` package has included `ccclon` and `ccclonw` functions to estimate the CCC for longitudinal data (CCCrn) that were the firstly available in R statistical software. Both functions estimates the CCC based on variance components of mixed-effects model for longitudinal data, however, the difference between them is that `ccclonw` uses a non-negative definite matrix of weights between different repeated measurements (Carrasco *et al.*, 2009). They have been published very recently, demonstrating the raising importance in estimation of the CCC for longitudinal data.

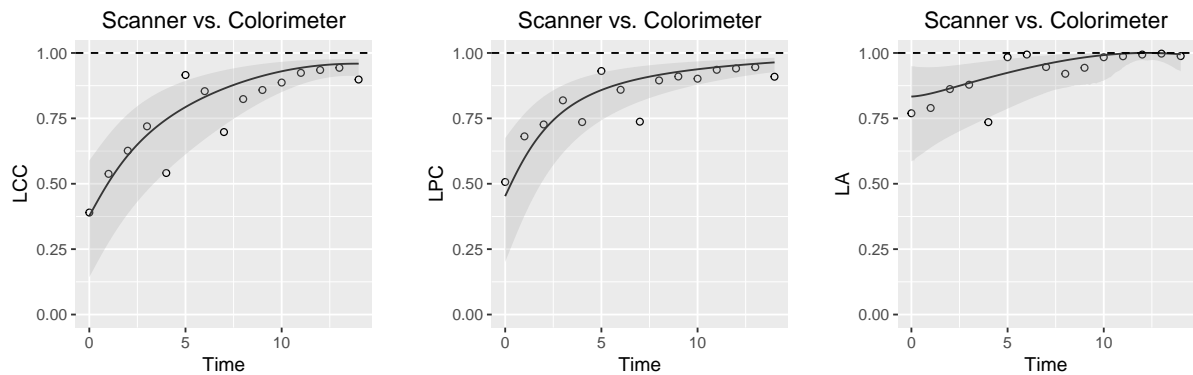


Figure 4.4: Estimate and 95% bootstrap confidence interval for the (a) longitudinal concordance correlation (LCC); (b) longitudinal Pearson correlation; and (c) longitudinal accuracy between observations measured on the equatorial region by the scanner and colorimeter with addition of points that represent the sample CCC, sample Pearson correlation coefficient, and sample accuracy, respectively

The **ccclon** as well as **ccclonw** functions have been introduced to produce a value that summarizes the interchangeability between methods in relation to all their measures rather than modeling the agreement as a function of time (Carrasco *et al.*, 2009). On the other hand, the **lcc** function in package **lcc** was developed to capture changes in the extent of the agreement profile among methods. Furthermore, this package also provides estimates and confidence intervals for LPC and LA that are important statistics to infer, respectively, about how the precision or accuracy measures at time $t_k = t$ could influence the LCC values in that time.

In the following example, the LCC of package **lcc** and CCCrm of package **cccrm** are estimated using the hue data analyzed in Section 4.5:

```
R> require(cccrm)
R> estccc<-ccclon(hue,"H_mean","Fruit","Time","Method")
CCC estimated by variance components:
  CCC      LL CI 95%      UL CI 95%      SE CCC
  0.83767698    0.72520268    0.90660774    0.04486742
```

The estimation of CCCrm shows an moderate agreement between methods, suggesting that image analysis of the equatorial peel region should be used to compute the mean hue. However, suppose that the researcher had stipulated the following condition: “ we would only take measurements on equatorial region using a colorimeter if the lower band of simultaneous confidence interval is greater than or equal to 0.90”. Thus, based on lower band of CCCrm (0.725) the researcher should not use the colorimeter to compute the mean hue. On the other hand, the lower band of LCC (Figure 4.4a) indicates that papaya’s equatorial region should be sampled through four equidistant points using a colorimeter from the ninth day. Clearly, this conclusion is only valid considering same experimental conditions. Moreover, this result shows

a possibility of interchangeable between methods and, consequently, reducing the handling time per fruit.

4.7 Discussion

The proposed longitudinal concordance correlation is a useful statistic to describe the agreement between methods over time based on polynomial mixed-effects models, allowing to capture changes in the extent of agreement over time. Our approach is flexible because it can accommodate balanced or unbalanced (dropouts) experimental designs and multiple methods. The argument `covar` included in the `lcc()` function allows for the inclusion of covariates in the linear predictor of the mixed-effects model to control systematic variations in the response. Other helpful feature of the `lcc` package is the ability to estimate the LCC, LPC and LA considering models with heterogeneous residual variance structures for different groups of observations, which could yield a strongly difference in the results obtained and conclusions for these statistics. Therefore, these arguments make the `lcc()` function more flexible to work with several types of datasets.

The statistical inference for estimators of $\rho_{jj'}(t_k)$, $\rho_{jj'}^{(p)}(t_k)$, and $C_{jj'}(t_k)$ can be made through bootstrap confidence intervals based on approximation from empirical distributions of them by the normal distribution or based on percentile of bootstrap sampling distribution of estimators. These CI methods are computationally intensive and are a limitation of the proposed methodology. The computations for hue data analysis (Section 4.5) took about 45 minutes to build the confidence intervals based on 8.000 bootstrap samples on Linux platform version 4.13.0-21-generic with an Intel® Core™ i7 processor of 2.40GHz speed and 4GB of RAM.

The `lcc` package uses the REML method, as default, for parameter estimations because it is less biased, less sensitive to outliers, and handles more effectively with high correlations when compared to ML estimation (Harville, 1977; Giesbrecht and Burns, 1985). However, we offer the user the possibility to change the estimation method to ML because this approach should be used when comparing models with nested fixed effects, but with the same random structure.

4.8 Future works

The `lcc` package is still in process of submitting to The Comprehensive R Archive Network (CRAN) and in its first version all the arguments proposed here will be considered. There is a number of desirable extensions of the package which could be included in future releases. The most important extension is the inclusion of correlation structures to model dependence among within-group errors. Some correlation structures were implemented in the `nlme` package such as compound symmetry, autoregressive-moving average and spatial correlation structures (Pinheiro and Bates, 2000) and they will be implemented in future extension of our package.

4.9 Conclusions

This chapter discussed the implementation of some methods developed for estimating longitudinal concordance correlation, longitudinal Pearson correlation and longitudinal accuracy with or without covariates in the R package `lcc`. The package also implements two bootstrap-based procedures to built confidence intervals of the estimated curves. Numerical and graphical summaries of the fitted LCC, LPC and LA as well as for their confidence intervals were implemented in order to make result interpretation easier. Moreover, the inclusion of standard classes of variance-covariance structures to model heteroscedasticity among within-group error with or without covariates increases the flexibility of our package to model longitudinal data.

Acknowledgement

The authors are grateful to CNPq (National Counsel of Technological and Scientific Development), University of São Paulo, and National University of Ireland through Science Foundation Ireland program, that supported this research project.

References

- Carrasco JL, King TS, Chinchilli VM (2009). “The concordance correlation coefficient for repeated measures estimated by variance components.” *Journal of biopharmaceutical statistics*, **19**(1), 90–105.
- Carrasco JL, Phillips BR, Puig-Martinez J, King TS, Chinchilli VM (2013). “Estimation of the concordance correlation coefficient for repeated measures using SAS and R.” *Computer Methods and Programs in Biomedicine*, **109**, 293–304.
- Chinchilli VM, Martel JK, Kumanyika S, Lloyd T (1996). “A Weighted Concordance Correlation Coefficient for Repeated Measurement Designs.” *Biometrics*, **52**(1), 341–353.
- Evans EA, Ballen FH (2015). “An Overview of Global Papaya Production , Trade , and Consumption.” *Technical report*, University of Florida, Florida.
- Giesbrecht FG, Burns JC (1985). “Two-Stage Analysis Based on a Mixed Model: Large-Sample Asymptotic Theory and Small- Sample Simulation Results.” *International Biometric Society*, **41**(2), 477–486.
- Harville DA (1977). “Maximum Likelihood Approaches to Variance Component Estimation and to Related Problems.” *Journal of the American Statistical Association*, **72**(358), 320–338.
- King TS, Chinchilli VM (2001). “A generalized concordance correlation coefficient for continuous and categorical data.” *Statistics in Medicine*, **20**(14), 2131–2147.

Konica Minolta (2003). *Precise colour communication, colour control from perception to instrumentation*. Konica Minolta Sensing.

Lin LI (1989). “A Concordance Correlation Coefficient to Evaluate Reproducibility.” *Biometrics*, **45**(1), 255–268.

Martin RJ, Szefler SJ, Chinchilli VM, Kraft M, Dolovich M, Boushey HA, Cherniack RM, Craig TJ, Drazen JM, Fagan JK, Fahy JV, Fish JE, Ford JG, Israel E, Kunselman SJ, Lazarus SC, Lemanske RF, Peters SP, Sorkness CA (2002). “Systemic effect comparisons of six inhaled corticosteroid preparations.” *American Journal of Respiratory and Critical Care Medicine*, **165**(10), 1377–1383.

Mendoza F, Aguilera JM (2004). “Application of image analysis for classification of ripening bananas.” *Journal of food science*, **69**(9), 471–477.

Oliveira TdP, Zocchi SS, Jacomino AP (2017). “Measuring color hue in “Sunrise Solo” papaya using flatbed scanner.” *Revista Brasileira de Fruticultura*, **39**(2), e–911.

Pinheiro J, Bates D, Debroy S, Sarkar D, R core team (2017). “nlme: linear and nonlinear mixed effects models.” URL <http://cran.r-project.org/package=nlme>.

Pinheiro JC, Bates DM (2000). *Mixed-Effects Models in S and S-PLUS*. Springer, New York.

R core Team (2017). “The R environment.” URL <https://www.r-project.org/>.

Rathnayake LN, Choudhary PK (2017). “Semiparametric modeling and analysis of longitudinal method comparison data.” *Statistics in Medicine*, **36**(13), 2003–2015.

Sancho LEG, Yahia EM, Martínez-Téllez MA, González-Aguilar GA (2010). “Effect of Maturity Stage of Papaya Maradol on Physiological and Biochemical Parameters.” *American Journal of Agricultural and Biological Science*, **5**(2), 194–203.

Warnes GR, Bolker B, Gorjanc G, Grothendieck G, Korosec A, Lumley T, MacQueen D, Magnusson A, Rogers J (2017). “gdata: Various R Programming Tools for Data Manipulation.” URL <https://cran.r-project.org/package=gdata>.

Wickham H (2009). *ggplot2: Elegant Graphics for Data Analysis*. New York. URL <http://ggplot2.org>.

5 CONCLUSIONS

In this thesis, we aimed to develop and extend statistical methods to help in the concordance analysis of agricultural data. Initially, we developed a longitudinal concordance correlation (LCC), longitudinal Pearson correlation (LPC), and longitudinal accuracy (LA) based on fixed effects and variance components of a polynomial mixed-effects regression model. We also developed methods to compute bootstrap-based confidence intervals for all components. In a small simulation study we demonstrated a satisfactory performance for LCC. The use of our approach in a real data application suggested that image analysis of whole peel region of papaya's fruit should be used to compute the mean hue rather than colorimeter or images from equatorial region.

We have been developing an R package called `lcc` for estimating LCC, LPC, and LA with or without covariates. The package allows for inclusion of heteroscedasticity among within-group error, different structures for variance-covariance matrix of random effects \mathbf{G} , and bootstrap-based procedure to build confidence intervals. Moreover, numerical and graphical summaries of these statistics were included in order to facilitate visualization and interpretations of results.

Further work includes extensions to the LCC approach in order to account for the longitudinal and spacial correlation among residuals. Improvements on the package developed here are still subject of ongoing research, and we appreciate any suggestion. Another extension would be a simulation study to compare several type of bootstrap confidence intervals (parametric and non-parametric). Finally, we would be happy to share the code of our package, which is not yet available in CRAN.

APPENDIX

Appendix I: Concordance correlation coefficient based on variance components

Consider a longitudinal study with N fruits, m devices (or methods), and n assessments. So, the expression (2.1) can be rewrite as

$$\begin{aligned} \rho_{jj'}(t) &= 1 - \frac{E[(Y_{ijk} - Y_{ij'k})^2]}{E_{Ind}[(Y_{ijk} - Y_{ij'k})^2]} \\ E[(Y_{ijk} - Y_{ij'k})^2] &= E(Y_{ijk}^2) - 2E(Y_{ijk}Y_{ij'k}) + E(Y_{ij'k}^2) \\ &= E(Y_{ijk}^2) - [E(Y_{ijk})]^2 + [E(Y_{ijk})]^2 + E(Y_{ij'k}^2) - [E(Y_{ij'k})]^2 + [E(Y_{ij'k})]^2 \\ &\quad - 2E(Y_{ijk}Y_{ij'k}) \\ &= Var(Y_{ijk}) + Var(Y_{ij'k}) + [E(Y_{ijk})]^2 + [E(Y_{ij'k})]^2 - 2E(Y_{ijk}Y_{ij'k}) \\ &= Var(Y_{ijk}) + Var(Y_{ij'k}) + [E(Y_{ijk})]^2 + [E(Y_{ij'k})]^2 - 2[Cov(Y_{ijk}, Y_{ij'k}) \\ &\quad + E(Y_{ijk})E(Y_{ij'k})] \\ &= Var(Y_{ijk}) + Var(Y_{ij'k}) + [E(Y_{ijk}) - E(Y_{ij'k})]^2 - 2Cov(Y_{ijk}, Y_{ij'k}) \\ E_{Ind}[(Y_{ijk} - Y_{ij'k})^2] &= Var(Y_{ijk}) + Var(Y_{ij'k}) + [E(Y_{ijk}) - E(Y_{ij'k})]^2 \\ \rho_{jj'}(t) &= 1 - \frac{Var(Y_{ijk}) + Var(Y_{ij'k}) + [E(Y_{ijk}) - E(Y_{ij'k})]^2 - 2Cov(Y_{ijk}, Y_{ij'k})}{Var(Y_{ijk}) + Var(Y_{ij'k}) + [E(Y_{ijk}) - E(Y_{ij'k})]^2} \\ &= 1 - \left[1 - \frac{2Cov(Y_{ijk}, Y_{ij'k})}{Var(Y_{ijk}) + Var(Y_{ij'k}) + [E(Y_{ijk}) - E(Y_{ij'k})]^2} \right] \\ &= \frac{2Cov(Y_{ijk}, Y_{ij'k})}{Var(Y_{ijk}) + Var(Y_{ij'k}) + [E(Y_{ijk}) - E(Y_{ij'k})]^2} \end{aligned}$$

Appendix II

Consider that matrices \mathbf{X} and \mathbf{L}_2 are both of full column rank and satisfy $\mathbf{L}_2\mathbf{X} = \mathbf{0}$ and \mathbf{V} is a positive definite matrix then

$$\mathbf{V} - \mathbf{V}\mathbf{L}_2(\mathbf{L}_2^T\mathbf{V}\mathbf{L}_2)^{-1}\mathbf{L}_2^T\mathbf{V} = \mathbf{X}(\mathbf{X}^T\mathbf{V}^{-1}\mathbf{X})^{-1}\mathbf{X}^T$$

and rearranging the terms we have to

$$\mathbf{L}_2(\mathbf{L}_2^T\mathbf{V}\mathbf{L}_2)^{-1}\mathbf{L}_2^T = \mathbf{V}^{-1} - \mathbf{V}^{-1}\mathbf{X}(\mathbf{X}^T\mathbf{V}^{-1}\mathbf{X})^{-1}\mathbf{X}^T\mathbf{V}^{-1} = \mathbf{P}.$$

Appendix III: Matrix Algebra

The theory used in this appendix was based on the book **Matrix Algebra From a Statistician's Perspective** (Harville, 2008).

Lemma 1: Let $\mathbf{F} = \{f_{is}\}$ and $\mathbf{B} = \{b_{is}\}$ represent $p \times q$ and $q \times r$ matrices of functions, defined on a set S , of a vector $\mathbf{x} = (x_1, x_2, \dots, x_m)^T$ of m variables. Suppose that \mathbf{A} is $q \times p$ matrix of constants or functions (defined on S) is continuous at every interior point S and such that $\mathbf{A}(\mathbf{x})$ does not vary with x_j . Then, at any interior point \mathbf{c} of S at which \mathbf{F} and \mathbf{B} are continuously differentiable with $\mathbf{F} : S \rightarrow \mathbb{R}^{p \times q}$ and $\mathbf{B} : S \rightarrow \mathbb{R}^{p \times r}$, then

$$\begin{aligned}\frac{\partial \mathbf{F}\mathbf{B}}{\partial x_j} &= \mathbf{F}\frac{\partial \mathbf{B}}{\partial x_j} + \frac{\partial \mathbf{F}}{\partial x_j}\mathbf{B}, \\ \frac{\partial \text{tr}(\mathbf{F})}{\partial x_j} &= \text{tr}\left(\frac{\mathbf{F}}{\partial x_j}\right), \\ \frac{\partial \text{tr}(\mathbf{AF})}{\partial x_j} &= \frac{\partial \text{tr}(\mathbf{FA})}{\partial x_j} = \text{tr}\left(\frac{\mathbf{F}}{\partial x_j}\mathbf{A}\right) = \text{tr}\left(\mathbf{A}\frac{\mathbf{F}}{\partial x_j}\right), \\ \frac{\partial \text{tr}(\mathbf{FG})}{\partial x_j} &= \frac{\partial \text{tr}(\mathbf{GF})}{\partial x_j} = \text{tr}\left(\mathbf{F}\frac{\mathbf{B}}{\partial x_j}\right) + \text{tr}\left(\mathbf{B}\frac{\mathbf{F}}{\partial x_j}\right) = \text{tr}\left(\frac{\mathbf{B}}{\partial x_j}\mathbf{F}\right) + \text{tr}\left(\frac{\mathbf{F}}{\partial x_j}\mathbf{B}\right).\end{aligned}$$

Definition 1: Let a_j and x_j represent the j th elements of \mathbf{a} and \mathbf{x} , respectively, and let a_{jk} represent the ik th element of \mathbf{A} . Then,

$$\frac{\partial(\mathbf{a}^T \mathbf{x})}{\partial \mathbf{x}} = \mathbf{a}^T, \quad \frac{\partial(\mathbf{x}^T \mathbf{Ax})}{\partial \mathbf{x}} = (\mathbf{A} + \mathbf{A}^T) \mathbf{x} \text{ and } \frac{\partial^2(\mathbf{x}^T \mathbf{Ax})}{\partial \mathbf{x} \partial \mathbf{x}^T} = \mathbf{A} + \mathbf{A}^T. \quad (5.1)$$

Note also that, in the special case where \mathbf{A} is symmetric, the results presented in (5.1) are simplify to

$$\frac{\partial(\mathbf{x}^T \mathbf{Ax})}{\partial \mathbf{x}} = 2\mathbf{Ax} \text{ and } \frac{\partial^2(\mathbf{x}^T \mathbf{Ax})}{\partial \mathbf{x} \partial \mathbf{x}^T} = 2\mathbf{A}.$$

Theorem 1: $|\mathbf{AB}| = |\mathbf{A}||\mathbf{B}|$ when \mathbf{A} and \mathbf{B} are square and of the same order.

Definition 2: If \mathbf{F} is twice continuously differentiable at an interior point \mathbf{c} of S , then \mathbf{F} is continuously differentiable at \mathbf{c} . Applying the chain rule, the first derivative of $|\mathbf{F}|$ is given by

$$\frac{\partial |\mathbf{F}|}{\partial x_j} = \text{tr} \left[\text{adj}(\mathbf{F}) \frac{\partial \mathbf{F}}{\partial x_j} \right],$$

where $\text{adj}(\mathbf{F})$ is the adjugate of \mathbf{F} . The adjugate of \mathbf{F} is the transpose of \mathbf{C} (cofactor matrix), that is, the $p \times q$ matrix whose (ij) entry is the (j, i) cofactor of \mathbf{F} ,

$$\text{adj}(\mathbf{F})_{ij} = \mathbf{C}_{ji} = (-1)^{i+j} F_{ji}, \quad i = 1, 2, \dots, p \text{ and } j = 1, 2, \dots, q.$$

Furthermore, if \mathbf{F} is nonsingular as well as continuously differentiable at c , then

$$\frac{\partial |\mathbf{F}|}{\partial x_j} = |\mathbf{F}| \text{tr} \left(\mathbf{F}^{-1} \frac{\partial \mathbf{F}}{\partial x_j} \right).$$

The second derivative of $|\mathbf{F}|$ is given by

$$\frac{\partial^2 |\mathbf{F}|}{\partial x_i \partial x_j} = |\mathbf{F}| \left[\text{tr} \left(\mathbf{F}^{-1} \frac{\partial^2 \mathbf{F}}{\partial x_i \partial x_j} \right) + \text{tr} \left(\mathbf{F}^{-1} \frac{\partial \mathbf{F}}{\partial x_i} \right) \text{tr} \left(\mathbf{F}^{-1} \frac{\partial \mathbf{F}}{\partial x_j} \right) \text{tr} \left(\mathbf{F}^{-1} \frac{\partial \mathbf{F}}{\partial x_i} \mathbf{F}^{-1} \frac{\partial \mathbf{F}}{\partial x_j} \right) \right]$$

The differentiation when we have the logarithm of the determinant is given by

$$\frac{\partial \ln |\mathbf{F}|}{\partial x_j} = \frac{1}{|\mathbf{F}|} \frac{\partial |\mathbf{F}|}{\partial x_j} = \text{tr} \left(\mathbf{F}^{-1} \frac{\partial \mathbf{F}}{\partial x_j} \right),$$

and

$$\frac{\partial^2 \ln |\mathbf{F}|}{\partial x_i \partial x_j} = \text{tr} \left(\mathbf{F}^{-1} \frac{\partial^2 \mathbf{F}}{\partial x_i \partial x_j} \right) + \text{tr} \left(\mathbf{F}^{-1} \frac{\partial \mathbf{F}}{\partial x_i} \mathbf{F}^{-1} \frac{\partial \mathbf{F}}{\partial x_j} \right).$$

Definition 3: Consider that \mathbf{F}^{-1} is continuously differentiable at \mathbf{c} , so the first and second differentiation of the inverse matrix \mathbf{F}^{-1} is given by

$$\frac{\partial \mathbf{F}^{-1}}{\partial x_j} = -\mathbf{F}^{-1} \frac{\partial \mathbf{F}}{\partial x_j} \mathbf{F}^{-1}$$

and

$$\frac{\partial^2 \mathbf{F}^{-1}}{\partial x_i \partial x_j} = -\mathbf{F}^{-1} \frac{\partial^2 \mathbf{F}}{\partial x_i \partial x_j} \mathbf{F}^{-1} + \mathbf{F}^{-1} \frac{\partial \mathbf{F}}{\partial x_i} \mathbf{F}^{-1} \frac{\partial \mathbf{F}}{\partial x_j} \mathbf{F}^{-1} + \mathbf{F}^{-1} \frac{\partial \mathbf{F}}{\partial x_j} \mathbf{F}^{-1} \frac{\partial \mathbf{F}}{\partial x_i} \mathbf{F}^{-1}$$

Definition 4: Suppose that \mathbf{A} and \mathbf{B} are continuously differentiable at \mathbf{c} . Then, $\mathbf{A}\mathbf{F}^{-1}\mathbf{B}$ is continuously differentiable at \mathbf{c} and (at $\mathbf{x} = \mathbf{c}$)

$$\frac{\partial (\mathbf{A}\mathbf{F}^{-1}\mathbf{B})}{\partial x_j} = \mathbf{A}\mathbf{F}^{-1} \frac{\partial \mathbf{B}}{\partial x_j} - \mathbf{A}\mathbf{F}^{-1} \frac{\partial \mathbf{F}}{\partial x_j} \mathbf{F}^{-1}\mathbf{B} + \frac{\partial \mathbf{A}}{\partial x_j} \mathbf{F}^{-1}\mathbf{B}.$$

In the special case where \mathbf{A} and \mathbf{B} are constant or do not vary with x_j , formula (5.2) simplifies to

$$\frac{\partial (\mathbf{A}\mathbf{F}^{-1}\mathbf{B})}{\partial x_j} = -\mathbf{A}\mathbf{F}^{-1} \frac{\partial \mathbf{F}}{\partial x_j} \mathbf{F}^{-1}\mathbf{B}.$$

Appendix IV: The first derivative of $\frac{\partial P}{\partial \psi_w}$

$$\begin{aligned} \frac{\partial \mathbf{P}}{\partial \psi_w} &= \frac{\partial}{\partial \psi_w} \left[\mathbf{V}^{-1} - \mathbf{V}^{-1} \mathbf{X} (\mathbf{X}^T \mathbf{V}^{-1} \mathbf{X})^{-1} \mathbf{X}^T \mathbf{V}^{-1} \right] \quad (\text{Using the Lemma 1 of Appendix III}) \\ &= \frac{\partial \mathbf{V}^{-1}}{\partial \psi_w} - \frac{\partial \mathbf{V}^{-1}}{\partial \psi_w} \mathbf{X} (\mathbf{X}^T \mathbf{V}^{-1} \mathbf{X})^{-1} \mathbf{X}^T \mathbf{V}^{-1} - \mathbf{V}^{-1} \mathbf{X} \frac{\partial (\mathbf{X}^T \mathbf{V}^{-1} \mathbf{X})^{-1}}{\partial \psi_w} \mathbf{X}^T \mathbf{V}^{-1} \\ &\quad - \mathbf{V}^{-1} \mathbf{X} (\mathbf{X}^T \mathbf{V}^{-1} \mathbf{X})^{-1} \mathbf{X}^T \frac{\partial \mathbf{V}^{-1}}{\partial \psi_w} \quad (\text{Using the Definition 3 and 4 of Appendix III}) \\ &= -\mathbf{V}^{-1} \frac{\partial \mathbf{V}}{\partial \psi_w} \mathbf{V}^{-1} + \mathbf{V}^{-1} \frac{\partial \mathbf{V}}{\partial \psi_w} \mathbf{V}^{-1} \mathbf{X} (\mathbf{X}^T \mathbf{V}^{-1} \mathbf{X})^{-1} \mathbf{X}^T \mathbf{V}^{-1} \\ &\quad - \mathbf{V}^{-1} \mathbf{X} (\mathbf{X}^T \mathbf{V}^{-1} \mathbf{X})^{-1} \mathbf{X}^T \mathbf{V}^{-1} \frac{\partial \mathbf{V}}{\partial \psi_w} \mathbf{V}^{-1} \mathbf{X} (\mathbf{X}^T \mathbf{V}^{-1} \mathbf{X})^{-1} \mathbf{X}^T \mathbf{V}^{-1} \\ &\quad + \mathbf{V}^{-1} \mathbf{X} (\mathbf{X}^T \mathbf{V}^{-1} \mathbf{X})^{-1} \mathbf{X}^T \mathbf{V}^{-1} \frac{\partial \mathbf{V}}{\partial \psi_w} \mathbf{V}^{-1}. \end{aligned} \tag{5.3}$$

Using the Appendix II, we can rewrite the expression (5.3) as

$$\begin{aligned}
\frac{\partial \mathbf{P}}{\partial \psi_w} &= -\mathbf{V}^{-1} \frac{\partial \mathbf{V}}{\partial \psi_w} \left[\mathbf{V}^{-1} - \mathbf{V}^{-1} \mathbf{X} (\mathbf{X}^T \mathbf{V}^{-1} \mathbf{X})^{-1} \mathbf{X}^T \mathbf{V}^{-1} \right] \\
&\quad + \mathbf{V}^{-1} \mathbf{X} (\mathbf{X}^T \mathbf{V}^{-1} \mathbf{X})^{-1} \mathbf{X}^T \mathbf{V}^{-1} \frac{\partial \mathbf{V}}{\partial \psi_w} \left[\mathbf{V}^{-1} - \mathbf{V}^{-1} \mathbf{X} (\mathbf{X}^T \mathbf{V}^{-1} \mathbf{X})^{-1} \mathbf{X}^T \mathbf{V}^{-1} \right] \\
&= -\mathbf{V}^{-1} \frac{\partial \mathbf{V}}{\partial \psi_w} \mathbf{P} + \mathbf{V}^{-1} \mathbf{X} (\mathbf{X}^T \mathbf{V}^{-1} \mathbf{X})^{-1} \mathbf{X}^T \mathbf{V}^{-1} \frac{\partial \mathbf{V}}{\partial \psi_w} \mathbf{P} \\
&= -\left[\mathbf{V}^{-1} - \mathbf{V}^{-1} \mathbf{X} (\mathbf{X}^T \mathbf{V}^{-1} \mathbf{X})^{-1} \mathbf{X}^T \mathbf{V}^{-1} \right] \frac{\partial \mathbf{V}}{\partial \psi_w} \mathbf{P} \\
&= -\mathbf{P} \frac{\partial \mathbf{V}}{\partial \psi_w} \mathbf{P}
\end{aligned}$$

Appendix V: Quadratic forms

The theory used in this appendix was based on the book **Linear Models in Statistics** (Rencher, 2007).

Theorem 2: If \mathbf{y} is a random vector with mean $\boldsymbol{\mu}$ and covariance matrix $\boldsymbol{\Sigma}$ and if \mathbf{A} is a symmetric matrix of constants, then

$$E(\mathbf{y}^T \mathbf{A} \mathbf{y}) = \text{tr}(\mathbf{A} \boldsymbol{\Sigma}) + \boldsymbol{\mu}^T \mathbf{A} \boldsymbol{\mu}$$

Theorem 3: If $\mathbf{y} \sim N_p(\boldsymbol{\mu}, \boldsymbol{\Sigma})$, then

$$\text{Var}(\mathbf{y}^T \mathbf{A} \mathbf{y}) = 2 \text{tr}[(\mathbf{A} \boldsymbol{\Sigma})^2] + 4 \boldsymbol{\mu}^T \mathbf{A} \boldsymbol{\Sigma} \mathbf{A} \boldsymbol{\mu}.$$

Theorem 4: If $\mathbf{y} \sim N_p(\boldsymbol{\mu}, \boldsymbol{\Sigma})$, then

$$\text{Cov}(\mathbf{y}, \mathbf{y}^T \mathbf{A} \mathbf{y}) = 2 \boldsymbol{\Sigma} \mathbf{A} \boldsymbol{\mu}.$$

Appendix VI: Diagnostic analysis

Although LMEM have good properties of the estimates, the model assumptions must be fulfilled. Thus, we presented the observed values versus the predicted values of the model (Figure A.1a); the normality of residuals (Figure A.1b); and the conditional residuals versus the predicted values (Figure A.1c) because if the assumptions is not fulfilled or the likelihood is not true, the REML estimates and their standard errors will be dramatically biased. The residuals analysis showed that there is not any trends in the graph of residuals versus predicted values. Furthermore, as less than 5% of observations are outside of the simulated envelope of normal plot (Figure A.1b), we can consider that assumption of normality of errors is adequate.

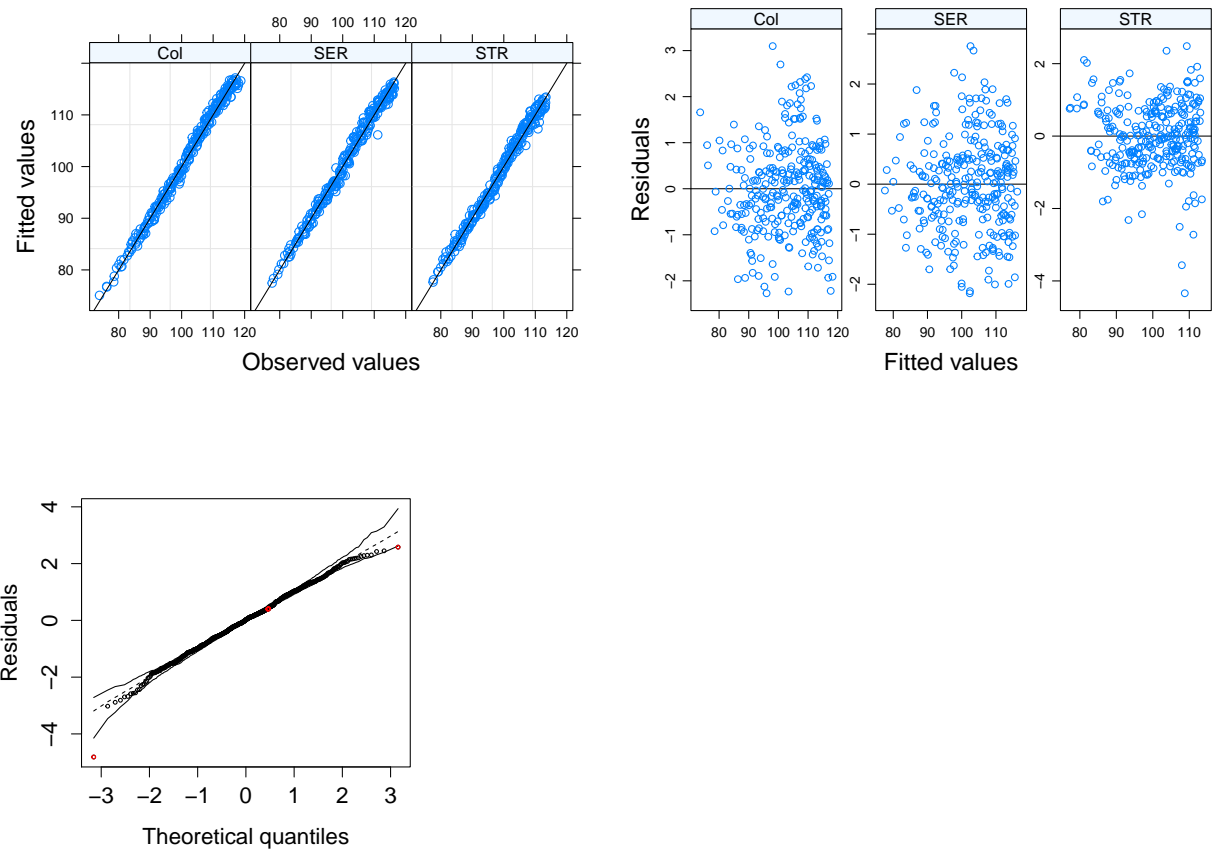


Figure A.1: (a) Observed values versus the predicted values of the model; (b) the normality of residuals; and (c) the conditional residuals versus the predicted values. Here ‘Col’ represent observations measured by colorimeter on equatorial region, ‘SER’ represent observations measured by scanner on equatorial region, and ‘STR’ represent observations measured by scanner on whole region

ANNEX

Annex A: Dataset

The entire dataset will be available to view from publication of second chapter about Longitudinal concordance correlation. This chapter already was accepted to publication in the Journal of Agricultural, Biological, and Environmental Statistics (JABES).

Table Annex 1: A small part of hue data of papaya fruits measured by two methods (Colorimeter or Scanner) on two peel regions (Equatorial or Whole) over time

n	Hue	Method	Region	Time	Fruit
1	116.54	Colorimeter	Equatorial	0	1
2	115.41	Colorimeter	Equatorial	0	2
3	116.98	Colorimeter	Equatorial	0	3
4	115.88	Colorimeter	Equatorial	0	4
5	115.71	Colorimeter	Equatorial	0	5
6	116.14	Colorimeter	Equatorial	0	6
7	114.44	Colorimeter	Equatorial	0	7
8	116.10	Colorimeter	Equatorial	0	8
9	115.18	Colorimeter	Equatorial	0	9
10	116.57	Colorimeter	Equatorial	0	10
...
278	113.90	Scanner	Equatorial	0	1
279	116.50	Scanner	Equatorial	0	2
280	116.86	Scanner	Equatorial	0	3
281	114.59	Scanner	Equatorial	0	4
282	113.38	Scanner	Equatorial	0	5
283	114.49	Scanner	Equatorial	0	6
284	116.67	Scanner	Equatorial	0	7
285	115.01	Scanner	Equatorial	0	8
286	113.58	Scanner	Equatorial	0	9
287	115.87	Scanner	Equatorial	0	10
288	115.10	Scanner	Equatorial	0	11
...
555	111.51	Scanner	Whole	0	1
556	114.60	Scanner	Whole	0	2
557	114.25	Scanner	Whole	0	3
558	112.73	Scanner	Whole	0	4
559	112.08	Scanner	Whole	0	5

Continued on next page

Table Annex 1 – continued from previous page

n	Hue	Method	Region	Time	Fruit
560	111.67	Scanner	Whole	0	6
561	112.81	Scanner	Whole	0	7
562	112.44	Scanner	Whole	0	8
563	111.44	Scanner	Whole	0	9
564	113.10	Scanner	Whole	0	10
565	113.30	Scanner	Whole	0	11
...
821	87.79	Scanner	Whole	13	20
822	89.84	Scanner	Whole	14	1
823	82.27	Scanner	Whole	14	2
824	92.79	Scanner	Whole	14	3
825	95.56	Scanner	Whole	14	6
826	87.29	Scanner	Whole	14	10
827	83.88	Scanner	Whole	14	13
828	81.90	Scanner	Whole	14	15
829	86.24	Scanner	Whole	14	17
830	82.53	Scanner	Whole	14	18
831	84.85	Scanner	Whole	14	20

Annex B: Programming in R

i) Used Package:

```
require(nlme)
```

ii) Reading the data:

```
dados<-read.csv2("dataset.csv",header=TRUE,dec=". ",sep=";")
dados$Fruit<-as.factor(dados$Fruit)
dados$Time<-as.numeric(dados$Time)
dados$Time<-log(dados$Time+1)
```

iii) Grouping the data from the function groupedData:

```
dataset<-groupedData(H_mean~Time|Fruit, data=dados)
dataset$Scan<-with(dataset,model.matrix(~Method-1)[,2])
```

iv) Selected model:

```

model<-lme(H_mean~Method+Time+I(Time^2)+I(Time^3)+Region+
  Method:Time+Method:I(Time^2)+Region:Time+Region:I(Time^2),
  random=pdBlocked(list(pdCompSymm(~Scan:Region-1),
  pdDiag(~1),
  pdSymm(~Time+I(Time^2)-1))),
  data=dataset,
  weights=varExp(form=~Time|Region, fixed = c(Whole=0)),
  method = "REML")

```

v) Longitudinal concordance correlation (LCC) function

a) Extracting the variance components

```

(sigma.b0_scan.eq<-getVarCov(model)[1,1])
(sigma.b0_scan.tot<-getVarCov(model)[2,2])
(sigma.b0_scan.eqtot<-getVarCov(model)[1,2])
(sigma.b0_2<-getVarCov(model)[3,3])
(sigma.b1_2<-getVarCov(model)[4,4])
(sigma.b2_2<-getVarCov(model)[5,5])
(sigma.b01_2=getVarCov(model)[3,4])
(sigma.b02_2=getVarCov(model)[3,5])
(sigma.b12_2<-getVarCov(model)[4,5])
varcomp<-summary(model)
(SE<-model$sigma^2)
(varcomp_col<-SE) # Colorimeter on equatorial region
(varcomp_ser<-SE) # Scanner on equatorial region
(varcomp_str<-SE) # Scanner on whole region
(varcomp_exp_col<-coef(varcomp$modelStruct$varStruct,
  uncons=F, allCoef=T)[1])
(varcomp_exp_ser<-coef(varcomp$modelStruct$varStruct,
  uncons=F, allCoef=T)[1])
(varcomp_exp_str<-coef(varcomp$modelStruct$varStruct,
  uncons=F, allCoef=T)[2])

```

b) Calculating the LCC

```

# Variance components (VC) associated with colorimeter
Var_col<-function(tempo) {
  sigma.b0_2+sigma.b1_2*tempo^2+sigma.b2_2*tempo^4+
  2*(sigma.b01_2*tempo+sigma.b02_2*tempo^2+sigma.b12_2*tempo^3)+
  varcomp_col*exp(2*varcomp_exp_col*(tempo))
}

```

```

# Variance components (VC) associated with scanner on equatorial region
Var_ser<-function(tempo) {
  sigma.b0_2+sigma.b0_scan.eq+sigma.b1_2*tempo^2+sigma.b2_2*tempo^4+
  2*(sigma.b01_2*tempo+sigma.b02_2*tempo^2+sigma.b12_2*tempo^3)+
  varcomp_ser*exp(2*varcomp_exp_ser*(tempo))
}

# Variance components (VC) associated with scanner on whole region
Var_str<-function(tempo) {
  sigma.b0_2+sigma.b0_scan.tot+sigma.b1_2*tempo^2+sigma.b2_2*tempo^4+
  2*(sigma.b01_2*tempo+sigma.b02_2*tempo^2+sigma.b12_2*tempo^3)+
  varcomp_str*exp(2*varcomp_exp_str*(tempo))
}

# Covariance between colorimeter and scanner
COV_2<-function(tempo) {
  sigma.b0_2+sigma.b1_2*tempo^2+sigma.b2_2*tempo^4+
  2*(sigma.b01_2*tempo+sigma.b02_2*tempo^2+sigma.b12_2*tempo^3)
}

# Covariance between scanner on equatorial and whole regions
COV_2s<-function(tempo) {
  sigma.b0_2+sigma.b0_scan.eqtot+sigma.b1_2*tempo^2+sigma.b2_2*tempo^4+
  2*(sigma.b01_2*tempo+sigma.b02_2*tempo^2+sigma.b12_2*tempo^3)
}

# Expected values for colorimeter
Ei1k_2<-function(tempo)
sum(c(1,0,tempo,tempo^2,tempo^3,0,0,0,0,0)*fixef(model))

# Expected values for scanner on equatorial region
Ei2k_2<-function(tempo)
sum(c(1,1,tempo,tempo^2,tempo^3,0,tempo,tempo^2,0,0)*fixef(model))

# Expected values for scanner on whole region
Ei3k_2<-function(tempo)
sum(c(1,1,tempo,tempo^2,tempo^3,1,tempo,tempo^2,tempo,tempo^2)*fixef(model))

```

```

# Longitudinal concordance correlation

## Colorimeter versus Scanner on equatorial region
rho.12_2 <- Vectorize(function(t) 2*COV_2(t)/(Var_col(t)+Var_ser(t)+  

  (Ei1k_2(t)-Ei2k_2(t))^2), "t")
## Colorimeter versus Scanner on whole region
rho.13_2 <- Vectorize(function(t) 2*COV_2(t)/(Var_col(t)+Var_str(t)+  

  (Ei1k_2(t)-Ei3k_2(t))^2), "t")
## Scanner on equatorial region versus whole region
rho.23_2 <- Vectorize(function(t) 2*COV_2s(t)/(Var_ser(t)+Var_str(t)+  

  (Ei2k_2(t)-Ei3k_2(t))^2), "t")

# Longitudinal pearson correlation (LPC) function
## Colorimeter versus Scanner on equatorial region
rho.pearson.12_2<-Vectorize(function(t) COV_2(t)/sqrt(Var_col(t)*Var_ser(t)), "t")
## Colorimeter versus Scanner on whole region
rho.pearson.13_2<-Vectorize(function(t) COV_2(t)/sqrt(Var_col(t)*Var_str(t)), "t")
## Scanner on equatorial region versus whole region
rho.pearson.23_2<-Vectorize(function(t) COV_2s(t)/sqrt(Var_ser(t)*Var_str(t)), "t")

# Longitudinal accuracy (LA) function
## Colorimeter versus Scanner on equatorial region
Cb.12_2<-function(t) rho.12_2(t)/rho.pearson.12_2(t)
## Colorimeter versus Scanner on whole region
Cb.13_2<-function(t) rho.13_2(t)/rho.pearson.13_2(t)
## Scanner on equatorial region versus whole region
Cb.23_2<-function(t) rho.23_2(t)/rho.pearson.23_2(t)

```

vi) Algorithm to nonparametric bootstrap confidence intervals

```

# Bootstrap function
fit_sim<-function(data,N){
  Dataset<-data
  sample_data<-sample(as.character(unique(Dataset$Fruit)),N,replace=TRUE)
  Frame<-list(NA)
  for(i in 1:N){
    Frame[[i]]<-subset(Dataset, Fruit==sample_data[i])
    Frame[[i]]$Fruit<-c(rep(i,length(Frame[[i]][,1])))
  }
}

```

```

data_sample<-do.call(rbind.data.frame, Frame)

dataset_lme<-groupedData(H_mean~Time|Fruit, data=data_sample)

fit.sim <- lme(H_mean~Method + Time + I(Time^2) + I(Time^3) +
  Region + Method:Time+Method:I(Time^2)+Region:Time+
  Region:I(Time^2),
  random=pdBlocked(list(pdCompSymm(~Scan:Region-1),
    pdDiag(~1),
    pdSymm(~Time+I(Time^2)-1))),
  weights=varExp(form=~Time|Region,fixed=c(Whole=0)),
  data=dataset_lme)

Betas<-fixef(fit.sim)
s.b0.ser<-getVarCov(fit.sim)[1,1]
s.b0.str<-getVarCov(fit.sim)[2,2]
s.b0.23<-getVarCov(fit.sim)[1,2]
s.b0<-getVarCov(fit.sim)[3,3]
s.b1<-getVarCov(fit.sim)[4,4]
s.b2<-getVarCov(fit.sim)[5,5]
s.b01<-getVarCov(fit.sim)[3,4]
s.b02<-getVarCov(fit.sim)[3,5]
s.b12<-getVarCov(fit.sim)[4,5]

varcomp<-summary(fit.sim)
SE<-fit.sim$sigma^2
varcomp_exp_col<-coef(varcomp$modelStruct$varStruct,
  uncons=F, allCoef=T)[1]
varcomp_exp_ser<-coef(varcomp$modelStruct$varStruct,
  uncons=F, allCoef=T)[1]
varcomp_exp_str<-coef(varcomp$modelStruct$varStruct,
  uncons=F, allCoef=T)[2]
Var_all<-data.frame(s.b0.ser,s.b0.str,s.b0.23,s.b0,s.b1,s.b2,s.b01,s.b02,s.b12,SE,
varcomp_exp_col,varcomp_exp_ser,varcomp_exp_str)

# Variance for observations measured by colorimeter on equatorial region
Var_col<-function(tempo) {
  s.b0+s.b1*tempo^2+s.b2*tempo^4+
  2*(s.b01*tempo+s.b02*tempo^2+s.b12*tempo^3)+
```

```

SE*exp(2*varcomp_exp_col*(tempo))
}

# Variance for observations measured by scanner on equatorial region
Var_ser<-function(tempo) {
s.b0+s.b0.ser+s.b1*tempo^2+s.b2*tempo^4+
2*(s.b01*tempo+s.b02*tempo^2+s.b12*tempo^3)+  

SE*exp(2*varcomp_exp_ser*(tempo))
}

# Variance for observations measured by scanner on whole region
Var_str<-function(tempo) {
s.b0+s.b0.str+s.b1*tempo^2+s.b2*tempo^4+
2*(s.b01*tempo+s.b02*tempo^2+s.b12*tempo^3)+  

SE*exp(2*varcomp_exp_str*(tempo))
}

Ei1k<-function(tempo) sum(c(1,0,tempo,tempo^2,tempo^3,0,0,0,0,  

0)*fixef(fit.sim))
Ei2k<-function(tempo) sum(c(1,1,tempo,tempo^2,tempo^3,0,tempo,  

tempo^2,0,0)*fixef(fit.sim))
Ei3k<-function(tempo) sum(c(1,1,tempo,tempo^2,tempo^3,1,tempo,  

tempo^2,tempo,tempo^2)*fixef(fit.sim))

COV.col<-function(tempo) {
s.b0+s.b1*tempo^2+s.b2*tempo^4+2*(s.b01*tempo+s.b02*tempo^2+s.  

b12*tempo^3)
}
COV.scan<-function(tempo) {
s.b0+s.b0.23+s.b1*tempo^2+s.b2*tempo^4+2*(s.b01*tempo+  

s.b02*tempo^2+s.b12*tempo^3)
}

# Calculating the longitudinal concordance correlation
rho.12 <- Vectorize(function(t) 2*COV.col(t)/(Var_col(t)+Var_ser(t)+  

(Ei1k(t)-Ei2k(t))^2), "t")
rho.13 <- Vectorize(function(t) 2*COV.col(t)/(Var_col(t)+Var_str(t)+  

(Ei1k(t)-Ei3k(t))^2), "t")

```

```

rho.23 <- Vectorize(function(t) 2*COV.scan(t)/(Var_ser(t)+Var_str(t)+  

(Ei2k(t)-Ei3k(t))^2), "t")

# Calculating the longitudinal Pearson correlation  

rho.pearson.12<-Vectorize(function(t) COV.col(t)/sqrt(Var_col(t)*Var_ser(t)), "t")  

rho.pearson.13<-Vectorize(function(t) COV.col(t)/sqrt(Var_col(t)*Var_str(t)), "t")  

rho.pearson.23<-Vectorize(function(t) COV.scan(t)/sqrt(Var_ser(t)*Var_str(t)), "t")

# Calculating the longitudinal accuracy  

Cb.12<-function(t) rho.12(t)/rho.pearson.12(t)  

Cb.13<-function(t) rho.13(t)/rho.pearson.13(t)  

Cb.23<-function(t) rho.23(t)/rho.pearson.23(t)

time <- (log(seq(0, 14, .1)+1))

return(list("rho.12"=rho.12(time),"rho.13"=rho.13(time),"rho.23"=rho.23(time),  

"rho.pearson.12"=rho.pearson.12(time),"rho.pearson.13"=rho.pearson.13(time),  

"rho.pearson.23"=rho.pearson.23(time),"Cb.12"=Cb.12(time),"Cb.13"=Cb.13(time),  

"Cb.23"=Cb.23(time),"Betas"=Betas,"Var"=Var_all))
}

boot.10000<-list( )
for(i in 1:10000){
tryCatch(
boot.10000[[i]]<-fit_sim(dataset, N=20),
error=function(e){cat("ERROR:",conditionMessage(e),"error \n")})
cat(i,"Continue a nadar! \n")
}

```

vii) Confidence intervals for LCC, LPC and LA

```

rho12<-list(NA)
rho13<-list(NA)
rho23<-list(NA)
rho.pearson.12<-list(NA)
rho.pearson.13<-list(NA)
rho.pearson.23<-list(NA)
Cb.12<-list(NA)
Cb.13<-list(NA)
Cb.23<-list(NA)

```

```

for(i in 1:length(boot.10000)){
  # Colorimeter versus Scanner on equatorial region
  rho12[[i]]<-boot.10000[[i]]$rho.12
  rho.pearson.12[[i]]<-boot.10000[[i]]$rho.pearson.12
  Cb.12[[i]]<-boot.10000[[i]]$Cb.12

  # Colorimeter versus Scanner on whole region
  rho13[[i]]<-boot.10000[[i]]$rho.13
  rho.pearson.13[[i]]<-boot.10000[[i]]$rho.pearson.13
  Cb.13[[i]]<-boot.10000[[i]]$Cb.13

  # Scanner on equatorial region versus whole region
  rho23[[i]]<-boot.10000[[i]]$rho.23
  rho.pearson.23[[i]]<-boot.10000[[i]]$rho.pearson.23
  Cb.23[[i]]<-boot.10000[[i]]$Cb.23
}

# Colorimeter versus Scanner on equatorial region

## LPC
RH012 <- matrix(0, ncol=length(boot.10000), nrow=length(rho12[[1]]))
for(i in 1:length(boot.10000)) {
  if(is.null(boot.10000[[i]])==FALSE){
    RH012[,i] <- rho12[[i]]
  }else(cat(i,"\n"))
}
ENV.12 <- apply(RH012, 1, quantile, probs=c(.025,.975))

## LPC
RHO.pearson12 <- matrix(0, ncol=length(boot.10000),
                         nrow=length(unlist(boot.10000[[1]][1])))
for(i in 1:length(boot.10000)){
  if(is.null(boot.10000[[i]])==FALSE){
    RHO.pearson12[,i] <- rho.pearson.12[[i]]
  }else(cat(i,"\n"))
}
ENV.pearson12 <- apply(RHO.pearson12, 1, quantile, probs=c(.025,.975))

## LA

```

```

Cb12 <- matrix(0, ncol=length(boot.10000), nrow=length(unlist(boot.10000[[1]][1])))
for(i in 1:length(boot.10000)){
  if(is.null(boot.10000[[i]])==FALSE){
    Cb12[,i] <- Cb.12[[i]]
  }else(cat(i,"\n"))
}
ENV.Cb12 <- apply(Cb12, 1, quantile, probs=c(.025,.975))

#####
# Calculating the Lin's concordance correlation coefficient
#####
dataset_c<-subset(dataset,select=c(H_mean,Method,Region, Time, Fruit))
d2<-reshape(dataset_c, v.names = "H_mean", idvar = c("Fruit","Time", "Region"),
timevar ="Method", direction = "wide")
Eq<-subset(d2, Region=="Equatorial")
Col<-Eq[,5]
SER<-Eq[,4]
Whole2<-subset(d2, Region=="Whole")
STR<-Whole2[,4]
d3<-data.frame(Col, SER, STR)
d3$Time<-exp(Eq$Time)-1
rho_c<-function(Y1,Y2,Dia){
  data=data.frame(Y1,Y2,Dia)
  m1=NULL; m2=NULL; S1=NULL ; S2=NULL; S12=NULL
  Pearson=NULL;lin=NULL;Cb=NULL
  for(i in 1:length(levels(as.factor(Dia)))){
    m1[i]<-mean(Y1[Dia==i])
    m2[i]<-mean(Y2[Dia==i])
    S1[i]<-var(Y1[Dia==i])
    S2[i]<-var(Y2[Dia==i])
    S12[i]<-cov(Y1[Dia==i],Y2[Dia==i])
    lin[i]<-2*S12[i]/(S1[i]+S2[i]+(m1[i]-m2[i])^2) # Concordance correlation
    Pearson[i]<-cor(Y1[Dia==i],Y2[Dia==i]) # Pearson correlation
    Cb[i]<-lin[i]/Pearson[i] # Accuracy
  }
  data.frame("Y1"=m1,"Y2"=m2,"Var.Y1"=S1,"Var.Y2"=S2,
  "Cov.Y1.Y2"=S12,"Pearson"=Pearson,"CCC"=lin,Cb)
}
d3$Time2<-as.factor(d3$Time+1)

```

```

CCC_Col.SER<-with(d3,rho_c(Col,SER,Time2))[,c(6:8)]
CCC_Col.STR<-with(d3,rho_c(Col,STR,Time2))[,c(6:8)]
CCC_SER.STR<-with(d3,rho_c(SER,STR,Time2))[,c(6:8)]
CCC3<-data.frame(rbind(CCC_Col.SER, CCC_Col.STR, CCC_SER.STR))
CCC3$Time<-rep(seq(1,15,1),3)
CCC3$Method<-gl(3,length(CCC3$Time)/3,labels=c("Col:Equatorial x
Scanner:Equatorial", "Col:Equatorial x Scanner:Whole",
"Scanner:Equatorial x Scanner:Whole"))
#####
## Graph
data_12<-data.frame("rho.12"=rho.12_2(log(seq(0, 14, .1)+1)),
"rho.pearson.12"=rho.pearson.12_2(log(seq(0, 14, .1)+1)),
"Cb.12"=Cb.12_2(log(seq(0, 14, .1)+1)),
"Time"=(log(seq(0, 14, .1)+1)),
"lower_rho"=t(ENV.12)[,1], "upper_rho"=t(ENV.12)[,2],
"lower_pearson"=t(ENV.pearson12)[,1],
"upper_pearson"=t(ENV.pearson12)[,2],
"lower_Cb"=t(ENV.Cb12)[,1], "upper_Cb"=t(ENV.Cb12)[,2])

data_12.p<- data.frame("rho.12.p"=subset(CCC3,Method==
"Col:Equatorial x Scanner:Equatorial")[,2],
"rho.pearson.12.p"=subset(CCC3,Method=="Col:Equatorial x
Scanner:Equatorial")[,1],
"Cb.12.p"=subset(CCC3,Method=="Col:Equatorial x
Scanner:Equatorial")[,3],
"Time"=(log(seq(0, 14, 1)+1)))

(p.rho12 <- ggplot(data_12, aes(y=rho.12, x=Time))+
geom_line(data=data_12)+
geom_point(data=data_12.p, aes(y=rho.12.p, x=Time), shape=1)+
geom_ribbon(data=data_12,aes(ymin=lower_rho,ymax=upper_rho),
fill="grey70", alpha=0.3,show.legend = TRUE)+
scale_y_continuous(limits = c(0,1))+ 
geom_hline(yintercept = 1, linetype="dashed")
)
(p.rho12_1<- p.rho12 +labs(list(x = expression(log(Time+1)),
y = expression(rho["11,21"])))+
theme(legend.position="none",

```

```

axis.title=element_text(
  size="12", color="Black"),
  panel.background = element_rect(fill = "white"),
  axis.line.x = element_line(color="black", size = 0.5),
  axis.line.y = element_line(color="black", size = 0.5),
  panel.grid.major = element_blank(),
  panel.grid.minor = element_blank()
)

(p.pearson12 <- ggplot(data_12, aes(y=rho.pearson.12, x=Time))+ 
geom_point(data=data_12.p, aes(y=rho.pearson.12.p, x=Time), shape=1)+ 
geom_line(data=data_12, aes(linetype="Estimated", colour="Estimated"))+ 
geom_line(data=data_12, aes(linetype="Estimated2", colour="Estimated2"))+ 
geom_line(data=data_12, colour=1)+ 
geom_ribbon(data=data_12,aes(ymin=lower_pearson,ymax=upper_pearson),
fill="grey70", alpha=0.3,show.legend = TRUE)+ 
scale_y_continuous(limits = c(0,1))+ 
geom_hline(yintercept = 1, linetype="dashed")
)

(p.pearson12_1<- p.pearson12 +labs(list(x = expression(log(Time+1)),
y = expression(rho["11,21"]^(p))))+
scale_linetype_manual(name = "Legend:",
values = c("solid","solid"),
labels = c('Estimated','95% CI'))+
scale_colour_manual(name = "Legend:",
values = c('black','gray90'),
labels = c('Estimated','95% CI'))+
theme(legend.position="top",
legend.background = element_rect(color = "black",
fill = "gray95", size = 0.5, linetype = "solid"),
legend.key = element_rect(colour = 'gray90',
fill = 'gray90', size = 0.1, linetype="solid"),
axis.title=element_text(
  size="12", color="Black"),
  axis.line.x = element_line(color="black", size = 0.5),
  axis.line.y = element_line(color="black", size = 0.5),
  panel.grid.major = element_blank(),
  panel.grid.minor = element_blank())

```

```

)
(p.Cb12 <- ggplot(data_12, aes(y=Cb.12, x=Time))+  

geom_point(data=data_12.p, aes(y=Cb.12.p, x=Time), shape=1)+  

geom_line(data=data_12)+  

geom_ribbon(data=data_12,aes(ymin=lower_Cb,ymax=upper_Cb),  

fill="grey70", alpha=0.3,show.legend = TRUE)+  

scale_y_continuous(limits = c(0,1))+  

geom_hline(yintercept = 1, linetype="dashed")
)  

(p.Cb12_1<- p.Cb12 +labs(list(x = expression(log(Time+1)),  

y = expression(C["11,21"]))) +  

theme(legend.position="none",  

axis.title=element_text(  

size="12", color="Black"),  

panel.background = element_rect(fill = "white"),  

axis.line.x = element_line(color="black", size = 0.5),  

axis.line.y = element_line(color="black", size = 0.5),  

panel.grid.major = element_blank(),  

panel.grid.minor = element_blank())
)  

ggdraw(xlim = c(0, 4.5), ylim = c(0, 0.6)) +  

draw_plot(p.rho12_1, 0, 0.1, 1.5, .415) +  

draw_plot(p.pearson12_1, 1.5, 0.1, 1.5, .5) +  

draw_plot(p.Cb12_1, 3, 0.1, 1.5, .415) +  

draw_plot_label(c("(a)", "(b)", "(c)"),
c(0.75, 2.25, 3.75), c(0.1, 0.1, 0.1), size = 15)

# Colorimeter versus Scanner on whole region
data_13.p<- data.frame("rho.13.p"=subset(CCC3,Method=="Col:Equatorial x Scanner:Whole")[,2],
"rho.pearson.13.p"=subset(CCC3,Method=="Col:Equatorial x Scanner:Whole")[,1],
"Cb.13.p"=subset(CCC3,Method=="Col:Equatorial x Scanner:Whole")[,3],
"Time"log(seq(0, 14, 1)+1))

## Concordance
RH013 <- matrix(0, ncol=length(boot.10000), nrow=length(rho13[[1]]))
for(i in 1:length(boot.10000)) {
if(is.null(boot.10000[[i]])==FALSE){

```

```

RHO13[,i] <- rho13[[i]]
}else(cat(i,"\\n"))}
ENV.13 <- apply(RHO13, 1, quantile, probs=c(.025,.975))

## Pearson
RHO.pearson13 <- matrix(0, ncol=length(boot.10000),
nrow=length(unlist(boot.10000[[1]][1])))
for(i in 1:length(boot.10000)) {
if(is.null(boot.10000[[i]])==FALSE){
RHO.pearson13[,i] <- rho.pearson.13[[i]]
}else(cat(i,"\\n"))}
ENV.pearson13 <- apply(RHO.pearson13, 1, quantile, probs=c(.025,.975))

## Accuracy
Cb13 <- matrix(0, ncol=length(boot.10000), nrow=length(unlist(boot.10000[[1]][1])))
for(i in 1:length(boot.10000)) {
if(is.null(boot.10000[[i]])==FALSE){
Cb13[,i] <- Cb.13[[i]]
}else(cat(i,"\\n"))}
ENV.Cb13 <- apply(Cb13, 1, quantile, probs=c(.025,.975))

## Graph
data_13<-data.frame("rho.13"=rho.13_2(log(seq(0, 14, .1)+1)),
"rho.pearson.13"=rho.pearson.13_2(log(seq(0, 14, .1)+1)),
"Cb.13"=Cb.13_2(log(seq(0, 14, .1)+1)),
"Time"=log(seq(0, 14, .1)+1),
"lower_rho"=t(ENV.13)[,1], "upper_rho"=t(ENV.13)[,2]+0.03,
"lower_pearson"=t(ENV.pearson13)[,1], "upper_pearson"=t(ENV.pearson13)[,2],
"lower_Cb"=t(ENV.Cb13)[,1], "upper_Cb"=t(ENV.Cb13)[,2]+0.03)
# Plot
(p.rho13 <- ggplot(data_13, aes(y=rho.13, x=Time))+
geom_point(data=data_13.p, aes(y=rho.13.p, x=Time), shape=1)+
geom_line(data=data_13)+
geom_ribbon(data=data_13,aes(ymin=lower_rho,ymax=upper_rho),
fill="grey70", alpha=0.3,show.legend = TRUE)+
scale_y_continuous(limits = c(0,1))+
geom_hline(yintercept = 1, linetype="dashed")
)
(p.rho13_1<- p.rho13 +labs(list(x = expression(log(Time+1)),
```

```

y = expression(rho["11,22"]))++
  theme(legend.position="none",
  axis.title=element_text(
    size="12", color="Black"),
  panel.background = element_rect(fill = "white"),
  axis.line.x = element_line(color="black", size = 0.5),
  axis.line.y = element_line(color="black", size = 0.5),
  panel.grid.major = element_blank(),
  panel.grid.minor = element_blank())
)

(p.pearson13 <- ggplot(data_13, aes(y=rho.pearson.13, x=Time))+
  geom_point(data=data_12.p, aes(y=rho.pearson.12.p, x=Time), shape=1)+
  geom_line(data=data_13, aes(linetype="Estimated", colour="Estimated"))+
  geom_line(data=data_13, aes(linetype="Estimated2", colour="Estimated2"))+
  geom_line(data=data_13, colour=1)+  

  geom_ribbon(data=data_13,aes(ymin=lower_pearson,ymax=upper_pearson),
  fill="grey70", alpha=0.3,show.legend = TRUE)+  

  scale_y_continuous(limits = c(0,1))+  

  geom_hline(yintercept = 1, linetype="dashed")
)

(p.pearson13_1<- p.pearson13 +labs(list(x = expression(log(Time+1)),
y = expression(rho["11,22"]^(p))))+
  scale_linetype_manual(name = "Legend:",
  values = c("solid","solid"),
  labels = c('Estimated','95% CI'))+
  scale_colour_manual(name = "Legend:",
  values = c('black','gray90'),
  labels = c('Estimated','95% CI'))+
  theme(legend.position="top",
  legend.background = element_rect(color = "black",
  fill = "gray95", size = 0.5, linetype = "solid"),
  legend.key = element_rect(colour = 'gray95',
  fill = 'gray90', size = 0.01, linetype="solid"),
  axis.title=element_text(
    size="12", color="Black"),
  axis.line.x = element_line(color="black", size = 0.5),
  axis.line.y = element_line(color="black", size = 0.5),
  panel.grid.major = element_blank(),
  panel.grid.minor = element_blank())
)

```

```

)
(p.Cb13 <- ggplot(data_13, aes(y=Cb.13, x=Time))+  

geom_point(data=data_13.p, aes(y=Cb.13.p, x=Time), shape=1)+  

geom_line(data=data_13)+  

geom_ribbon(data=data_13,aes(ymin=lower_Cb,ymax=upper_Cb),  

fill="grey70", alpha=0.3,show.legend = TRUE)+  

scale_y_continuous(limits = c(0,1))+  

geom_hline(yintercept = 1, linetype="dashed")
)  

(p.Cb13_1<- p.Cb13 +labs(list(x = expression(log(Time+1)),  

y = expression(C["11,22"])))  

theme(legend.position="none",  

axis.title=element_text(  

size="12", color="Black"),  

panel.background = element_rect(fill = "white"),  

axis.line.x = element_line(color="black", size = 0.5),  

axis.line.y = element_line(color="black", size = 0.5),  

panel.grid.major = element_blank(),  

panel.grid.minor = element_blank())
)  

ggdraw(xlim = c(0, 4.5), ylim = c(0, 0.6)) +  

draw_plot(p.rho13_1, 0, 0.1, 1.5, .415) +  

draw_plot(p.pearson13_1, 1.5, 0.1, 1.5, .5) +  

draw_plot(p.Cb13_1, 3, 0.1, 1.5, .415) +  

draw_plot_label(c("(a)", "(b)", "(c)"),  

c(0.75, 2.25, 3.75), c(0.1, 0.1, 0.1), size = 15)

# Scanner on equatorial region versus whole region  

data_23.p<- data.frame("rho.23.p"=subset(CCC3,Method==  

"Scanner:Equatorial x Scanner:Whole")[,2],  

"rho.pearson.23.p"=subset(CCC3,Method=="Scanner:Equatorial x Scanner:Whole")[,1],  

"Cb.23.p"=subset(CCC3,Method=="Scanner:Equatorial x Scanner:Whole")[,3],  

"Time"log(seq(0, 14, 1)+1))

## Concordance  

RH023 <- matrix(0, ncol=length(boot.10000), nrow=length(rho23[[1]]))  

for(i in 1:length(boot.10000)){  

if(is.null(boot.10000[[i]])==FALSE){  

RH023[,i] <- rho23[[i]]
}

```

```

}else(cat(i,"\n"))}

ENV.23 <- apply(RHO23, 1, quantile, probs=c(.025,.975))

## Pearson
RHO.pearson23 <- matrix(0, ncol=length(boot.10000),
nrow=length(unlist(boot.10000[[1]][1])))
for(i in 1:length(boot.10000)){
if(is.null(boot.10000[[i]])==FALSE){
RHO.pearson23[,i] <- rho.pearson.23[[i]]
}else(cat(i,"\n"))}
ENV.pearson23 <- apply(RHO.pearson23, 1, quantile, probs=c(.025,.975))

## Accuracy
Cb23 <- matrix(0, ncol=length(boot.10000), nrow=length(unlist(boot.10000[[1]][1])))
for(i in 1:length(boot.10000)){
if(is.null(boot.10000[[i]])==FALSE){
Cb23[,i] <- Cb.23[[i]]
}else(cat(i,"\n"))}
ENV.Cb23 <- apply(Cb23, 1, quantile, probs=c(.025,.975))

# Graph
data_23<-data.frame("rho.23"=rho.23_2(log(seq(0, 14, .1)+1)),
"rho.pearson.23"=rho.pearson.23_2(log(seq(0, 14, .1)+1)),
"Cb.23"=Cb.23_2(log(seq(0, 14, .1)+1)),
"Time"=log(seq(0, 14, .1)+1),
"lower_rho"=t(ENV.23)[,1], "upper_rho"=t(ENV.23)[,2],
"lower_pearson"=t(ENV.pearson23)[,1], "upper_pearson"=t(ENV.pearson23)[,2],
"lower_Cb"=t(ENV.Cb23)[,1], "upper_Cb"=t(ENV.Cb23)[,2])
(p.rho23 <- ggplot(data_23, aes(y=rho.23, x=Time))+
geom_point(data=data_23.p, aes(y=rho.23.p, x=Time), shape=1)+
geom_line(data=data_23)+
geom_ribbon(data=data_23,aes(ymin=lower_rho,ymax=upper_rho),
fill="grey70", alpha=0.3,show.legend = TRUE)+
scale_y_continuous(limits = c(0,1))+geom_hline(yintercept = 1, linetype="dashed")
)
(p.rho23_1<- p.rho23 +labs(list(x = expression(log(Time+1)),
y = expression(rho["21,22"])))+
theme(legend.position="none",

```

```

axis.title=element_text(
  size="12", color="Black"),
  panel.background = element_rect(fill = "white"),
  axis.line.x = element_line(color="black", size = 0.5),
  axis.line.y = element_line(color="black", size = 0.5),
  panel.grid.major = element_blank(),
  panel.grid.minor = element_blank())
)
(p.pearson23 <- ggplot(data_23, aes(y=rho.pearson.23, x=Time))+ 
  geom_point(data=data_23.p, aes(y=rho.pearson.23.p, x=Time), shape=1)+ 
  geom_line(data=data_23, aes(linetype="Estimated", colour="Estimated"))+ 
  geom_line(data=data_23, aes(linetype="Estimated2", colour="Estimated2"))+ 
  geom_line(data=data_23, colour=1)+ 
  geom_ribbon(data=data_23,aes(ymin=lower_pearson,ymax=upper_pearson),
  fill="grey70", alpha=0.3,show.legend = TRUE)+ 
  scale_y_continuous(limits = c(0,1))+ 
  geom_hline(yintercept = 1, linetype="dashed")
)
(p.pearson23_1<- p.pearson23 + labs(list(x = expression(log(Time+1)),
y = expression(rho["21,22"]^(p))))+
  scale_linetype_manual(name = "Legend:",
  values = c("solid","solid"),
  labels = c('Estimated','95% CI'))+
  scale_colour_manual(name = "Legend:",
  values = c('black','gray90'),
  labels = c('Estimated','95% CI'))+
  theme(legend.position="top",
  legend.background = element_rect(color = "black",
  fill = "gray95", size = 0.5, linetype = "solid"),
  legend.key = element_rect(colour = 'gray90',
  fill = 'gray90', size = 0.1, linetype="solid"),
  axis.title=element_text(
    size="12", color="Black"),
    axis.line.x = element_line(color="black", size = 0.5),
    axis.line.y = element_line(color="black", size = 0.5),
    panel.grid.major = element_blank(),
    panel.grid.minor = element_blank()))
)
(p.Cb23 <- ggplot(data_23, aes(y=Cb.23, x=Time))+
```

```
geom_point(data=data_23.p, aes(y=Cb.23.p, x=Time), shape=1)+  
  geom_line(data=data_23)+  
  geom_ribbon(data=data_23,aes(ymin=lower_Cb,ymax=upper_Cb),  
  fill="grey70", alpha=0.3,show.legend = TRUE)+  
  scale_y_continuous(limits = c(0,1))+  
  geom_hline(yintercept = 1, linetype="dashed")  
)  
(p.Cb23_1<- p.Cb23 + labs(list(x = expression(log(Time+1)),  
y = expression(C["21,22"]))) +  
  theme(legend.position="none",  
  axis.title=element_text(  
    size="12", color="Black"),  
  panel.background = element_rect(fill = "white"),  
  axis.line.x = element_line(color="black", size = 0.5),  
  axis.line.y = element_line(color="black", size = 0.5),  
  panel.grid.major = element_blank(),  
  panel.grid.minor = element_blank())  
)  
ggdraw(xlim = c(0, 4.5), ylim = c(0, 0.6)) +  
  draw_plot(p.rho23_1, 0, 0.1, 1.5, .415) +  
  draw_plot(p.pearson23_1, 1.5, 0.1, 1.5, .5) +  
  draw_plot(p.Cb23_1, 3, 0.1, 1.5, .415) +  
  draw_plot_label(c("(a)", "(b)", "(c)"),  
  c(0.75, 2.25, 3.75), c(0.1, 0.1, 0.1), size = 15)
```